DEVELOPMENT OF SOLID LIPID NANOPARTICLES FOR SUSTAINED RELEASE OF ANTICANCER AGENTS

MD MUSHFIQ HOSSAIN AKANDA [BSc (Hons.)]

A thesis submitted in partial fulfilment of the requirements of the University of Greenwich for the degree of Doctor of Philosophy

September, 2015

UNIVERSITY
of
GREENWICH

DECLARATION

"I certify that this work has not been accepted in substance for any degree, and is not concurrently being submitted for any degree other than that of Doctor of Philosophy (PhD) being studied at the University of Greenwich. I also declare that this work is the result of my own investigations except where otherwise identified by references and that I have not plagiarised the work of others".

…………………………..

MD MUSHFIQ HOSSAIN AKANDA (CANDIDATE)

PhD SUPERVISOR

DR. DIONYSIOS DOUROUMIS   ………………………….

Date: 16/09/2015

ACKNOWLEDGEMENTS

ABSTRACT

A brief introduction to solid lipid nanoparticles (SLN) is provided and the reasoning behind the use of SLN over other colloidal carriers, such as emulsions and liposomes, are discussed. SLN has many advantageous such as controlled drug release, non-biotoxicity of the carrier, increased bioavailability of drug and lower overall cost. Techniques for the production of SLN, drug incorporation, loading capacity and drug release mechanisms are reviewed. The potential of SLN in anti-cancer drug delivery systems is highlighted.

SLN formulations of two different lipids (tristearin, stearic acid), used as carriers for the encapsulation of the anticancer drug substance curcumin (CRC), have been investigated. The physicochemical characteristics of the CRC-SLNs were investigated by particle size, zeta potential and stability measurements. In addition transmission electron microscopy was used to study the morphology of the SLNs and differential scanning calorimetry (DSC) as well as X- ray diffraction (XRD) were used to evaluate the physical state of the drug in the SLN formulations after freeze drying. The release pattern of CRC-SLN showed sustained release over five days, Moreover, encapsulation efficiency at the range of 92-95% indicated the loosely ordered crystal lattice of lipid matrix, which facilitated a higher drug payload.

The anti-cancer effects of CRC encapsulated SLN formulations (both loaded and unloaded) were evaluated using a human prostate cancer cell line (LNCaP). Blank SLN (BL-SLN) did not show any anti-tumour activity; CRC encapsulated SLN (CRC-SLN) displayed anti-tumour activity. Both lipid based CRC loaded SLNs reduced the LNCaP cell viability to almost 0% at a CRC concentration of 100 µg/ml. Cellular uptake studies confirmed the internalisation of CRC-SLN which was found to be localized in the cytoplasm around the nucleus. Flow cytometric studies confirmed the early and late apoptosis inducing ability of CRC-SLNs.

Retinoic acid (RTA) loaded SLN, optimized by tuning the process parameters (pressure and temperature) and using various lipid grades to produce nano-dispersions, displayed enhanced anticancer activity. The RTA-SLN dispersions were produced by high-pressure homogenization and characterized in terms of particle size, zeta potential, drug entrapment efficiency, transmission electron microscopy (TEM), atomic force microscopy (AFM), X-ray diffraction (XRD) and *in vitro* drug release. Anticancer efficiency was evaluated by incubating RTA-SLN with LNCaP cells, and demonstrated reduced cell viability with increasing drug concentrations (9.5% at 200 ug/ml) while blank SLN showed negligible cytotoxicity. Cellular uptake studies of SLNs showed localization within the cytoplasm of the

cell and flow cytometry analysis showed an increase in the fraction of cells expressing early apoptotic markers, suggesting that the RTA-SLN is able to induce apoptosis in LNCaP cells.

Both empty and loaded (curcumin) nanostructured lipid carriers (NLC) were characterized in relation to their size, zeta potential and polydispersity index. The drug entrapment efficiency and *in vitro* drug release behaviour of these NLC formulations were also investigated. Analysis of the shape and morphology (using transmission electron microscopy (TEM) and laser diffraction) revealed spherical shaped NLC with a uniform particle size distribution. Cellular uptake studies revealed the internalisation of CRC-NLC, which appear to be localized in the cytoplasm around the nucleus. Flow cytometry studies were performed to evaluate apoptosis inducing abilities of CRC-NLC, as at a CRC concentration of 100 µg/ml, the CRC-NLC treated cells showed 12.2% (early) and 76.9% (late) apoptotic cells. Nude mice bearing prostate cancer xenografts exhibited significant suppression upon administering CRC loaded NLC formulations, with no significant weight loss. The efficacy of CRC-NLC treatment group with CRC only group in comparison with the CRC group showed 40% tumour volume suppression.

Unconjugated SLN were conjugated with transferrin for specific (active) delivery of CRC into LNCaP prostate cancer cells. SLNs prepared by high-pressure homogenization were characterised for particle size, zeta potential and drug loading. The transferrin conjugated to SLN was quantified by the Bradford assay. *In vitro* and *in vivo* studies of SLN for passive and active delivery of CRC to LNCaP prostate cancer cells were evaluated. *In vivo* studies of tumour regression efficiency showed CRC-SLN formulations to be more effective in suppressing tumour growth compared to the free drug. In addition the transferrin conjugated SLN also demonstrated a higher anti-tumour activity in tumour bearing mice compared to the non-conjugated formulation. The tumour mass was significantly suppressed by 61% and 79% for CRC-SLN and Tf-CRC-SLN, respectively, when compared with the control group.

Table of Contents

CONTENTS

List of Figures

List of Tables

ABBREVIATIONS

Abbreviation	Meaning
BL- PR	Blank precirol
BL- SA	Blank stearic acid
BL- TL	Blank trilaurin
BL- TS	Blank tristearin
CRC	Curcumin
CRC- PR	Curcumin loaded precirol
CRC- SA	Curcumin loaded Stearic acid
CRC- TL	Curcumin loaded trilaurin
CRC- TS	Curcumin loaded tristearin
DSC	Differential scanning calorimetry
FACS	Fluorescence activated cell sorting
FACS	Fluorescence activated cell sorting
RTA	Retinoic acid
RTA- SA	Retinoic acid loaded stearic acid
RTA- SLN	Retinoic acid loaded SLN
RTA- TS	Retinoic acid loaded tristearin
SLN	Solid lipid nanoparticles
TEM	Transmission electron microscopy
XRD	X-ray diffraction
Tf	Transferrin
CRC-SLN	Curcumin loaded SLN
Tf-CRC-SLN	Transferrin conjugated curcumin loaded SLN
BL-SLN	Blank SLN
BL-Tf-SLN	Transferrin conjugated blank SLN
NLC	Nanostructured lipid carriers
BL-NLC	Blank NLC
CRC-NLC	CRC Loaded NLC

CONFERENCE PRESENTATIONS

Akanda, M. H., Douroumis, D. (2014), Formulation of solid lipid nanoparticles for sustained release of anti-cancer drugs. (American Association of Pharmaceutical Science) Student Chapter at University of Greenwich, UK (Poster Presentation).

Akanda, M. H., Douroumis, D. (2014), Development of Curcumin & Retinoic Acid loaded solid lipid nanoparticles, Academy of Pharmaceutical Society at Hertfordshire University, UK (Poster Presentation).

Akanda, M. H., Douroumis, D. (2014), Development and characterisation of retinoic acid loaded solid lipid nanoparticles. (American Association of Pharmaceutical Science) student chapter at University of Greenwich, UK (Poster Presentation).

Akanda, M. H., Slipper, I. J., Douroumis, D. (2013), Formulation of solid lipid nanoparticles loaded with curcumin. (American Association of Pharmaceutical Science) Student Chapter at University of Greenwich, UK (Poster Presentation).

Akanda, M. H., Douroumis, D. (2012), Formulation of solid lipid nanoparticles for sustained release of anti-cancer drugs, Academy of Pharmaceutical Society at Nottingham University, UK (Poster Presentation).

CHAPTER ONE: INTRODUCTION

1.1. Overview

Solid lipid nanoparticles are colloidal delivery system made from solid (under room temperature) lipid, (Wissing, Kayser et al., 2004). Diameter of solid lipid nanoparticles by photo correlation spectroscopy is between 50 to 500nm. SLN can, unlike polymeric nanoparticles, can be produced by conveniently by different methods, such as high pressure homogenization. The obtained solid lipid nanoparticles can be stabilized by surfactant such as lecithin, Tween 80, Pluronic 68 or the combination of different surfactant (Muller, Maer et al., 2000; Muller, Hommoss et al., 2009). Solid lipid nanoparticles are invented in early 90s. It is the latest development of lipid based colloidal delivery system after nanoemulsion, liposome. Nanoemulsions are made from lipids that are liquid under room temperature. It quickly generated broad public attention and within few years. The first safe emulsion for parental nutrition delivery was invented by Wretlind, which marks the beginning of emulsion as colloidal delivery for lipophilic drugs. After years of research some of them are successively commercialized, Diprivan (1980). Research review reported that applying oil in water emulsions were able to reduce injection dosage and thereby minimize side effect. O/W emulsion was designed and applied for drug delivery. Products such as Diazemuls and Diazepam-Lipuro were developed and put into market (Muller, Maer et al., 2000). Despite of the advantages, major limitations of these emulsions are also obvious: poor physical stability of drug containing emulsion. Encapsulation of drugs is able to cause agglomeration, drug expulsion and poor ability to offer protection to liable compounds. Another lipid based carrier developed earlier is liposome, which normally composed of phospholipid. It is invented as early as 1965 with focus on cosmetic market (Muller, Maer et al., 2000). After one decade of research, several products such as lung surfactant for pulmonary instillation were put into market. However, the total number of successful product is rather limited when compared to emulsion. Major obstacle is lack of commercially available production method. In another word, liposome product is only feasible in lab scale. For polymeric nanoparticles, it has been under intensive research for 50 years. However, this delivery system is well commercialized like lipid based delivery system. Similar to the problem encountered by liposome, polymeric particles is difficult to be produced in large quantity. What is worse, it has been reported that polymeric particle has poor tolerability. It is believe that polymeric lipid nanoparticles are able to penetrate through cell membrane and leads to cytotoxic effect when degrades inside cell (Muller, Maer et al., 2000).

1.2. What is SLN?

SLN was first introduced in 1991; they represent alternative carrier systems to other traditional colloidal carriers namely oil in water emulsions, liposomes, micro-particles and polymeric nanoparticles (Eldem et al., 1991). SLN consists of spherical lipid particles in the nano-meter size range (Figure 1.1).
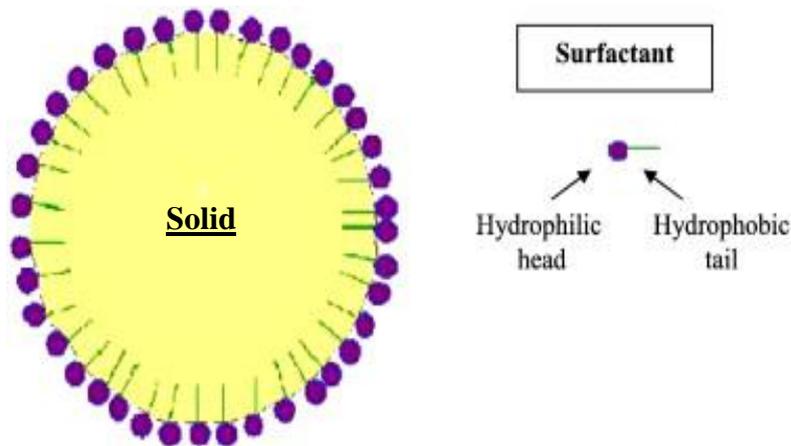
Figure 1. 1. A diagrammatic representation of SLN

SLN is used for the controlled and targeted delivery of drugs. The drugs are part of the solid lipid matrix. SLN is stabilized by a surfactant layer, which may consist of a single surfactant, but is normally composed of a mixture of surfactants (Cavalli et al., 2002). Generally a solid lipid that is used in such delivery systems melts at temperatures exceeding body temperature (37°C). Some of these lipids are fatty acids, steroids, waxes, triglycerides, acyl-glycerols or a combination thereof. Different classes and ratios of emulsifiers have been successfully utilized to stabilize SLNs. Some of the most common emulsifiers are lecithin, bile salts (such as sodium taurocholate), non-ionic emulsifiers such as ethylene oxide/propylene oxide copolymers, sorbitan esters, fatty acid ehoxylates etc. SLN is claimed to be advantageous when compared to any other colloidal carriers. SLN is known to combine the advantages and avoid the disadvantages associated with numerous colloidal carrier systems (Mehnert et al., 2001). SLN does have several disadvantages e.g., unpredictable particle growth or unexpected drug expulsion from the lipid core are known to be common phenomena (Mehnert et al., 2001). Table 1.1 shows the advantages and disadvantages of using SLN as drug delivery systems (Mukherjee et al., 2011).

Table 1. 2. Advantages and disadvantages of using SLN

Advantages of SLN	Disadvantages of SLN
1. Target based drug delivery system.	1. Particle growth.
2. Drug released for prolonged time.	2. High pressure induced drug degradation.
3. Less expensive.	3. Unpredictable gelation tendency.
4. Used for poorly water soluble drugs.	4. Drug expulsion after polymeric transition during storage
5. Long term stability	
6. Can be administered via different routes.	
7. No bio-toxicity of the carrier.	

1.3. SLN production procedures

1.3.1. General ingredients

General ingredients for the production of SLN include solid lipid(s), emulsifiers and water. The term lipid is used here in a broad sense; these lipids can include triglycerides (e.g. tristearin), partial glycerides (e.g. Imwitor), fatty acids (e.g. stearic acid), steroids (e.g. cholesterol) and waxes (e.g. cetyl palmitate). Emulsifiers help to stabilize the lipid dispersion. It has been found that a combination of emulsifiers may prevent particle agglomeration (Mehnert et al., 2001). Table 1.2 shows a list of excipients that can be used for the preparation of SLN.

Table 1. 3. An overview of ingredients that are commonly used for the preparation of SLN

Triglycerides (lipids)	Hard fat types	Surfactants
• Tricapin	• Glyceryl monostearate	• Soybean lechitin
• Trilaurin	• Glyceryl behenate	• Egg lechitin
• Trimyristin	• Glyceryl palmitostearate	• Phosphatidylcholine
• Tripalmitin	• Cetyl palmitate	• Poloxamer 188
• Tristearin	• Stearic acid	• Poloxamer 182
• Tristeain	• Palmitic acid	• Poloxamer 407
• Hydrogenated coco-glycerides		• Ploxamine 908
		• Polysorbate 20

1.4. Methods of preparing solid lipid nanoparticles

1.4.1. High pressure homogenisation

1.4.1.1. Hot homogenisation

High temperature is used in hot homogenisation techniques. The temperature is kept above the melting point of the lipid(s); drug is dissolved in the melted lipid(s) and the mixture is dispersed in a hot surfactant solution. The pre-emulsion is made by mixing drug, lipid(s) and surfactant, which is then pre- by using an ultra turrax pre- homogeniser for 3 minutes. The solution is then passed through a homogenizer for 5 minute depending on the pressure (Almeida et al., 2007). Figure 1.2 shows a schematic diagram of the hot homogenisation technique for the production of SLN.

Melting of the lipid and
dissolving/dispersing of the drug in the lipid

Dispersion of the drug loaded lipid in a hot
aqueous surfactant mixture

Pre-mix using a stirrer to form a coarse pre-
emulsion

High Pressure homogenization at a
temperature above lipid melting point

Hot o/w nanoemulsion

*Solidification of the nanoemulsion
by cooling down to room
temperature*

Solid lipid nanoparticles (SLN)

Figure 1. 2. Flow chart for preparing SLN using a hot high pressure homogenizer

1.4.1.2. Cold homogenisation

In the cold HPH technique, lipid is melted above its melting point and drug is dissolved or dispersed in it. The system is cooled down by means of dry ice or liquid nitrogen. After solidification, the lipid mass is grounded using ball or mortar milling to yield lipid micro-particles in a range between 50 and 100 μm. Then a micro-emulsion is formed by adding these micro-particles into cold surfactant solution with stirring. This suspension is passed through a high pressure homogenizer at/or below room temperature and the micro-particles are broken down to nanoparticles. Lipid particles prepared using the cold HPH technique possess a slightly higher PI and mean particle size compared to the ones obtained by hot HPH technique (Chaturvedi et al., 2012).

1.4.2. Solvent emulsification evaporation

The lipid is dissolved in water immiscible organic solvents e.g., chloroform, which is then emulsified in an aqueous phase before evaporation of the solvent under condition of reduced pressure. This method is suitable for the incorporation of highly thermolabile drugs due to avoidance of heat during the preparation but presence of solvent residues in the final dispersion may create problems due to regulatory concern (Chaturvedi et al., 2012).

1.4.3. Micro-emulsion technique

A warm micro-emulsion is prepared containing molten lipid, surfactant and co-surfactant is added with stirring. This solution is then dispersed in cold water while stirring. Excess water can be removed by freeze drying. This method has certain advantages which include no need for specialized equipment, energy for production is not required and scale-up production of lipid nanoparticles is possible. Disadvantage of the microemulsion technique is the dilution of the particles suspension with water, thus removal of excess water need additional efforts. In addition, high concentrations of surfactants and co-surfactants, in the formulation raise regulatory concern (Chaturvedi et al, 2012).

1.4.4. Ultra-sonication

SLN can be obtained by high speed stirring using ultra-sonication. This method was used for the production of an oil in water emulsion in which high speed stirring was applied to the melted lipid phase and hot aqueous dispersion of surfactant. After cooling the resulting emulsion, solid particles of lipid were obtained. The main drawback of this method is the use of a high amount of surfactant without which the production of nanometre size particles is not

possible. Physical instability and micro sized range of particles are some of the disadvantages of this technique (Souto et al., 2007).

1.4.5. Supercritical fluid method

This technique is considered to be a relatively new approach for SLN production. There are several variations in this platform technology for powder and nanoparticle preparation. In this method, a gas such as carbon dioxide is used as a solvent. SLN can be prepared by the rapid expansion of supercritical carbon dioxide solutions (RESS) method. The gas mainly used in this process is carbon dioxide because of its non-toxicity, low critical temperature and pressure. Some of the advantages of this technique include no usage of organic solvents and ability to produce nanoparticle and micro-particles in the form of dry powders (Ekambaram et al., 2011).

1.4.6. Double emulsion based method

Warm w/o/w double micro-emulsions can be prepared in two steps. Firstly, w/o micro-emulsion is prepared by adding an aqueous solution containing drug to a mixture of melted lipid, surfactant and co-surfactant at a temperature slightly above the melting point of lipid to obtain a clear system. In second step, w/o prepared micro-emulsion is added to a mixture of water, surfactant and co-surfactant to obtain a clear w/o/w system. SLN can be obtained by dispersing the warm micro double emulsions in cold then washed with dispersion medium by ultra-filtration system. Multiple emulsions have inherent instabilities due to coalescence of the internal aqueous droplets within the oil phase, coalescence of the oil droplets, and rupture of the layer on the surface of the internal droplets. In case of SLN production, they have to be stable for few minutes, the time between the preparations of the clear double micro-emulsions and its quenching in cold aqueous medium, which is possible to achieve (Ekambaram et al., 2011).

1.4.7. Solvent emulsification diffusion method

Using this method an average diameter of particle sizes between 50-100 nm can be obtained. One of the advantages of this technique is the avoidance of high temperatures during preparation. In this technique lipid is generally dissolved in the organic phase in a water bath at 50°C and used as an acidic aqueous phase in order to adjust the zeta potential to form coacervation of SLN, and then easy separation can be done by centrifugation. The SLN suspension was quickly produced. The entire dispersed system can then be centrifuged and re-suspended in distilled water (Trotta et al., 2003).

1.5 Advantages of using high pressure homogenization technique

High pressure homogenizer proved to be a very effective dispersing technique in the preparation of SLN. A reduction of the average particle size from 474 to 155 nm was obtained in a study after the first homogenization cycle (800 bar). Results reported by several other investigators show similar reduction in particle sizes from the homogenization method (Muller et al., 1995).

The dispersing grade of SLN depends on the power density and the power distribution in the dispersion volume. High power densities result in more effective particle disruption. High pressure homogenizers reach by far the highest power densities (10^{12} –10^{13} energy input. W/m^3). A homogeneous distribution of the power density is necessary to obtain narrow size distributions. Otherwise, particles localized in different volumes of the sample will experience different dispersing forces and therefore, the degree of particle disruption will vary within the sample volume. Inhomogeneous power distributions are observed in high-shear homogenizers and ultrasonifiers. High pressure homogenizers are characterized by a homogenous power distribution due to the small size of the homogenizing gap (25–30 mm) (Mehner et al., 2001).

1.6. Influence of ingredient composition on product quality

1.6.1. Influence of lipid

According to Mader et al., (2001) the critical parameters for the formation of nanoparticles are related to the usage of different lipids. Some of the examples are the velocity of lipid crystallization, the lipid hydrophilicity (influence on several self-emulsifying properties) and the shape of the lipid crystals, which in turn also influences the surface area (Siekmann et al., 1992). Moreover, most of the lipids used represent a mixture of several chemical compounds, and the quality of these chemical compounds can vary from different suppliers or vary for different batches from the same supplier. These small differences in the lipid composition can possibly have considerable impact on the quality of SLN dispersion (e.g. by changing the zeta potential, retarding crystallization processes etc). According to Ahlin et al., (1998) lipid composition can supposedly influence the particle size of SLN that is produced by high shear homogenization. Increasing the lipid content over 5–10% in most cases results in larger particles (including micro-particles) and broader particle size distributions (Siekmann et al., 1994).

1.6.2. Influence of emulsifiers

The choice of the emulsifiers and their concentration is of great impact on the quality of the SLN dispersion (Mehnert et al., 2001). Either surfactant or surfactant mixture affects the particle size of the lipid nanoparticles. According to Mehnert et al., (2001) SLN exhibited a much smaller particle size when the surfactant amount was increased. The decrease in surfactant concentration resulted in increase of particle size during storage. One of the most characteristics of surfactant is, it decreases the surface tension between the interface of the particles causing portioning of the particles and thereby increasing the surface area (Ekambaram et al., 2011).

1.7. Secondary production steps

1.7.1. Stability of the drug and solid lipid nanoparticles

Stability considerations that are relevant to SLNs are; the chemical stability of the drug and the physical stability of SLN. Prevention of degradation reactions such as hydrolysis is an important chemical stability parameter and examples for physical stability issues include the prevention of particle size growth and polymorphic changes of the solid lipid. Lipids and surfactants must be chosen carefully and should be mutually compatible to improve the chemical stability (Lim et al., 2004).

Particle size distribution determines the bio-distribution, shelf-life and route of administration of SLN formulation. The SLN dispersion should possess a narrow size distribution to avoid particle size growth due to Ostwald ripening. Ostwald ripening is a thermodynamically driven process, in which smaller particles dissolve and redeposit onto the surface of larger particles. This process occurs because smaller particles have larger surface area and higher surface energy and hence higher Gibbs free energy than the larger particles. All systems tend to attain lowest Gibbs free energy. In other words, larger particles are more energetically stable and favoured over smaller particles. Ostwald ripening can be reduced by minimizing polydispersity in the particle size but it cannot be prevented (Ekambaram et al., 2011).

In SLN dispersions there are three types of instabilities. These are creaming, flocculation and coalescence. In creaming process the less dense phase migrates to top of the dispersion under the influence of buoyancy or centripetal force. Creaming causes the SLN particles to come close to each other which in turn also initiate Ostwald ripening, flocculation and coalescence.

It has been reported that creaming phenomenon can be prevented by matching the density of the lipid and the aqueous phase. Flocculation is a process in which the nanoparticles are held together in loose associations by weak van der Waals forces. Coalescence is a process in which the nanoparticles fuse to form larger particles. The electrostatic repulsion and steric hindrance between particles produced in the presence of surfactants have been found to inhibit flocculation (Porter et al., 1994).

Electrostatic repulsion produces an electrical double layer around each nanoparticle in SLN dispersion. The electrical double layer comprises of two parts: an inner region (stern layer), in which the ions are tightly bound and an outer diffuse region, in which the ions are less firmly attached. A notional boundary forms between particles and ions within this diffuse layer. Ions within the boundary move with the particle and the ions outside the boundary do not move with the particle. This notional boundary is called as slipping plane. The potential at the slipping plane is known as zeta potential. The magnitude of the zeta potential is an important determinant of the stability of SLN dispersions. As the zeta potential increases, the magnitude of electrostatic repulsion between the particles also increases, hence the particles will tend to repel each other and there is no tendency to flocculate. Colloidal dispersions with a zeta potential of more positive than +30 mV and negative than -30mV are considered to be stable. Steric effects also play an important role in the stability of SLN dispersion by hindering the particles from coming close to each other and thus preventing flocculation 14 and coalescence. The polyoxyethylene chain present in non-ionic surfactants extends in the aqueous medium in the form of a coil and providing steric hindrance. Optimum surfactant concentration and sufficient chain length ($\geq$ 20 ethylene oxide units) will impart steric effect mediated formulation stability. For long-term stability a balance between electrostatic repulsion and steric effect must be obtained (Porter et al., 1994).
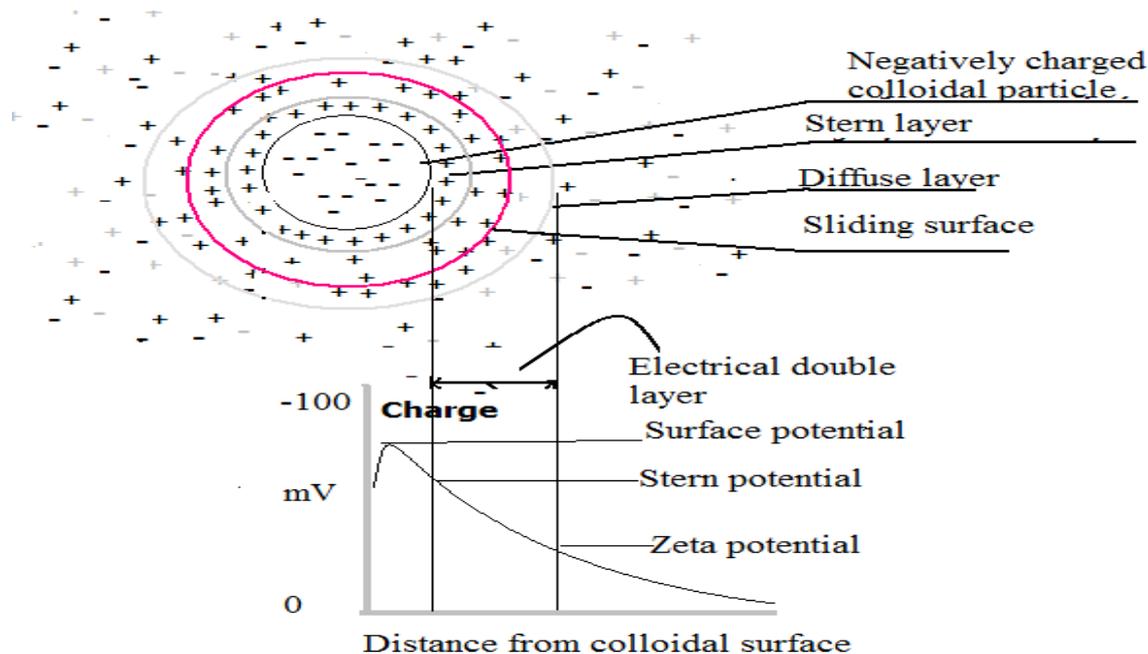
Figure 1. 3. A schematic definition of zeta potential. (Modified from www.malvern.com)

1.7.2. Lyophilisation

Lyophilisation can play an important part to increase the chemical and physical stability of SLN over extended period of time. Lyophilisation had been required to achieve long term stability for a product containing hydrolysable drugs or a suitable product for per-oral administration. Transformation into the solid state would prevent the Oswald ripening and avoid hydrolytic reactions. In case of freeze drying of the product, all the lipid matrices used, can form larger solid lipid nanoparticles with a wider size distribution due to presence of aggregates between the nanoparticles. The conditions of the freeze drying process and the removal of water promote the aggregation among SLNs. An adequate amount of cryo-protectant (such as sucrose, lactose, mannitol, polyethylene glycol etc) can protect the aggregation of solid lipid nanoparticles during the freeze drying process (Ohshima et al., 2009).

1.7.3. Spray drying

Compared to lyophilisation spray drying is cheaper. Usage of spray drying is more encouraged when the lipids melting point is more than 70°C. According to Mehnert et al., (2001) the best results with spray drying were obtained with SLN concentration of 1% in a solution of trehalose in water or 20% trehalose in ethanol-water mixture. The addition of

carbohydrates and low lipid content favour the preservation of the colloidal particle size in spray drying. Muller et al (1998) illustrated that melting of the lipid can be minimized by using ethanol–water mixtures instead of pure water due to cooling leads to small and heterogeneous crystals, the lower inlet temperatures.

1.8. Drug incorporation and drug release from SLN

1.8.1. Drug incorporation

Three different models for the incorporation of active ingredients into SLN have been extensively studied by Muller et al., (2000). These are homogeneous matrix model, drug-enriched shell model and drug-enriched core model. The structure that is obtained is a function of formulation composition, such as lipid, active compound, surfactant, and also of the production conditions (hot vs cold homogenization). A homogeneous matrix with molecularly dispersed drug or drug being present in amorphous clusters is thought to be mainly obtained when applying the cold homogenisation method and when incorporating very lipophilic drugs in SLN with the hot homogenisation method (Yadav et al., 2013).

During the cold homogenisation method the bulk lipid matrix contains the dissolved drug in molecularly dispersed form, which afterwards is mechanically broken down high pressure homogenization leading to the formation of nanoparticle. In hot homogenisation method the produced oil droplet is being cooled and crystallised. It is to note that no phase separation between lipid and drug occurs during the cooling process.

Drug enriched outer shell can be obtained when phase separation occurs during the cooling process from liquid oil droplet to the formation of solid lipid nanoparticles. According to Muller et al (2000) the lipid can precipitate first forming a practically compound free lipid core. Also during the forming process of lipid core the concentration of active compound in the remaining liquid lipid increases continuously. Finally the compound enriched shell crystallises, this model is assumed to give away a very fast release which is highly desired in various SLN applications. Core enriched with active compound can be formed when the opposite occurs, which means the active compound starts precipitating first and the shell will have distinctly less drug. This leads to a membrane controlled release governed by the Fick law of diffusion. The structure of SLN formed clearly depends on the chemical nature of active compound and excipients and the interaction thereof. In addition, the structure can be influenced or determined by the production conditions (Muller et al., 2000).

Solid solution

Drug enriched shell

Lipid shell

Drug molecularly dispersed

Lipid core

Drug enriched core
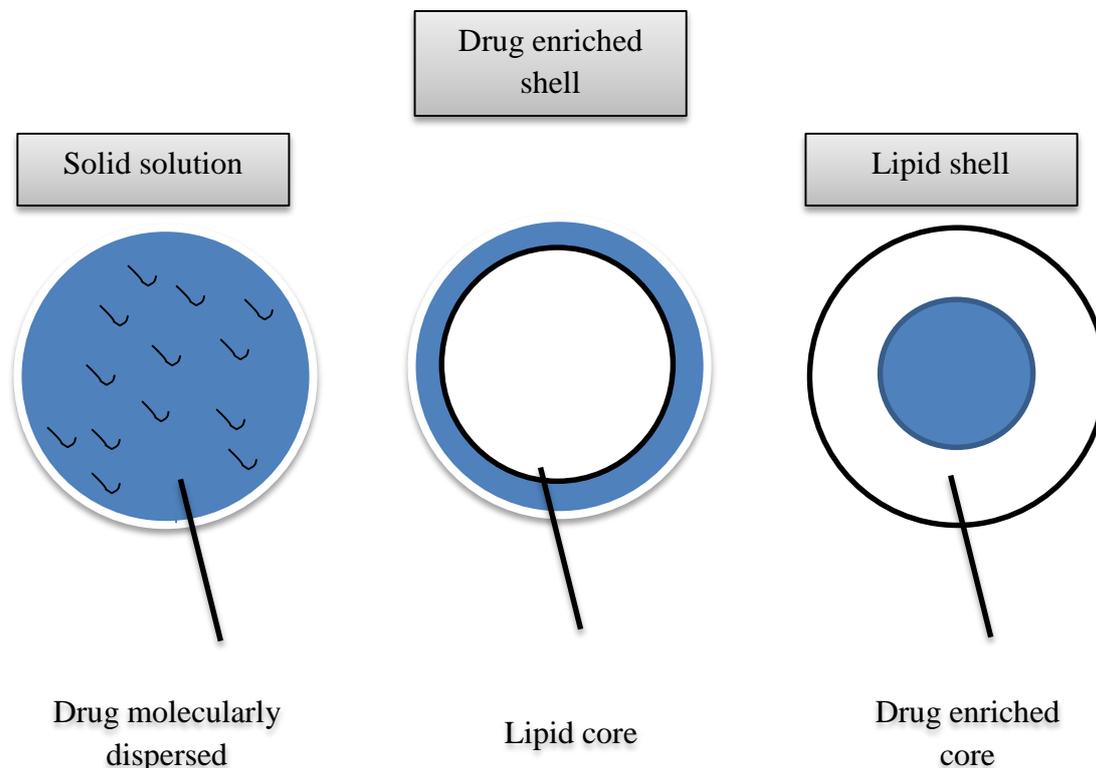
Figure 1. 4. Illustration of different drug incorporation model

1.8.2. Drug release from SLN

Üner (2007) have intensively investigated the effect of formulation parameters and production conditions on the release profile of SLN. For example, they investigated the release profile as a function of production temperature. In most cases, burst release is observed from SLN. An initial burst release is afterwards followed by a prolonged release, this process is called biphasic. It has also been observed that the burst release phenomenon only takes place when hot homogenization is used and very high temperatures are applied. For particles that travel through circulation system, prolonged release is desired, (Subedi, Kang et al., 2009). Fabricated Doxorubicin solid lipid nanoparticles with mean diameter of 199nm using glyceryl caprate and dimethyl sulfoxide via high pressure homogenization method. Prolonged release of doxorubicin was observed in another research by (Xie, Zhu et al., 2009). Doxorubicin-loaded solid lipid nanoparticles (SLN) were fabricated using tetradecanoic acid, palmitic acid, stearic acid respectively. On the other hand, biphasic release patterns are completely non-existent when cold homogenisation is used. The release kinetics

can also depend on the release conditions (sink or non-sink conditions, release medium etc.) Surfactant concentration can also play a vital role in burst release. Different studies has suggested that high surfactant concentration can lead to high burst release. This was explained by redistribution effects of the active compound between the lipid and the water phase during the heating up process and subsequently the cooling down process after production of the hot oil in water emulsion during the hot homogenization process. Solubility of active compound in the water phase increases due to the heating of lipid/water mixture and the compound partitions from the melted lipid droplet to the water phase. After the homogenization procedure is done the lipid core starts to crystallize with still a relatively high amount of active compounds in the water phase. Further cooling leads to super saturation of the compound in the water phase, then the compounds partitions back into the lipid phase; a solid core has already started forming leaving only the liquid outer shell for compound accumulation. So it can be observed that as the solubility in water phase goes higher so does the burst effect. Solubility increases drastically when increased temperature and increased surfactant concentrations are used (Mehnert et al., 2001).

1.9. Biological and pharmaceutical aspects of SLN

SLN is considered to be suitable for parenteral drug delivery because of their small size. SLN may be injected intravenously and used to target drugs to particular organs.

Upon administration into the systemic circulation, several colloidal carriers such as liposomes and polymeric nanoparticles are rapidly cleared by cells of reticuloendothelial system (RES). RES usually reside in the spleen, liver and in the form of Kupffer cells in the liver consisting of phagocytic cells, which is considered to be the major part of the immune system. RES is known to remove drug carriers within minutes identified as foreign objects. (Moghimi et al., 2003). Clearance by RES is beneficial only when the spleen (or) liver, lymph nodes are the target tumour site for other type of cancers RES is known to be the major barrier. When colloidal carrier surface is modified with hydrophilic polymer it increases the blood circulation time and resistance to clearance by RES. This type of surface modification of drug delivery systems by polymers is called long circulating drug carriers. Polyethylene glycols have been employed widely to get the stearic stabilization of colloidal carriers. Polyethylene glycol having electrical neutrality, chain flexibility, lack of functional group and high hydrophilicity which prevent it from interacting with biological components unnecessarily. Other hydrophilic molecules have been tried are brij 68, brij 78, pluronic F188 (Chimmiri et

al., 2012). In order to facilitate drug targeting a reticuloendothelial system avoidance facility these block polyoxyethylene polypropylene copolymers like pluronic F188 can be used, in which the hydrophobic portion of the molecule forms the nanoparticle matrix while the water soluble polyoxyethylene block forms a hydrophilic coating on the SLN increase the tumour accumulation and anticancer activity of drugs (Zara et al., 1999). The administered particles are cleared from the circulation by liver and spleen Because of the small size of SLN (below 1μm), these lipid nanoparticle formulations can be used for systemic body distribution with a minimal risk of blood clotting and aggregation, which can lead to embolism. SLN can also provide a sustained release of drug when administered intravenously. Drug encapsulated inside the lipid core can be released gradually on erosion (e.g. degradation by enzymes) or by diffusion from the particles (Wissing et al., 2004).

1.10. Use of SLN in various cancer therapies

Cancer is a condition where cells in a specific part of the body both grows and reproduces in an uncontrollable manner. The cancerous cells are known to invade and destroy surrounding healthy tissues, which includes organs as well. Apart from a few cancer types (e.g. breast cancer), for which hormonal therapy or immunotherapy is used, cytotoxic drugs are used as the major form of chemotherapy for cancer (Ewesuedo et al., 2003). Particulate drug carrier systems can great promise to improve the therapeutic effectiveness and safety profile of this conventional form of cancer chemotherapy (Wong et al., 2007). Because of the numerous advantages that SLN can offer, this relatively new drug carrier is considered be an emerging drug carrier system in the field of anticancer drug delivery.

A tumour is normally associated with a defective, leaky vascular architecture as a result of the poorly regulated nature of tumour angiogenesis. Moreover, the interstitial fluid within a tumour is usually inadequately drained by a poorly formed lymphatic system. Due to this phenomenon, submicron sized particulate matter may preferentially extravasate into the tumour and be retained there. This is often quoted as the "enhanced permeability and retention" EPR effect (Y. Matsumura & H. Maeda, 1986). This EPR effect can be taken advantage of by a properly designed nanoparticle system such as SLN to achieve passive tumour targeting. By doing this, the aforementioned poor tissue specificity problem can be partly solved. Furthermore, with the advances in surface-engineering technology, the biodistribution of SLN can be further manipulated by modifying the surface Physico-chemical properties of SLN to target them to the tissue of particular interest (Mehnert et al.,

2001). As a result of this, the chances of drugs reaching the tumour sites can be further enhanced and systemic drug toxicity can be reduced. Cytotoxic drug delivery systems such as polymeric nanoparticles and liposomes possess several problems in terms of physical stability, protection of labile drugs from degradation and controlled release. SLN tends not to demonstrate such disadvantages (Wissing et al., 2004). Delivery of drugs from active form to solid tumours can be difficult. It is known that most anticancer agents have a large volume if distribution upon i.e. administration and subsequently narrow therapeutic index due to a high level of toxicity in healthy tissues. Through the successful encapsulation of these drugs in a drug delivery system, such as SLN, the volume of distribution can be significantly reduced and the concentration of drug in the tumour site can be increased (Speth et al., 1988). SLN formulations of different anticancer agents have been shown to be less toxic than the free drug. Table 1.3 shows a list of anti-cancer drug encapsulated SLN. Although there is still a lack of clinical studies of the use of SLN for cancer treatment, preclinical studies using cell culture systems or animal models have so far been very promising (Pardeshi et al., 2012).

Table 1. 4. A summary of SLN formulations used for delivery of drugs with anticancer properties and the significant works based on these formulations (Wong et al., 2007).

Drug	Research Group	Focus of studies
Anticancer drugs		
Camptothecin	Yang 1	SLN preparation and characterisation.
	Yang 2	SLN characterisation , pharmacokinetics and biodistribution studies in mice.
Doxorubucin	Gasco	SLN preparation and characterisation.
	Serpe/Gasco	*In vitro* evaluation in colon cancer cell line.
	Wu 1	In drug-resistant breast cancer cell lines.
	Wu 2	*In vitro* evaluation of doxorubicin.
Etoposide	Murthy	SLN studies in tumour bearing mice.

Paclitaxel	Gasco	SLN preparation and characterisation.
	Lee	SLN preparation, *in vitro*, *in vivo* cytotoxicity.
	Muller	SLN preparation and characterisation.
	Zhang	*In vitro* evaluation in colon cancer cell line.
Retinoic Acid	Kim	SLN preparation and characterisation.
Verapamil	Wu	Verapamil SLN preparation and characterisation.

1.10.1. Breast cancer

Breast cancer is one of the most frequently occurring cancers in women and the second leading cause of cancer deaths in women. Among the major challenges in effective breast cancer chemotherapies are inadequate drug concentrations reaching the tumour, their rapid elimination, systemic toxicity and adverse effects. SLN has the potential to overcome current chemotherapeutic barriers in breast cancer treatment and to solve the problems associated with traditional chemotherapy and multidrug resistance (Bassiouni et al., 2012). Chemo-resistance or multidrug resistance can generally result from either of the two means firstly, by physically impairing delivery to the tumour (e.g., poor absorption, increased metabolism/excretion, and/or poor diffusion of drugs into the tumour mass); secondly, through intracellular mechanisms that raise the threshold for cell death. It is widely known that nanoparticles are beneficial tumour targeting vehicles due to their passive targeting properties by the enhanced permeability and retention (EPR) effect. Another added advantage in SLN drug delivery system is the development of proteins (transferrin) and commercial antibody conjugated SLN formulations for active targeting of breast cancer (Du et al., 2007).

1.10.2. Colorectal cancer

Colorectal cancer is considered to be the second leading cause of cancer-related deaths in United States, and also known to be the most common cancer in several other western countries. SLN have been proposed as a new approach of drug carrier for colorectal cancer.

SLN carrying cholesteryl butyrate, doxorubicin and paclitaxel had previously been developed (Nielsen et al., 1996).

1.10.3. Lung cancer

One of the leading causes of cancer related deaths worldwide is lung cancer. Adenocarcinoma, squamous cell carcinoma, and large-cell carcinoma, which together make up the majority of lung cancers, are referred to as ''non-small cell lung cancers'' (NSCLCs). Patients with early stage NSCLC are typically treated with surgery with a 5 year survival rate ranging from 25% to 80%. This survival rate also depends vastly on the stage of the disease (Bonomi, 1998). The causes of lung cancers are generally characterized by mutations in p53 gene (Sidransky et al., 1996). These mutations can lead to an exponential loss of tumour-suppressor function, increase drug resistance, loss of mutational repair, increase of angiogenesis, inhibition of cells and proliferation of apoptosis (Bennett et al., 1993). SLNs have gained increasing attention as a promising colloidal carrier system. As a substitution for viral delivery systems it was reported the use of p53 gene/cationic lipid complexes for the treatment of early endobronchial cancer (Zou et al., 1998).

1.10.4. Prostate cancer

Prostate cancer is known to be one of the most important cancer (Jo et al., 2008) in men, especially in the industrialized countries of the western world. According to several reports the incidence of prostate cancer has been increasing over the last decade. The reason behind this rapid increase of incidence is thought to be because of the heterogeneous and peculiar nature of individual cancers, and moreover the inability to target therapies to neoplastic cells (Sanna et al., 2014). The usage of SLN as a drug delivery system considered to be advantageous for inhibition of prostate cancer cells, such as LNCaP. One of the many advantages of using SLN is because of the usage of well tolerated compound's while making these nanoparticles, and moreover the avoidance of organic solvents, alongside good physical stability (Jesus et al., 2010). SLN have a great potential as a drug delivery system for prostate cancer cells since it is capable of enhanced accumulation in the target tissue through a passive targeting mechanism (*i.e.* enhanced permeability and retention effect, EPR), an increased accumulation and cell uptake through receptor-mediated endocytosis can be obtained if specific binding agents are attached on the surface of SLNs.

1.10.5. Brain tumour

The incidences of primary brain tumours in the United States have been estimated at approximately 43,800 per year (Mathur et al., 2011). SLN is considered to be one of the best nanoscale lipid based compound for brain tumour drug delivery. Although the exact mechanism by which these SLNs cross BBB (Blood Brain Barrier) is still unknown, internalization is hypothesized to be mediated by endocytosis of SLN's by endothelial cells. Endocytosis procedure is initiated by the successful absorption of circulating plasma proteins to the SLN surface (Nagayama et al., 2007). Drug loading and any sort of possible drug degradation can be altered by lipid matrix. Drug unloading within the tumour tissues can also be controlled. This control can be achieved by the respective surface coating of the SLN with tis constituent lipids (Wissing et al., 2004). Different studies suggested that nanoparticles with tween (surfactants) resulted in transport of drugs across the blood brain barrier (Kreuter, 2004). SLN have the potential to revolutionize both preoperative and intraoperative brain tumour detection.

1.11 Human Prostate Cancer Cells

Prostate cancer affects many men in the West but rarely occurs in Japan or China. Some epidemiological factors that may be important in this are described elsewhere in this volume. Prostate cancer has become the most common malignancy and the second highest cause of cancer death in Western society. The disease is very heterogeneous in terms of grade, genetics oncogene/tumor suppressor gene expression, and its biological, hormonal, and molecular characteristics are extremely complex. Growth of early prostate cancer requires 5α-dihydrotestosterone produced from testosterone by the 5α- reductase enzyme system; such prostate cells are described as androgen dependent (AD). Subsequently, the prostate cancer cells may respond to androgen but do not require it for growth; these cells are androgen sensitive (AS). Because of the requirement for androgen for growth of prostate cancer, patients whose tumors are not suitable for surgical intervention or radiotherapy may be treated by hormonal intervention, either continuous or intermittent, to prevent prostate cancer cell growth (Paul et al., 2000). This leads to periods of remission from disease, but almost invariably, the prostate cancer recurs, by which time the prostate cancer cells have become androgen-independent (AI) (Laufer et al., 2000). This may be accompanied by changes in the androgen receptor (AR), which may undergo mutation , amplification , or loss. Prostate cancer cells metastasize to various organs but particularly to local lymph nodes and to skeletal bone. Important antigens expressed by prostate cancer cells include prostate-specific

antigen (PSA), which has been used both for screening for prostate cancer and for management of patients with the disease (Polascik et al., 1999). Prostate-specific membrane antigen (PSMA) is produced in two forms that differ in the normal prostate, benign hyperplasia of the prostate, and prostate cancer (Su et al., 1995). Interactions between epithelial cells and stroma appear to be very important in allowing prostate cells to grow and form tumors, partly because of paracrine pathways that exist in this tissue (Russel et al., 1998). Prostate cancer rarely arises spontaneously in animals, and the human cancer cells are particularly difficult to grow in culture as long-term cell lines (Russell et al., 1998). Elsewhere in this book, methods for growing primary cultures of the prostate, for immortalizing prostate cells, and for isolating prostate stem cells are described. This chapter describes the commonly used prostate cancer cell lines, their preferred media for growth, and some of their important uses, including inoculation into mice to produce bony metastases.

1.12. Marketed products and current studies on SLN

Since early nineties, researchers turned their attention to lipid nanoparticles because of their nontoxicity and cost/effectiveness relationship (Muller et al., 1995). In spite of the advantages, formulating with lipid nanoparticles has been suffering some drawbacks. Because of the gastro intestinal tract (GIT) conditions, most of promising drugs do not reach clinical trials. The stability of particles must be comprehensively tested due to pH changes and ionic strength as well as the drug release upon enzymatic degradation (Mathur et al., 2010).. Lipid nanoparticles absorption through GIT occurs via transcellular (through M cells or enterocytes) or paracellular (diffusion between cells). If the major drug uptake occurs through M cells, the portal vein to the liver is bypassed, resulting in higher drug concentrations to the lymph rather than to plasma (Harms et al., 2011). Despite the low number of lipid nanoparticles formulations on the market for drug delivery, Mucosolvan retard capsules (Boehringer Ingelheim) is a story of success (Cegla et al., 1988). Mucosolvan retard capsules was the first generation. It was produced by highspeed stirring of a melted lipid phase in a hot surfactant solution obtaining an emulsion. This emulsion was then cooled down to room temperature obtaining the so-called "lipid nanopellets for oral administration" (Uner et al., 2007). Successful *in vivo* studies also include rifampicin, isoniazid, and pyrazinamide that are used in tuberculosis treatment. These drugs achieved higher bioavailability when incorporated into SLN compared to the free solutions. Rifampicin has poor cellular penetration which requires high doses to reach effective concentrations. Rifamsolin is a rifampicin-loaded SLN under preclinical phase by AlphaRx. The

methodology employed for production is acceptable by the regulatory agencies and has been addressed by various papers and patents (Wei et al 2010). Poor water-soluble drugs, as camptothecin, vinpocetine, and fenofibrate, can have their solubilization improved if incorporated into SLN (Mathur et al., 2010). Another example is insulin, commonly administered parenterally in the treatment of diabetes mellitus. Injections are often painful and must be administered daily, which result in low patient compliance (Harms et al, 2011). Unfortunately, oral administration of insulin, produced by solvent emulsification-evaporation method based on a w/o/w double emulsion, has limitations such as low bioavailability due to degradation in the stomach, inactivation and degradation by proteolytic enzymes, and low permeability across the intestinal epithelium because of lack of lipophilicity and high molecular weight (Harms et al., 2011). The main advantages of incorporate insulin into SLN would be the enhancement of transmucosal transport and protection from the degradation in the GIT.

1.13. Curcumin - an anticancer agent

Curcumin (diferuloymethane) is the chief component of the spice turmeric and it is known to be derived from the rhizome of the East Indian plant *Curcuma longa*. *Curcuma longa* is a member of the Zingiberacae (ginger) family of botanicals and is a perennial plant that is native to Southeast Asia (Ishita et al., 2004). As shown in Figure 1.5, turmeric contains a class of compounds known as the curcuminoids, comprised of curcumin, demethoxycurcumin and bisdemethoxycurcumin (Wilken et al., 2012). Curcumin is the principal curcuminoid and consists of approximately 2-5% of turmeric; it is responsible for the yellow colour of the spice as well as the majority of turmeric's therapeutic effects (Ishita et al., 2004). Curcumin has anti-inflammatory, antioxidant, anti-parasitic and anticancer properties (Guermonprez et al., 2002). It targets transcription factors, cytokines, cell adhesion molecules, surface receptors, growth factors and kinases (Lantz et al., 2005). Curcumin directly binds to a variety of surface and intracellular proteins causing direct cellular pathway inhibition or activation of secondary cellular responses (Kutluay et al., 2008).
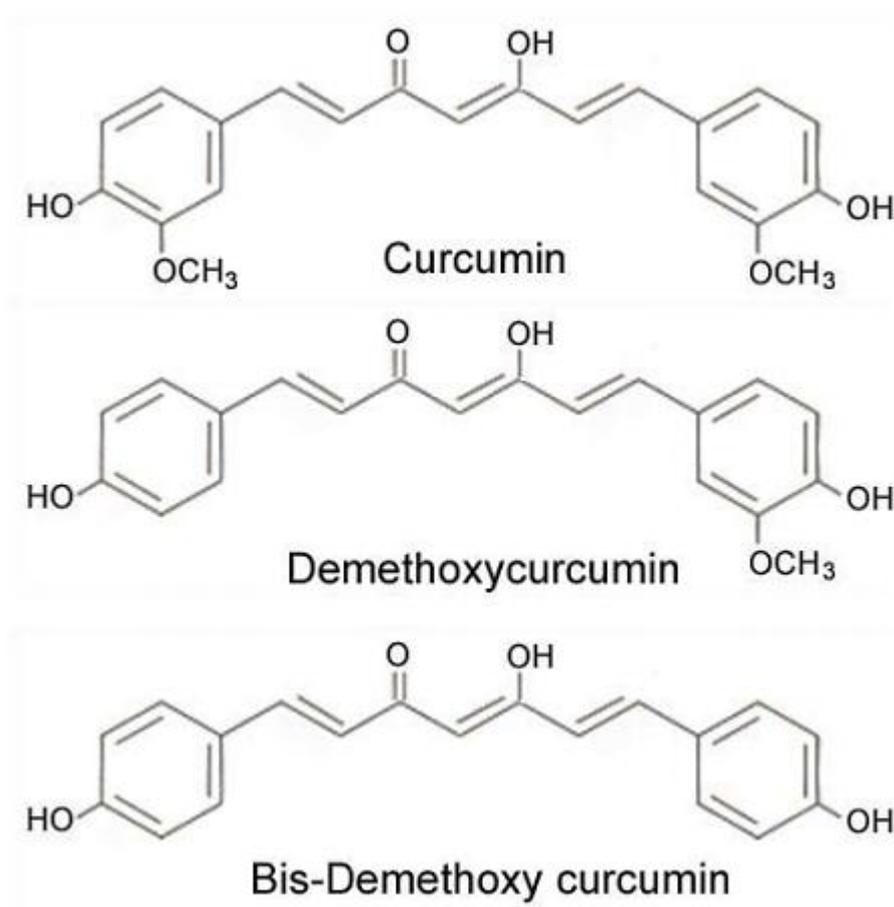
Figure 1. 5. Structure of the curcuminoids; curcumin, dethoxycurcumin and bisdemethoxycurcumin (Wilken et al., 2011)

1.13.1. Anti-cancer activity: suppression of carcinogenesis

The potency of curcumin has been evaluated in multiple human carcinomas, which includes; melanoma, head, neck, breast, colon, prostate and ovarian cancers (Schulze et al., 2004). The mechanisms of action followed by Curcumin in exerting its anti-cancer effects are comprehensive and diverse. Curcumin can efficiently target many levels of regulation in the processes of cellular growth and apoptosis (Wilken et al., 2011). Apart from the vertical effects of curcumin on various transcription factors, oncogenes and signalling proteins, curcumin has also the capabilities of acting at various temporal stages of carcinogenesis. These stages start from the initial stages leading to DNA mutations through the process of tumour genesis, growth and metastasis (Figure 1.6).

Cell Cycle Arrest

↑ p16   ↑ CDK inhibitors

↑ p53   ↓ Cyclin D1

↑ p14ARF ↓ Cyclin E

Other growth factors

↓ IL-6

↓ IL-8

Apoptosis

↑ p53   ↓ Bcl-2

↑ Bax   ↓ Bcl-xL

↑ Bad   ↓ NFκB

↑ Bim   ↓ pAKt

↓ mTOR

Curcumin

Angiogenesis & Metastasis

↓ COX-2

↓ MMP-9

↓ MMP-10

↓ VEGF

Iκ Kβ

↓

NFκB

↓

Increased Transcription of TNF-α, COX-2, MMp-9, IL-6, IL-8 and others

Autophagy

↑ Lysosomal proteases, phosphatases, lipases
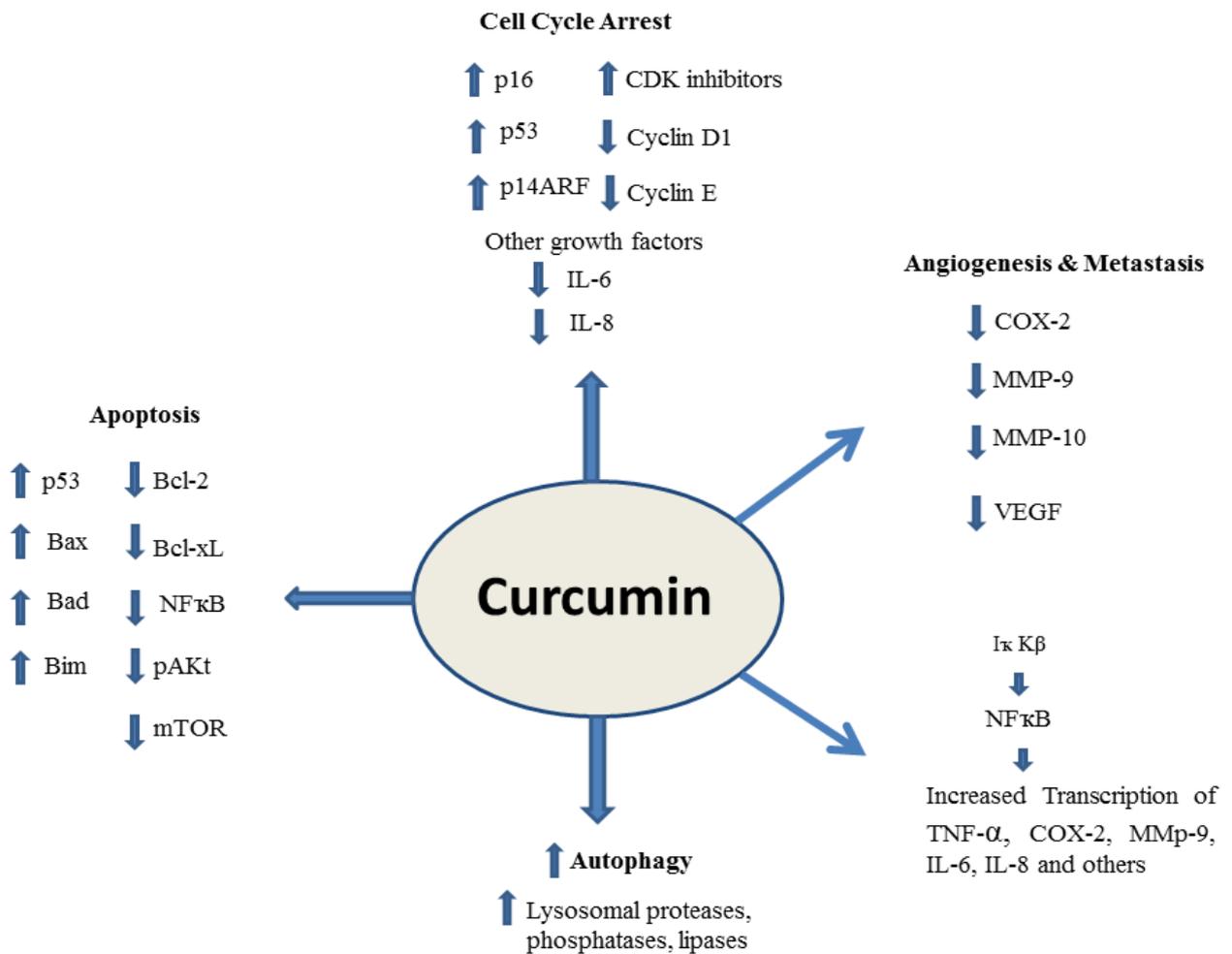
Figure 1. 6. Overview of the anticancer effects of curcumin (Wilken et al., 2011)

Curcumin suppresses the activation of NF-κB via inhibition of IκKB activity, leading to suppression of many NF-κB regulated genes involved in tumourigenesis including TNF, COX-2, cyclin D1, c-myc, MMP-9 and interleukins. Curcumin is involved in cell cycle control and stimulation of apoptosis via up regulation of p16 and p53. In addition, curcumin is a modulator of autophagy and has inhibitory effects on tumour angiogenesis and metastasis via suppression of a variety of growth factors including VEGF, COX-2, MMPs and ICAMs (Wilken et al., 2011)**.** Due to curcumin's potent anti-oxidant and free radical quenching properties it plays an important role in exerting the inhibitory effects on the initial stages of carcinogenesis. Studies reveal that curcumin has the ability of suppressing UV irradiation-induced DNA mutagenesis and cause an induction of the cellular functions (Oda, 1995). In addition to the inhibitory effects on the production of nitric oxide (NO) and the ability to scavenge DNA damaging superoxide radicals, curcumin also affects both the Phase I and Phase II enzymes of the hepatic cytochrome p450 enzyme system involved in the oxidation and detoxification of toxic substances. As curcumin has significant effects on cell growth

with tis multiple targeting capabilities, it possesses a lot of promise as a potential chemotherapeutic agent for many human cancers (Wilken et al., 2011).

1.14. Retinoic acid as an anticancer agent

Retinoids are natural and synthetic compounds of similar structure and the term retinoids refers to entire compounds including both naturally occur and synthetic retinol (vitamin A) metabolites and analogues. So far, three generations of retinoids have been developed. Retinoic acid (RA) is a physiologically active form of a metabolic product of vitamin A. It belongs to the first generation retinoids. It is a yellow or light orange crystalline powder with a molecular weight of 300.44. It is a poorly water insoluble substance while several experimental studies have shown the antiproliferative activity of RA in both *in vitro* and *in vivo* (Li et al., 2011). Many researchers have examined the ability of retinoids to treat various diseases such as acute promyelocytic leukaemia (APL), Kaposi's sarcoma, head and neck squamous cell carcinoma, ovarian carcinoma, bladder cancer, prostate cancer and neuroblastoma (Gacche et al., 2013). The mechanism of action of RA in chemoprevention and therapy of cancers involves modulation of cell proliferation and differentiation (Freemantle et al., 2003). Retinoids exert their effects by modulation of gene expression by two distinct classes of nuclear receptors: retinoic acid receptors (RAR α, β, γ) and rexinoid receptors (RXR α, β, γ). The receptors belong to the steroids or thyroid hormone super-family (Dutta et al., 2009). These nuclear RA receptors are the final mediators of RA action on gene expression that may lead to cell differentiation, inhibited growth and ultimately cell death (Li et al., 2011).

1.14.1 Mechanism of action of retinoic acid

Retinoic acid is the most potent form of a trophic factor vitamin A (retinol), and it has been proved effective to inhibit cancer cell survival or to induce apoptosis in a variety of cancers (Chen et al., 2012). In human body, vitamin A converts into RA (retinoic acid) through two oxidation steps. First the retinol is taken up from the blood and bound to CRBP (cellular retinol-binding protein) in the cytoplasm.
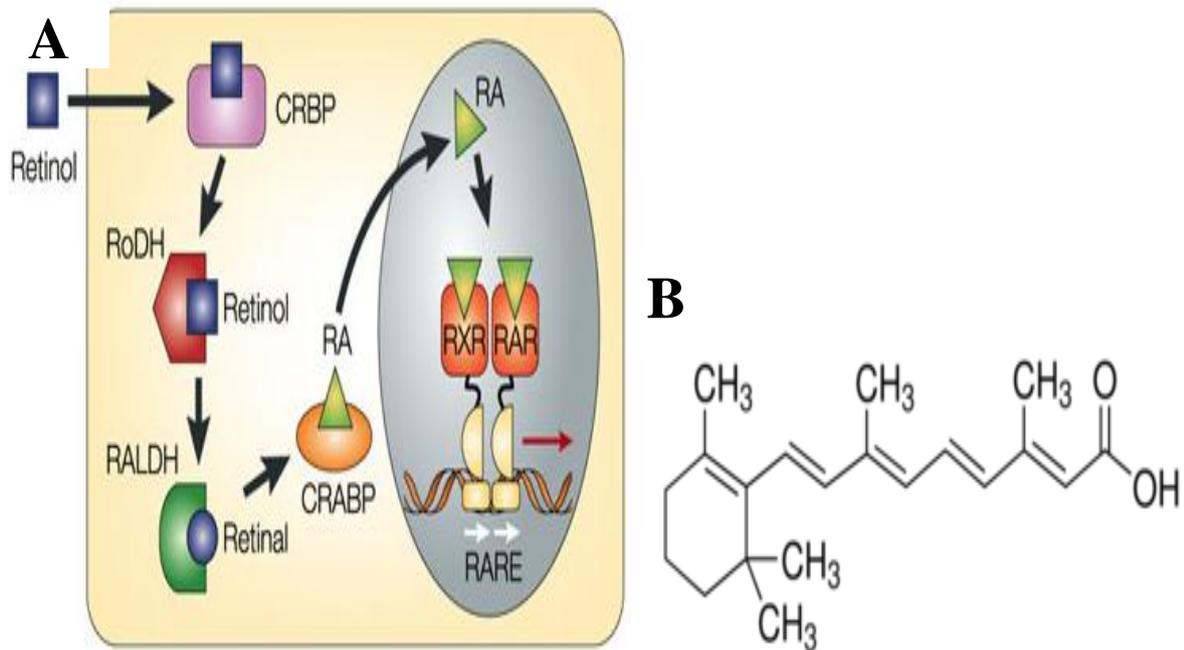
Figure 1. 7. A) The cellular mechanism of retinoic acid (RA) action, B) chemical structure of RA (Maden et al., 2002)

Afterwards the retinol dehydrogenase (RoDH) enzymes metabolize retinol to retinal, and then retinal is metabolized to RA by retinaldehyde dehydrogenases (RALDHs). RA is bound in the cytoplasm by CRABP (cellular RA-binding protein). RA enters the nucleus and binds to the RA receptors (RARs) and the retinoid X receptors (RXRs), which themselves heterodimerize and bind to a sequence of DNA known as the RARE (RA-response element). This activates transcription of the target gene (Maden et al., 2002). RAR-RXR heterodimers activated by RA regulates the transcription of the target gene and control various physiological functions such as, vision, immune function, cell proliferation, and differentiation (Chen et al., 2012).

1.15. Key Objectives of research

The current investigations were designed with the aim of developing anti-cancer drug encapsulated solid lipid nanoparticles, which are capable of enhancing the bioavailability of the drug. Here are the main aims and objectives of my research that were considered to be an integral part while conducting several studies.

Objective 1: Successful utilization of the hot homogenization method for the formulation of curcumin and retinoic acid loaded solid lipid nanoparticles and evaluate these formulations physico-chemically using parameters such as, size, zeta potential and entrapment efficiency, and techniques including transmission electron microscopy, differential scanning calorimetry and *in vitro* release studies.

Objective 2: Perform *in vitro* cytotoxicity studies using microplate analysis and apoptosis investigations using flow cytometry techniques to evaluate the potency of anti-cancer drug encapsulated SLNs. Fluorescent activated cell sorting analysis and fluorescent microscope for the confirmation of cellular uptake of curcumin and retinoic acid loaded solid lipid nanoparticles.

Objective 3: Preparation of curcumin loaded nanostructured lipid carriers (NLC) by using the hot homogenization method. Characterize the NLCs with respect to size, zeta potential and scanning electron microscopy. Further evaluation of NLC in terms of their cytotoxicity towards LNCaP prostate cancer cells both *in vitro* and *in vivo*.

Objective 4: Develop both transferrin conjugated and unconjugated solid lipid nanoparticles loaded with curcumin, with the conjugated SLN in order to test their anti-cancer properties on LNCaP prostate cancer cells, both *in vitro* and *in vivo*.

1.13. References

1. Aggarwal, B. B., & Harikumar, K. B. (2009). Potential therapeutic effects of curcumin, the anti-inflammatory agent, against neurodegenerative, cardiovascular, pulmonary, metabolic, autoimmune and neoplastic diseases. *The international journal of biochemistry & cell biology*, *41*(1), 40-59.

2. Ahlin, P., Kristl, J., & Smid-Korbar, J. (1998). Optimization of procedure parameters and physical stability of solid lipid nanoparticles in dispersions. *Acta pharmaceutica*, *48*(4), 259-267.

3. Almeida, A. J., & Souto, E. (2007). Solid lipid nanoparticles as a drug delivery system for peptides and proteins. *Advanced drug delivery reviews*, *59*(6), 478-490.

4. An overview of the zeta potential. (2012). Retrieved January 2014, from Particle sciences,drug development services: http://www.particlesciences.com/news/technical-briefs/2012/overview-of-zeta-potential.html

5. Bassiouni, Y., & Faddah, L. (2012). Nanocarrier-Based Drugs: The Future Promise for Treatment of Breast Cancer. *Journal of applied pharmaceutical science*, *2*(05), 225-232.

6. Bennett, W. P., Colby, T. V., Travis, W. D., Borkowski, A., Jones, R. T., Lane, D. P.. & Harris, C. C. (1993). p53 protein accumulates frequently in early bronchial neoplasia. *Cancer research*, *53*(20), 4817-4822.

7. Bonomi, P. (1998, August). Review of selected randomized trials in small cell lung cancer. In *Seminars in oncology* (Vol. 25, No. 4 Suppl 9, pp. 70-78).Bonomi P. (1998). Review of selected randomized trials in small cell lung cancer. *Oncology,4(9) 70-78.*

8. Cavalli, R., Gasco, M. R., Chetoni, P., Burgalassi, S., & Saettone, M. F. (2002). Solid lipid nanoparticles (SLN) as ocular delivery system for tobramycin. *International journal of pharmaceutics*, *238*(1), 241-245.

9. Cegla, U. H. (1988). [Long-term therapy over 2 years with ambroxol (Mucosolvan) retard capsules in patients with chronic bronchitis. Results of a double-blind study of 180 patients]. *Praxis und klinik der pneumologie,* 42(9), 715-721.

10. Chattopadhyay, I., Biswas, K., Bandyopadhyay, U., & Banerjee, R. K. (2004). Turmeric and curcumin: Biological actions and medicinal applications. *Current science*, *87*(1), 44-53.

11. Chaturvedi, S. P., & Mishra, A (2012). Production technique of lipid nanoparticles. *Research jJournal of pharmaceutical, biological and chemical sciences,* 3(3), 525-541.

12. Chen, M. C., Huang, C. Y., Hsu, S. L., Lin, E., Ku, C. T., Lin, H., & Chen, C. M. (2012). Retinoic acid induces apoptosis of prostate cancer DU145 cells through Cdk5 overactivation. *Evidence-based complementary and alternative medicine*, *2012*.

13. Chimmiri, P., Rajalakshmi, R., Mahitha, B., Ramesh, G., & Noor Ahmed, V. H. (2012). Solid lipid nanoparticles: a novel carrier for cancer therapy. *Int Journal of biological pharmaceutical research, 3*(3), 405-413.

14. Contri, R. V., Fiel, L. A., Pohlmann, A. R., Guterres, S. S., & Beck, R. C. (2011). Transport of substances and nanoparticles across the skin and *in vitro* models to evaluate skin permeation and/or penetration. *Nanocosmetics and nanomedicines*, 2(3), 71-83.

15. Du, W., Hong, L., Yao, T., Yang, X., He, Q., Yang, B., & Hu, Y. (2007). Synthesis and evaluation of water-soluble docetaxel prodrugs-docetaxel esters of malic acid. *Bioorganic & medicinal chemistry*, *15*(18), 6323-6330.

16. Dutta, A., Sen, T., Banerji, A., Das, S., & Chatterjee, A. (2009). Studies on multifunctional effect of all-trans retinoic acid (ATRA) on matrix metalloproteinase-2 (MMP-2) and its regulatory molecules in human breast cancer cells (MCF-7). *Journal of oncology*, 12(19), 88-95*2009*.

17. Ekambaram, P., Sathali, A.A.H & Priyanka, K. (2011). Solid lipid nanoparticles: A review. *Scientific reviews and chemical communications*, 2(1), 80-102.

18. Eldem, T.,Speise, P, Hincal, A. (1991) Optimization of spray-dried and congealed lipid microparticles and characterization of their surface morphology by scanning electron microscopy. *Pharmaveutical research, .* 8(3), 47-54.

19. Ewesuedo, R. B., & Ratain, M. J. (2003). Principles of cancer chemotherapy. *In Oncologic Therapies* (pp. 19-66). Springer Berlin Heidelberg.

20. Freemantle, S. J., Spinella, M. J., & Dmitrovsky, E. (2003). Retinoids in cancer therapy and chemoprevention: promise meets resistance. *Oncogene*, *22*(47), 7305-7315.

21. Freitas, C., & Muller, R. H. (1998). Spray-drying of solid lipid nanoparticles (SLN TM). *European Journal of Pharmaceutics and Biopharmaceutics*, *46*(2), 145-151.

22. Gacche, R. N., & Meshram, R. J. (2013). Targeting tumour micro-environment for design and development of novel anti-angiogenic agents arresting tumour growth. *Progress in biophysics and molecular biology*, *113*(2), 333-354.

23. Guermonprez, P., Valladeau, J., Zitvogel, L., Théry, C., & Amigorena, S. (2002). Antigen presentation and T cell stimulation by dendritic cells. *Annual review of immunology*, *20*(1), 621-667.

24. Harms, M., & Müller-Goymann, C. C. (2011). Solid lipid nanoparticles for drug delivery. *Journal of drug delivery science and technology,* 21(1), 89-99.

25. Harris, A. L., & Hochhauser, D. (1992). Mechanisms of multidrug resistance in cancer treatment. *Acta Oncologica*, *31*(2), 205-213.

26. Huss, W. J., Lai, L., Barrios, R. J., Hirschi, K. K., & Greenberg, N. M. (2004). Retinoic acid slows progression and promotes apoptosis of spontaneous prostate cancer. *The prostate*, *61*(2), 142-152.

27. Kreuter, J. (2004). Influence of the surface properties on nanoparticle-mediated transport of drugs to the brain. *Journal of nanoscience and nanotechnology*,*4*(5), 484-488.

28. Kutluay, S. B., Doroghazi, J., Roemer, M. E., & Triezenberg, S. J. (2008). Curcumin inhibits herpes simplex virus immediate-early gene expression by a mechanism

independent of p300/CBP histone acetyltransferase activity.*Virology*, *373*(2), 239-247.

29. Lantz, R. C., Chen, G. J., Solyom, A. M., Jolad, S. D., & Timmermann, B. N. (2005). The effect of turmeric extracts on inflammatory mediator production.*Phytomedicine*, *12*(6), 445-452.

30. Li, R. J., Ying, X., Zhang, Y., Ju, R. J., Wang, X. X., Yao, H. J., & Lu, W. L. (2011). All-trans retinoic acid stealth liposomes prevent the relapse of breast cancer arising from the cancer stem cells. *Journal of controlled release*,*149*(3), 281-291.

31. Lim, S. J., Lee, M. K., & Kim, C. K. (2004). Altered chemical and biological activities of all-trans retinoic acid incorporated in solid lipid nanoparticle powders. *Journal of controlled release*, *100*(1), 53-61.

32. Maden, M. (2002). Retinoid signalling in the development of the central nervous system. *Nature reviews neuroscience*, *3*(11), 843-853.

33. Maden, M. (2007). Retinoic acid in the development, regeneration and maintenance of the nervous system. *Nature reviews neuroscience*, *8*(10), 755-765.

34. Mathur, V., Satrawala, Y., Rajput, M. S., Kumar, P., Shrivastava, P., & Vishvkarma, A. (2011). Solid lipid nanoparticles in cancer therapy. *International journal of drug delivery*, *2*(3), 212-223..

35. Mathur, V., Satrawala, Y., Rajput, M. S., Kumar, P., Shrivastava, P., & Vishvkarma, A. (2010). Solid lipid nanoparticles in cancer therapy .*International journal of drug delivery,* 2(3).

36. McCormick, D. L., Rao, K. V. N., Steele, V. E., Lubet, R. A., Kelloff, G. J., & Bosland, M. C. (1999). Chemoprevention of rat prostate carcinogenesis by 9-cis-retinoic acid. *Cancer research*, *59*(3), 521-524.

37. Mehnert, W., & Mäder, K. (2001). Solid lipid nanoparticles: production, characterization and applications. *Advanced drug delivery reviews*, *47*(2), 165-196.

38. Moghimi, S. M., & Szebeni, J. (2003). Stealth liposomes and long circulating nanoparticles: critical issues in pharmacokinetics, opsonization and protein-binding properties. *Progress in lipid research*, *42*(6), 463-478.

39. Mueller, R. H., MaÈder, K., & Gohla, S. (2000). Solid lipid nanoparticles (SLN) for controlled drug delivery–a review of the state of the art. *European journal of pharmaceutics and biopharmaceutics*, *50*(1), 161-177.

40. Mukherjee, S., Ray,S. & Thakur R.S. (2009). Solid lipid nanoparticles : Modern formulation in drug delivery system. *Indian journal ofJ pPharmaceutical sSciences* ,2009; 71(4), 349-358.

41. Muller, R. H., Mader, K., & Gohla, S. (2000). Solid lipid nanoparticles (SLN) for controlled drug delivery-a review of the state of the art. *European journal of pharmaceutics and biopharmaceutics*, *50*(1), 161-177.

42. Nagayama, S., Ogawara, K. I., Fukuoka, Y., Higaki, K., & Kimura, T. (2007). Time-dependent changes in opsonin amount associated on nanoparticles alter their hepatic uptake characteristics. *International journal of pharmaceutics*,*342*(1), 215-221.

43. Nielsen, D., Maare, C., & Skovsgaard, T. (1996). Cellular resistance to anthracyclines. *General Pharmacology: The vascular system*, *27*(2), 251-255.

44. Oda, Y. (1995). Inhibitory effect of curcumin on SOS functions induced by UV irradiation. *Mutation research letters*, *348*(2), 67-73.

45. Ohshima, H., Miyagishima, A., Kurita, T., Makino, Y., Iwao, Y., Sonobe, T., & Itai, S. (2009). Freeze-dried nifedipine-lipid nanoparticles with long-term nano-dispersion stability after reconstitution. *International journal of pharmaceutics*,*377*(1), 180-184.

46. Padhye, S. G., & Nagarsenker, M. S. (2013). Simvastatin solid lipid nanoparticles for oral delivery: Formulation development and *In vivo* evaluation. *Indian journal of pharmaceutical sciences*, *75*(5), 591.

47. Pardeike, J., Hommoss, A., & Müller, R. H. (2009). Lipid nanoparticles (SLN, NLC) in cosmetic and pharmaceutical dermal products. *International journal of pharmaceutics*, *366*(1), 170-184.

48. Pardeshi, C., Rajput, P., Belgamwar, V., Tekade, A., Patil, G., Chaudhary, K., & Sonje, A. (2012). Solid lipid based nanocarriers: An overview/Nanonosači na bazi čvrstih lipida: Pregled. *Acta pharmaceutica*, *62*(4), 433-472.

49. Paul, R. and Breul, J. (2000) Antiandrogen withdrawal syndrome associated with prostate cancer therapies: Incidence and clinical significance. *Drug safety,* 2(3), 381–390.

50. Pinto, J. F., & Muller, R. H. (1999). Pellets as carriers of solid lipid nanoparticles (SLN) for oral administration of drugs. *Pharmazie*, *54*(7), 506-509.

51. Polascik, T. J., Oesterling, J. E., and Partin, A. W. (1999) Prostate specific antigen: A decade of discovery—what have we learned and where are we going. *Journal of urology,* 162(11), 293–306.

52. Ponchel, G., Montisci, M. J., Dembri, A., Durrer, C., & Duchêne, D. (1997). Mucoadhesion of colloidal particulate systems in the gastro-intestinal tract. *European journal of pharmaceutics and biopharmaceutics*, *44*(1), 25-31.

53. Porter, M. R. Handbook of surfactants. 1994.

54. Potta, S. G., Minemi, S., Nukala, R. K., Peinado, C., Lamprou, D. A., Urquhart, A., & Douroumis, D. (2010). Development of solid lipid nanoparticles for enhanced solubility of poorly soluble drugs. *Journal of biomedical nanotechnology*, *6*(6), 634-640.

55. Roy Choudhury, S., Karmakar, S., Banik, N. L., & Ray, S. K. (2011). Targeting angiogenesis for controlling neuroblastoma. *Journal of oncology*, 22(31), 312-323.*2012*.

56. Russell, P. J., Bennett, S., and Stricker, P. (1998) Growth factor involvement in progression of prostate cancer. *Clinical Chemotherapy,* 44(11), 705–723

57. Sanna, V., Lubinu, G., Madau, P., Pala, N., Nurra, S., Mariani, A., & Sechi, M. (2015). Polymeric Nanoparticles Encapsulating White Tea Extract for Nutraceutical Application. *Journal of agricultural and food chemistry*, *63*(7), 2026-2032.

58. Schmidt, B. M., Ribnicky, D. M., Lipsky, P. E., & Raskin, I. (2007). Revisiting the ancient concept of botanical therapeutics. *Nature chemical biology*, *3*(7), 360-366.Schmidt, B.M., Ribnicky, D.M., Lipsky, P.E. & Raskin, I. (2007) Revisiting the ancient concept of botanical therapeutics, *Nature chemical biology 3*(7): 360–366.

59. Schulze-Tanzil G, Mobasheri A, Sendzik J, John T, Shakibaei M (2004). Effects of curcumin (diferuloylmethane) on nuclear factor kappaB signaling in interleukin-1beta-stimulated chondrocytes. *Annals of the new york academy of sciences*, *1030*(1), 578-586.

60. Serpe, L., Catalano, M. G., Cavalli, R., Ugazio, E., Bosco, O., Canaparo, R., ... & Zara, G. P. (2004). Cytotoxicity of anticancer drugs incorporated in solid lipid nanoparticles on HT-29 colorectal cancer cell line. *European journal of pharmaceutics and biopharmaceutics*, *58*(3), 673-680.

61. Sidransky, MD, D., & Hollstein, Ph. D, M. (1996). Clinical implications of the p53 gene. *Annual review of medicine*, *47*(1), 285-301.Sidransky, MD, D., & Hollstein, Ph. D, M. (1996). Clinical implications of the p53 gene. *Annual review of medicine*, *47*(1), 285-301.

62. Siekmann, B., & Westesen, K. (1992). Submicron-sized parenteral carrier systems based on solid lipids. *Pharmcopia. pharmacological letters, . Lett*, *1*(3), 123-126.

63. Siekmann, B., & Westesen, K. (1994). Melt-homogenized solid lipid nanoparticles stabilized by the nonionic surfactant tyloxapol. I. Preparation and particle size determination. *Pharmcopia pharmacological letters*, 1(*3)*, 123-12694-197.

64. Souto, E. B., & Muller, R. H. (2007). Lipid nanoparticles (solid lipid nanoparticles and nanostructured lipid carriers) for cosmetic, dermal, and transdermal applications. *Drugs and the pharmaceutical sciences*, 166, 213.

65. Speth, P. A. J., Van Hoesel, Q. G. C. M., & Haanen, C. (1988). Clinical pharmacokinetics of doxorubicin. *Clinical pharmacokinetics*, *15*(1), 15-31.

66. Su, S. L., Huang, I. P., Fair, W. R., Powell, C. T., and Heston, W. D. W. (1995) Alternatively spliced variants of prostate-specific membrane antigen RNA: Ratio of expression as a potential measurement of progression. *Cancer research,* 55(2), 1441–1443

67. Subedi, R. K., Kang, K. W., & Choi, H. K. (2009). Preparation and characterization of solid lipid nanoparticles loaded with doxorubicin. *European journal of pharmaceutical sciences*, *37*(3), 508-513.

68. Trotta, M., Debernardi, F., & Caputo, O. (2003). Preparation of solid lipid nanoparticles by a solvent emulsification–diffusion technique. *International journal of pharmaceutics*, *257*(1), 153-160.

69. Üner, M., & Yener, G. (2007). Importance of solid lipid nanoparticles (SLN) in various administration routes and future perspectives. *International journal of nanomedicine*, *2*(3), 289.

70. Üner, M., & Yener, G. (2007). Importance of solid lipid nanoparticles (SLN) in various administration routes and future perspectives. *International journal of nanomedicine*, 2(3), 289.

71. Van Engeland, M., Nieland, L. J., Ramaekers, F. C., Schutte, B., & Reutelingsperger, C. P. (1998). Annexin V-affinity assay: a review on an apoptosis detection system based on phosphatidylserine exposure. *Cytometry*,*31*(1), 1-9.

72. Wei, W., Shi, S. J., Liu, J., Sun, X., Ren, K., Zhao, D., ... & Gong, T. (2010). Lipid nanoparticles loaded with 10-hydroxycamptothecin–phospholipid complex developed for the treatment of hepatoma in clinical application. *Journal of drug targeting*, 18(7), 557-566.

73. Weiss, J., Decker, E. A., McClements, D. J., Kristbergsson, K., Helgason, T., & Awad, T. (2008). Solid lipid nanoparticles as delivery systems for bioactive food components. *Food biophysics*, *3*(2), 146-154.

74. Wilken, R., Veena, M. S., Wang, M. B., & Srivatsan, E. S. (2011). Curcumin: A review of anti-cancer properties and therapeutic activity in head and neck squamous cell carcinoma. *Molecular cancer biology Cancer*, *10*(12), 1-19.

75. Wissing, S. A., Kayser, O., & Muller, R. H. (2004). Solid lipid nanoparticles for parenteral drug delivery. *Advanced drug delivery reviews*, *56*(9), 1257-1272.

76. Wissing, S. A., Kayser, O., & Müller, R. H. (2004). Solid lipid nanoparticles for parenteral drug delivery. *Advanced drug delivery reviews*, *56*(9), 1257-1272.

77. Wong, H. L., Bendayan, R., Rauth, A. M., Li, Y., & Wu, X. Y. (2007). Chemotherapy with anticancer drugs encapsulated in solid lipid nanoparticles.*Advanced drug delivery reviews*, *59*(6), 491-504.

78. Wong, H. L., Bendayan, R., Rauth, A. M., Li, Y., & Wu, X. Y. (2007). Chemotherapy with anticancer drugs encapsulated in solid lipid nanoparticles. *Advanced drug delivery reviews*, *59*(6), 491-504.

79. Xie, S., Zhu, L., Dong, Z., Wang, X., Wang, Y., Li, X., & Zhou, W. (2011). Preparation, characterization and pharmacokinetics of enrofloxacin-loaded solid lipid nanoparticles: influences of fatty acids. *Colloids and surfaces biointerfaces*, *83*(2), 382-387.

80. Yadav, N. E. H. A., Khatak, S. U. N. I. L., & Sara, U. V. (2013). Solid lipid nanoparticles: a review. *International Journal of pharmaceutics*, *5*(2), 8-18.

81. Zara, G. P., Cavalli, R., Fundaro, A., Bargoni, A., Caputo, O., & Gasco, M. R. (1999). Pharmacokinetics of doxorubicin incorporated in solid lipid nanospheres (SLN). *Pharmacological research*, *40*(3), 281-286.

82. Zou, Y., Zong, G., Ling, Y. H., Hao, M. M., Lozano, G., Hong, W. K., & Perez-Soler, R. (1998). Effective treatment of early endobronchial cancer with regional administration of liposome-p53 complexes. *Journal of the national cancer institute*, *90*(15), 1130-1137.

CHAPTER 2: PREPARATION AND CHARACTERIZATION OF CURCUMIN ENCAPSULATED SLN FORMULATIONS

2.1 Introduction

Curcumin (CRC) is known to be the principal active component extracted from rhizomes of turmeric and is also vastly used in China and India as a traditional herb. It possesses several pharmacological activities, including anti-oxidant, anti-inflammatory, anti-cancer and anti-depressant properties. Alongside all these pharmacological effects CRC is also known to enhance wound healing (Giri et al., 2009). Over the past few years the usage of CRC as a promising new natural chemical for chemoprevention has been studied extensively. These studies reveal that CRC acts on multiple molecular targets to selectively kill tumour cells with low intrinsic toxicity (Ravindran et al., 2009). Curcumin has been reported to be both a potent inhibitor of nuclear factor-kappa B (NF-kappa B) and to reverse multidrug resistance by down regulating P-glycoprotein expression in resistant cells (Park et al., 2008) and it has been also administered in combination with other chemotherapeutic agents, such as paclitexal, doxorubicin and cisplatin, to achieve synergistic anti-tumour effects in many resistant cell lines. Even though CRC does possess promising anti-tumour activities, its poor solubility and stability in aqueous systems alongside its rapid metabolism has drastically limited its clinical application (Anand et al., 2007). In order to eradicate these limitations several CRC delivery carriers have been investigated including cyclodextrin complexation, solid dispersion, liposomes, phospholipid complexes and polymeric nanoparticles (Sun et al., 2013). Each of these drug delivery systems presents various drawbacks such as poor physical stability, drug leakage and the potential toxicity of the excipients. Solid lipid nanoparticles (SLN) are considered to be a relatively novel type of colloidal drug delivery system that successfully combines the merits of liposomes and polymeric nanoparticles. As a result SLNs has the ability to provide both stability of the solid matrix and also biological compatibility of lipid carriers avoiding the limitations related to liposomes and polymeric nanoparticles. The drawbacks of liposomes and polymeric nanoparticles that SLN avoids are the undesired stability problems and toxicity of the bulk (Sun et al., 2013). According to Mehnert et al., (2001) SLNs have been reported to increase the bioavailability of incorporated drugs, alongside its easy scale up and high biocompatible characteristics. However, even with all these advantages the physicochemical characteristics of the SLN must be taken into account

(Mehnert et al., 2001). The coexistence of other colloidal structures and the interaction of the drug and lipid matrix are of particular interest. So, a broad spectrum of analytical techniques is needed to acquire information about the previously mentioned properties. In these studies many SLN formulations that were prepared via hot homogenization and incorporated with a hydrophobic anticancer drug (CRC) are subjected to detailed physicochemical characterization. The melting behaviours were investigated by DSC. The shape of SLN was revealed by SEM. Particle size analysis, charge determination, X-ray diffraction (XRD) of freeze dried SLNs were also carried out. Moreover the drug release profiles and the determination of encapsulation efficiency were also conducted.

2.2 Materials

Curcumin was purchased from Sigma-Aldrich (Dorset, UK). Stearic acid (SA), Tristearin (TS) and Trilaurin (TL) were purchased from Sigma-Aldrich. Precirol® ATO 5 (PR) was purchased from Gattefosse. Poloxamer 188 was kindly donated by BASF (Ludwigshafen, Germany). All the other chemicals and solvents were of analytical and high-performance liquid chromatography (HPLC) grade.

2.3 Methods

2.3.1 Preparation of SLN

SLN is prepared by high pressure homogenization. The lipid phase, consisting of stearic acid/precirol/tristearin/trilaurin was coarsely emulsified in water phase by a high speed dispersion device. The pre-emulsion was then further processed with a high pressure homogenizer (Micro DeBee, South Easton, USA).

In brief, appropriate amounts of the lipid, poloxamer 188 (table 2.1) were weighed accurately and heated above the melting point of the lipid. For CRC loaded SLN the drug was separately dissolved in ethanol (3ml) and then added in the molten lipid. The drug containing melt lipid was dispersed in a hot aqueous phase and homogenized with an Ultra-Turrax T25 (IKA®-WERKE GMBH, Staufen, Germany) homogenizer to form a pre-emulsion. The produced coarse dispersion was then transferred and homogenized in a Micro DeBee (South Easton, MA, USA) high pressure homogenizer at 15,000 PSI for 7 minutes at 70°C. The hot nano-dispersions were left to cool down and allow lipid to crystallize by forming lipid nanoparticles with a solid matrix. The SLN formulations used in this study are depicted in Table 2.1

2.3.2 Particle size analysis and zeta potential

The particle size distribution and zeta potential of the produced preparations were determined by dynamic light scattering photon correlation spectroscopy (PCS) using a Malvern Zetasizer Nano-ZS (Malvern, UK). The dispersion were adequately diluted with distilled water and measured in triplicate. The z-average and the PDI were applied for the evaluation of the particle size. The determined particle size range is 0.6 nm-6 μm.

2.3.3 Lyophilisation of SLN

The empty and CRC loaded SLN dispersions were freeze dried without the addition of cryo-protectants using an Advantage freeze dryer (Biopharm Process Systems, UK). The lyophilisation process was carried out by cooling the samples from 20ºC to -50ºC at 0.5ºC/min under atmospheric pressure and samples were held at -50ºC for 2 hours. After 2 hours the pressure was reduced to 30 mTor and the sample plates were heated to -10ºC and the samples were dried under this condition for 48 hours. Afterwards the plate was slowly heated at 0.2ºC/min to 20ºC and the pressure is reduced to 10 mTor for 2 hours to remove residue water

2.3.4 X-ray powder diffraction

Samples of pure and loaded curcumin, including empty SLN formulations were evaluated using Bruker D8 Advance (Coventry, UK) in theta-theta mode, Cu anode at 40 kV and 40 mA, parallel beam Goebel mirroe, 0.2 mm exit slit, Lynxeye position sensitive detector (PSD) with a 3° opening and LynxIris at 6.5 mm, sample rotation at 15 rpm. The sample was scanned from 5° to 45° 2θ with a step size of 0.02° 2θ and a counting time of 0.2s per step; 176 channels active on the PSD making a total counting time of 35.2 s per step.

2.3.5 Differential scanning calorimetry

Differential scanning calorimetry (DSC) measurements of pure and loaded curcumin, including empty SLN formulations were carried out on a Mettler Toledo DSC 823 apparatus (Schwerzenbach, Switzerland). Approximately, 3-5 mg samples were accurately weighed on standard aluminium pans. An empty pan was used as a reference. A scan rate of 10 °C/min was employed to heat up the samples from 20 up to 220 °C. Analysis was performed under a nitrogen purge (60mL/min). Calorimetric parameters were analysed using STARe Software.

2.3.6 Determination of encapsulation efficiency

The amount of CRC in the nanoparticles was determined spectrophotometrically at λmax of 425nm. A calibration curve was established by using UV–vis spectrophotometer and the calibration curve showed good linearity (with R^2 value of 0.991) of concentrations ranging from $1 - 20\mu g/ml$. The process followed was similar to the one carried out by D. Douroumis et al (2011). In brief, 1 ml of SLN nanosuspension was centrifuged at 40,000 rpm, for 30 min at 25 °C. The pellets of CRC loaded SLN was then dissolved in Acetonitrile and the absorbance of the dissolved pellet were measured after appropriate dilutions. Amount of drug in the pellet gave a direct measure of the extent of drug entrapped.

The DL and encapsulation efficiency (EE%) were calculated by using Equations (1) and (2).

$$\text{Drug loading} \quad = \quad \frac{Amount\ of\ curcumin\ in\ SLNs}{Amount\ of\ SLNs}\ x\ 100 \quad \text{……………..} (1)$$

$$\text{Entrapment efficiency} = \quad \frac{Drug\ loading}{Theoretical\ drug\ loading}\ x\ 100 \quad \text{……………..} (2)$$

2.3.7 Drug release properties of CRC-SLN

1ml of SLN formulation was transferred into a cellulose dialysis bag (molecular weight cut-off: 10,000), which was then suspended in a beaker containing a mixture of double-distilled water and ethanol (50:50, v/v) as the dissolution medium. (Yang et al., 2007) The beaker was then placed in a shaker bath with a set temperature of 37°C. At various time intervals, the whole content of the beaker was emptied and replaced with another 20ml of dissolution medium. Drug content was analysed using UV at λmax of 425nm.

2.4 Results and discussion

2.4.1 Particle size distribution and zeta potential

The development of SLN formulations was initially assessed by preparing various blank SLN formulations of different lipids and surfactants. The percentage of the lipids and the surfactant was kept at 500mg and 250mg respectively, while the water phase remained at 30ml. The lipid and surfactant amount was fixed at 500mg and 250 mg after a series of method development, where if the lipid or surfactant amount was altered above the mentioned amount resulted in rapid flocculation. These flocculated dispersions were not suitable for either particle size or zeta potential experiments. A possible reason behind that can be because, an increasing amount of lipid can increase particle size and also the

possibilities of dispersion instability increases at the same time too due to Oswald ripening. Surfactant amount however, was kept below the lipid amount to avoid SLN particle surface deformation (Freitas et al., 1999). The lipids used for preparing SLN dispersions were tristearin, stearic acid, precirol and trilaurin, while the surfactant used was poloxamer 188. The particle size and zeta potential of both blank SLN and CRC loaded SLNs were measured immediately after the preparation process where the optimized formulations showed narrow and monomodal particle size distribution. The particle size of blank SLN formulations remained at the range of 140-150 nm. The zeta potential of empty formulations varied from 13-19 mV while the polydispersity index was kept less than 0.2 for all formulations. Curcumin loaded SLNs were prepared successfully by the high pressure homogenization technique at temperatures above 75°C. Interestingly, tristearin and stearic acid based SLNs exhibited monomodal size distribution while trilaurin and Precirol showed bimodal size distribution. In case of precirol's approximately 70% of particles were around 280nm and another 30% showing a particle size of 1108nm. Similar results were obtained for trilaurin SLNs where two different particle size distribution peaks were revealed (Figure 2.1). This type of particle size distribution was a clear indication of SLN dispersion instability. The unstable behaviour of the dispersion was further identified by measuring the zeta potential of both CRC-TL and CRC-PR samples, which was found out to be 0.3-1.7 mV. An explanation of the observed aggregation may involve an intrinsic thermodynamic instability of the nanoparticle system with dispersed molecules of the surfactant in the lipid. There is a possibility that the concentration of surfactant used for preparing both CRC-PR and CRC-TL was interfering with particle surface where the surfactant molecules were compressed at the particle surface forming loops and tails which finally initiated a bridging between the primary nanoparticles. (Freitas et al., 1999). However, this was not the case for CRC tristearin and stearic acid loaded formulations where both dispersions showed narrow particle size distributions between 217-220 nm. They also presented very good polydispersity index (0.07-0.08) and the zeta potential was approximately at the range of -8.1 mV to -8.3 mV, which is a sign of moderate stability of the SLN (Table 2.2). Higher values of zeta potential indicate high electric charge on the surface of the SLNs, which can cause strong repellent forces among particles to prevent aggregation of the SLN dispersion (Yousefi et al., 2009). After six months of observation the SLN dispersions remained stable with a slight increase on particle size, varying at the range of 5-10 nm (table 2.3). Moreover the changes in zeta potential of these SLN formulations were not significant which is also an indication of stability. Due to

the stable characteristics of tristearin and stearic acid SLNs these two formulations were chosen for further experimental evaluations.

Table 2. 1 Blank SLN dispersions made by various lipid/surfactant compositions

Lipid	Lipid (mg)	P188 (mg)	Particle size (nm)	Zeta (mV	PI
Tristearin	500	250	148.4 ±3.1	-19.20 ±1.61	0.11 ±0.03
Stearic Acid	500	250	145.1 ±2.7	-18.74 ±2.77	0.10 ±0.02
Precirol	500	250	143.4 ± 1.2	-15.47 ±0.13	0.08 ±0.03
Trilaurin	500	250	149.2 ± 5.5	-13.32 ±0.23	0.07 ±0.04

SLN formulations of BL- TS (Blank Tristearin), BL- SA (Blank stearic acid), BL- PR (Blank precirol) and BL- TL (Blank trilaurin). Each formulation was measured three times and the mean as well as the standard deviation of the mean is presented**.**

Table 2. 2 CRC loaded SLN dispersions made by various lipid/surfactant compositions

Lipid	Lipid (mg)	P188 (mg)	CRC (mg)	Particle size (nm)	Zeta Potential (mV)	PI
Tristearin	500	250	50	216.6 ±2.8	-8.33 ±1.09	0.08 ±0.01
Stearic acid	500	250	50	218.5 ±3.7	-8.11 ±0.12	0.07 ±0.03
Precirol	500	250	50	1108±4.1	-0.33 ± 0.21	0.28 ± 0.09
Trilaurin	500	250	50	4235± 9.2	-1.75 ± 0.67	0.25 ± 0.06

SLN formulations of CRC- TS (Curcumin loaded tristearin), CRC- STR (Curcumin loaded stearic acid), CRC- PRL (Curcumin loaded precirol) and CRC- TRL (Curcumin loaded trilaurin). Formulation was measured in triplicates

Table 2. 3 Stability of SLN dispersions after 1, 3 and 6 months.

	Months	Particle size (nm)		Zeta Potential (mV)	
		Empty	**Loaded**	**Empty**	**Loaded**
CRC-TS	1	151.3 ±3.5	222.2 ±2.5	-19.05 ±2.2	-8.09 ±1.7
	3	155.5 ±2.8	223.3 ±1.9	-18.21 ±2.4	-7.99 ±0.5
	6	157.1 ±1.1	226.7 ±2.0	-17.05 ±4.3	-7.96±0.3
CRC-STR	1	147.3 ±0.9	221.4 ±2.5	-18.55 ±1.3	-8.08 ±0.1

	3	151.1 ±3.6	225.1 ±2.6	-18.11 ±1.2	-7.95 ±0.5
	6	154.8 ±3.3	227.6 ±1.4	-18.01 ±0.1	-7.93 ±0.2

Figure 2. 1 (a) Particle size distribution of CRC- PR (nm). (b) Zeta potential (mV) of CRC-PR. (c) Particle size distribution of CRC- TL (nm). (d) Zeta potential (mV) of CRC-TL.
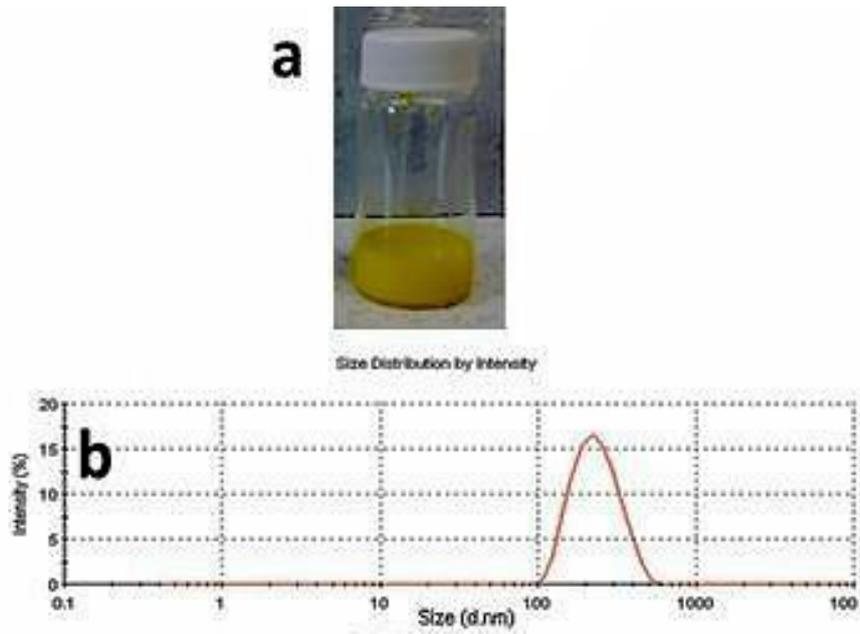
Figure 2. 2 (a) CRC-TS SLN dispersion. (b) Particle size distribution of CRC-TS (nm).
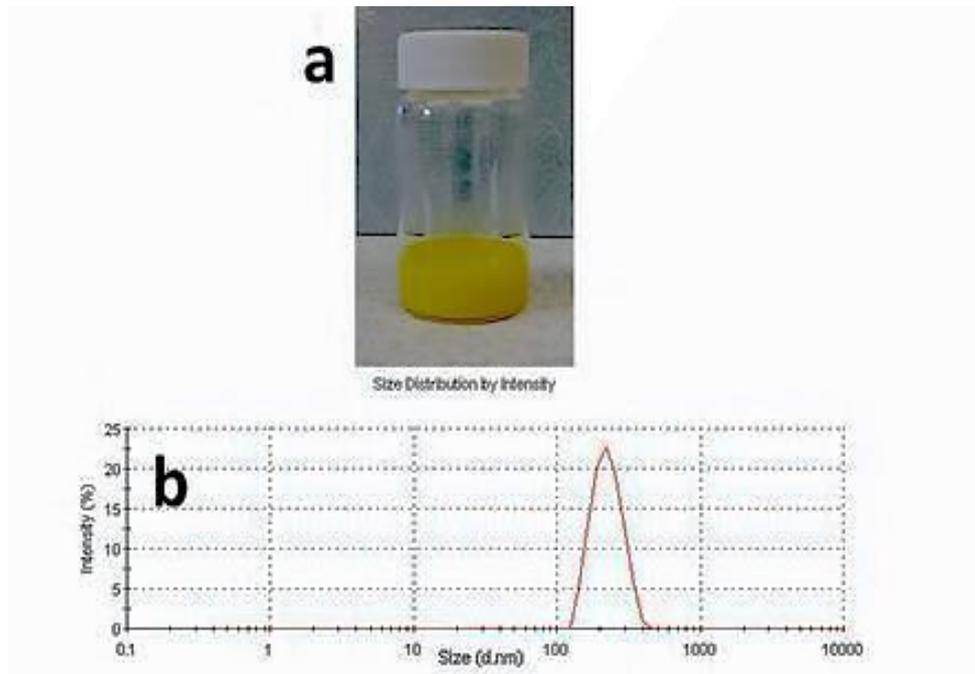
Figure 2. 3 (a) CRC-SA SLN dispersion. (b) Particle size distribution of CRC-SA (nm).

2.4.2 XRD results

XRD experiments were conducted in order to investigate the crystalline/amorphous characteristics of all SLN dispersions (after freeze drying). Amouphous compounds presented in the SLN showed very broad peaks which were distinguishable in comparison to the sharp peaks belonging to the crystalline form. XRD also gave information about the crystalline-amorphous ratios for the various bulk materials (lipid,surfactant,drug) and for the SLNs.
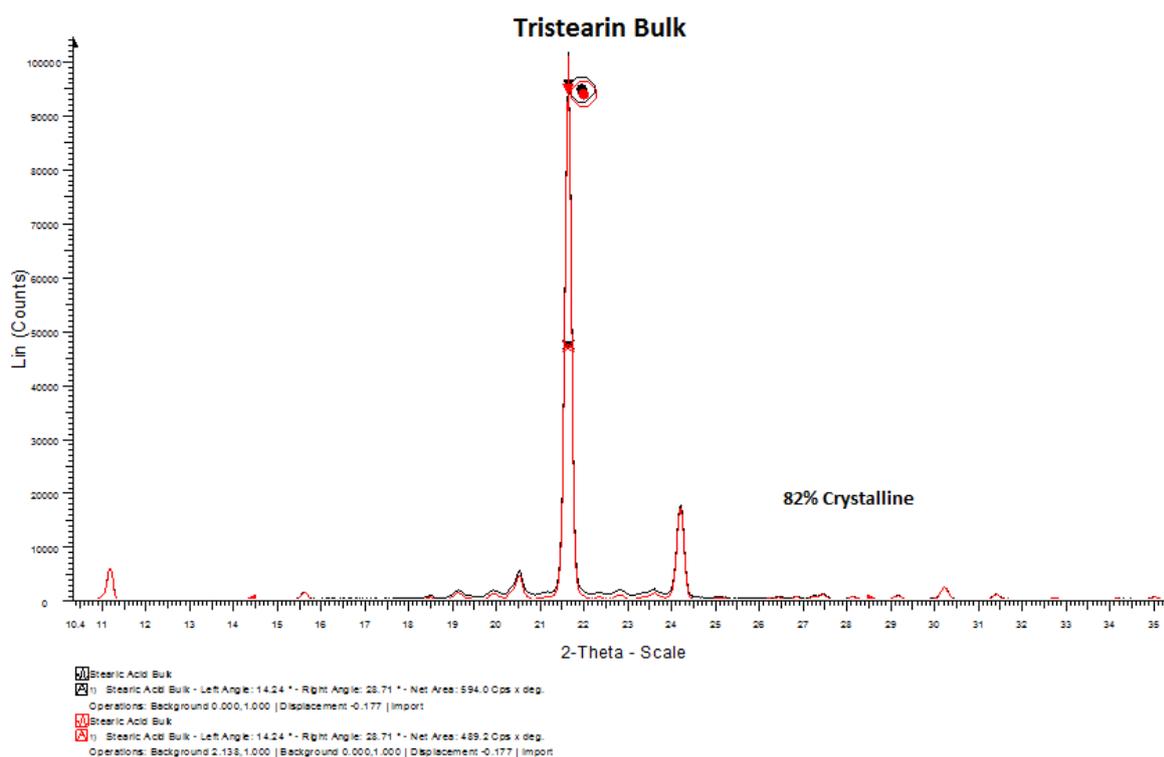
Figure 2. 4 XRD diffractogram of bulk tristearin

The XRD results from bulk tristearin showed very sharp peaks which indicated the crystalline nature of the lipid (Figure 2.4). The estimation of the area under the curve the ratio of crystalline to amorphous was found to be :

Tristearin crystalline : amorphous = 82:18

The results acquired from the P188 diffractograms showed 54% crystallinity(Figure 2.5). Further investigation performed on the bulk stearic acid also presented distinct intensity peaks in the XRD diffractogram (Figure 2.6) with above 80% crystallinity. The XRD diffraction patterns of pure curcumin showed almost 100% crystallinity (Figure 2.7).
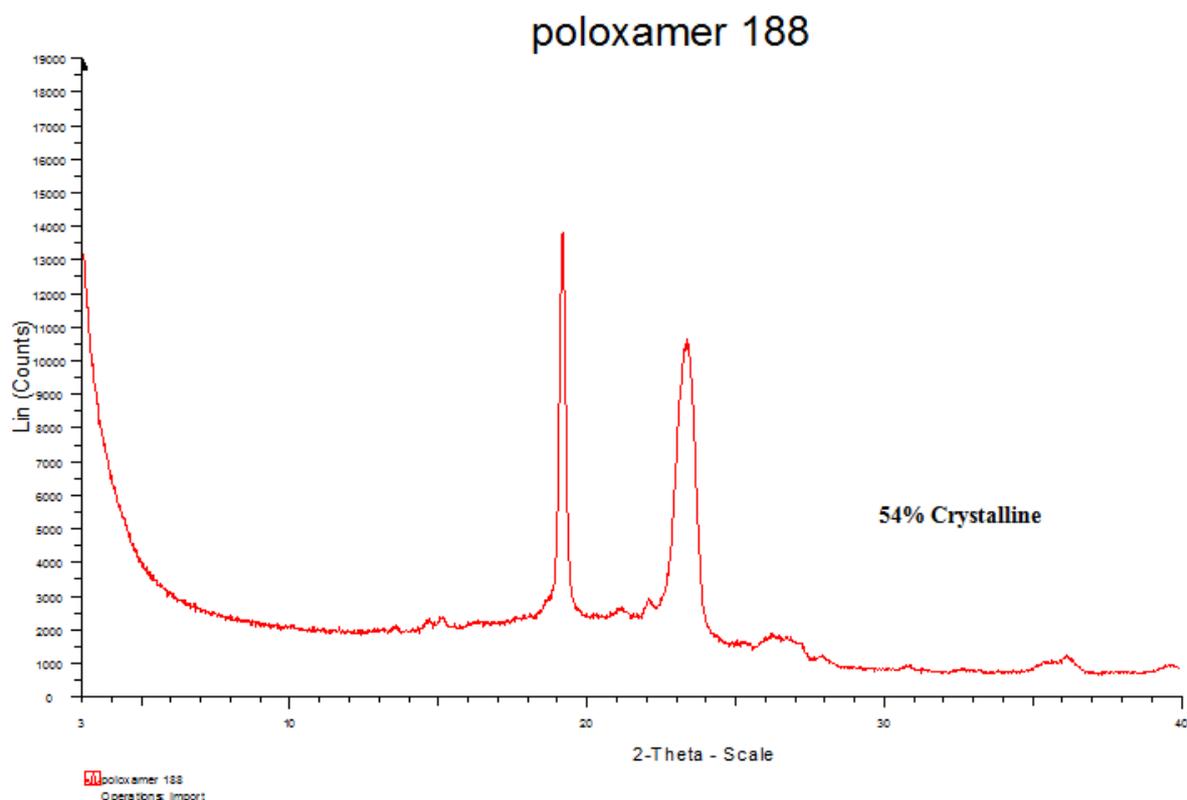
Figure 2. 5 XRD diffractogram of poloxamer 188

From diffraction patterns of BL- TS and CRC- TS it was clear that less ordered crystals were majority. The XRD results also confirmed the absense of crystalline curcumin form in CRC-TS. The absence of CRC intensity peaks in the CRC- TS diffractograms suggested that the CRC is entrapped in the lipid core of SLNs (Mulik et al., 2012). The X-ray diffraction pattern of CRC- TS was broader and with lower intensity than that of the bulk matrix. The crystalline and amorphous ration of CRC- TS SLN was 39:61, which is an indication that less ordered crystals were more abundant in this CRC loaded SLN formulation.
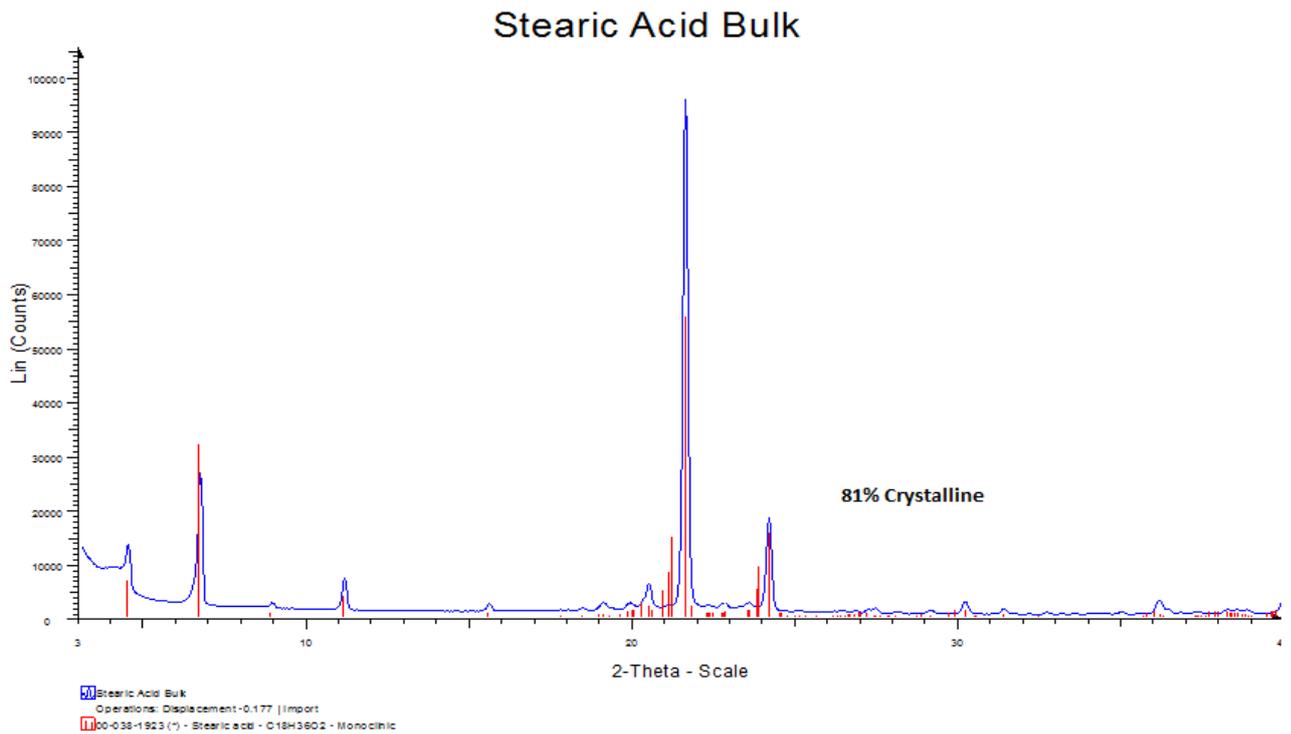
Figure 2. 6 XRD diffractogram of stearic acid
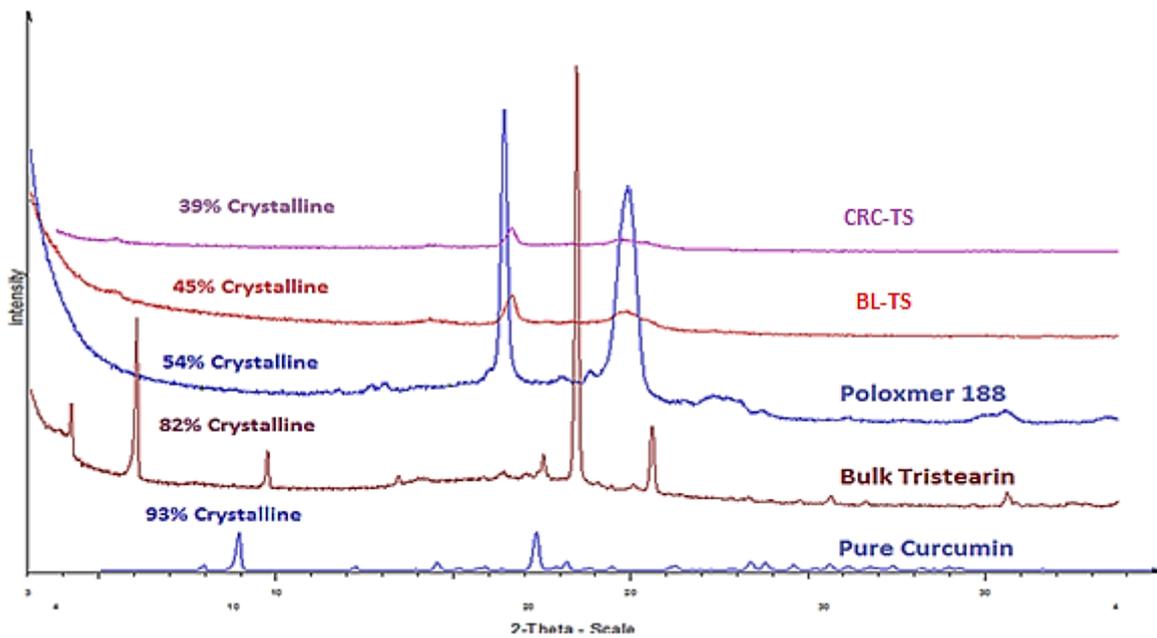
Figure 2. 7 XRD diffractograms of pure curcumin, poloxamer 188, bulk tristearin, BL- TS (blank tristearin), CRC- TS (Curcumin loaded tristearin).
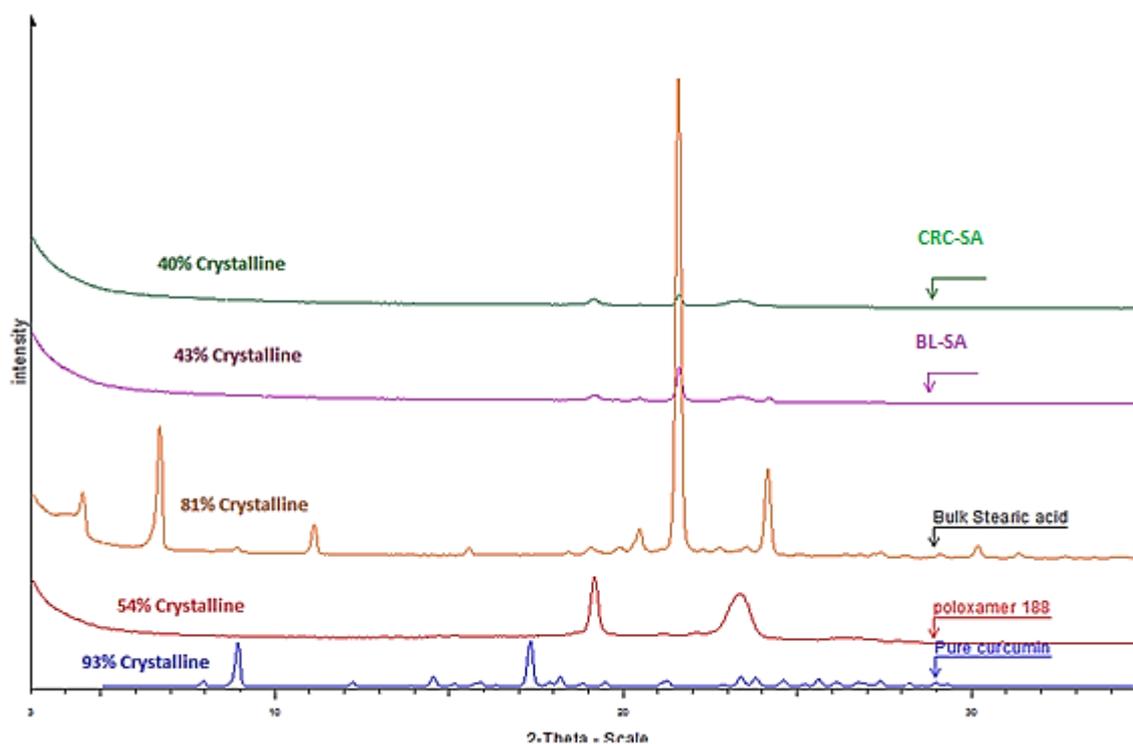
Figure 2. 8 XRD diffractograms of pure curcumin, poloxamer 188, bulk stearic acid, BL- SA (blank stearic acid), CRC- SA (Curcumin loaded stearic acid).

The diffraction pattern of BL- SA and CRC- SA were also analysed. As shown in Figure 2.8, the diffraction patterns of both CRC-SA and BL- SA showed increased amorphpicity compared to the tristearin formulations. The crystallinity percentage of CRC- SA and BL- SA were 40% and 43% respectively. However, for stearic acid SLNs the diffraction patterns of CRC- TS and BL- TS did not show any significant difference which is an indication that the addition of curcumin has not either altered or enhanced the nature of SLNs. Moreover, similarly to the tristearin based SLNs, no distinct intensity CRC peaks were present in the stearic acid based SLN diffraction patterns. A possible explanation to this observation is that the CRC is entrapped in the lipid core of SLNs in molecular dispersion form.

2.4.3 Differential scanning calorimetry

DSC has been extensively used to investigate the crystallinity of colloidal lipid matrices (Jie Liu et al.,2007). Bulk stearic acid, poloxamer 188 and curcumin showed melting endothermic peaks at 69.82°C ,51.81°C and 175.74°C respectively (Figure 2.9). In addition the enthalpies for the bulk SA, P188 and curcumin were -228.39 J/g, -126.37 J/g and -100.29 J/g.

46
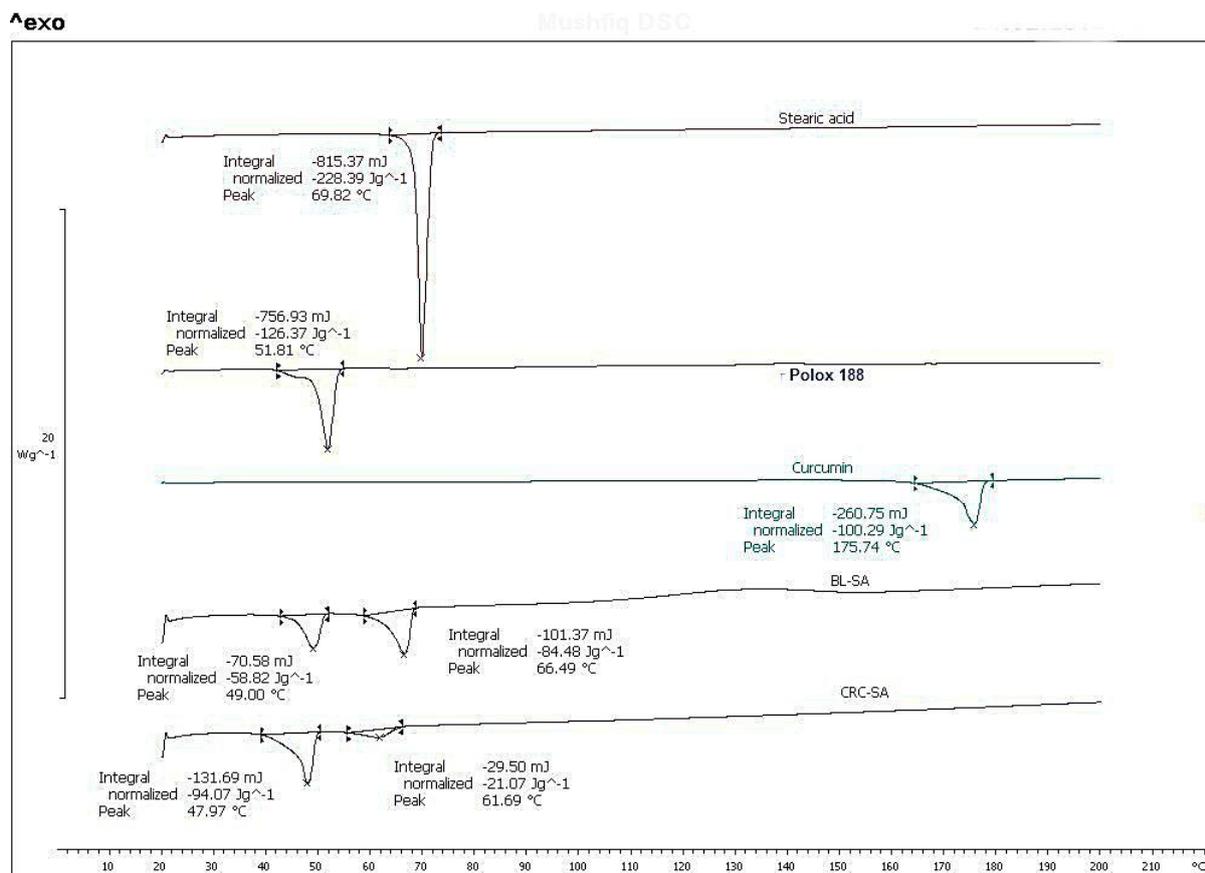
Figure 2. 9 DSC thermographs of curcumin, bulk stearic acid, poloxamer 188, BL-SA and CRC-SA

The crystallization behaviour of freshly prepared blank SLN and CRC loaded SLNs differed distinctively from bulk material. The melting endotherms of blank and CRC loaded are broadened and melting point is also reduced. The broadening of the heating peaks and the reduction of the melting point indicate an increased number of lattice defects (Siekmann, 1994). Another interesting observation was the decreasing enthalpy of SLN formulations compared to bulk materials. These findings can confirm the entrapment of curcumin inside the nanoparticles in a molecular dispersion form (Mulik et al., 2012). Moreover, the sharp melting endotherm of CRC was absent in DSC of CRC-SA formulations (Figure 2.9). The reason is that CRC is completely solubilised in the lipid matrix due to melting of drug in lipid (Padhye et al., 2013).

47
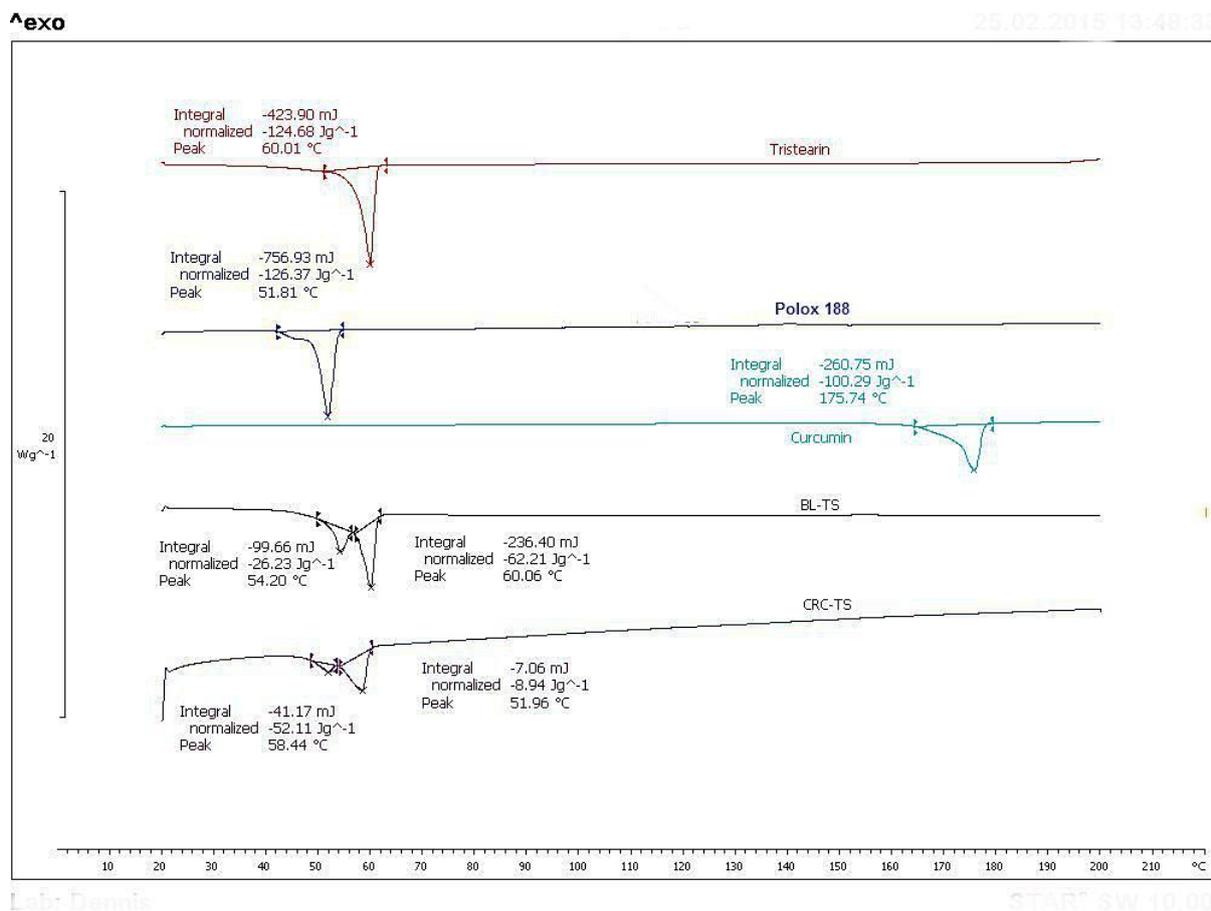
Figure 2. 10 DSC thermographs of curcumin, bulk tristearin, polox P188, BL-TS and CRC-TS.

Tristearin based SLN formulations exhibited similar DSC heating peaks when compared to stearic acid based SLN's (Figure 2.10). The bulk tristearin, poloxamer P188 and bulk CRC ahowed melting endotherm peaks at 60.01°C, 51.81°C and 100.29°C respectively. The SLN formulations exhibited two endothermic peaks, atributed to the lipid and surfactant melting peaks. As previously obsereved the DSC heating curves were broadened and the melting peaks were reduced significantly, suggesting an increased number of lattice defects. Moreover, while comparing the enthalpy of CRC loaded SLN formulations with the enthalpy of the drug a substantial reduction in enthalpy was observed. As mentioned above this is an indication that curcumin's is molecularly dispersed in the lipid matrix. Again no CRC melting endothermic peaks were observed in the CRC-TS heating curves which is either because CRC solubilised in the lipid matrix due to the melting of drug in lipid (Padhye *et al.*, 2013) or this might confirmes its entrapment of CRC in the lipid matrix (Juvonen *et al.*, 2012)

2.4.4 Determination of encapsulation efficiency and drug loading

The encapsulation efficiency of both tristearin and stearic acid based SLNs showed good encapsulation efficiency, while stearic acid based SLNs showed higher encapsulation efficiency (91.7%) compared to tristearin (90.9%). Different studies suggested that curcumin is poorly soluble in water (Sun et al., 2013). However it is well known that the solubility of compounds in the lipid matrix is one of the critical factors that determine drug payload and incorporation efficiency in the SLNs. Even then the solubility of curcumin has improved by addition of surfactants. Thus, the curcumin is incorporated in the lipid core of SLNs which in turn facilitate very high entrapment efficiency (Tiyaboonchai et al., 2007). Figure 2.11 represents a bar chart comparing the encapsulation efficiency of CRC-SA and CRC-TS where, both lipids based CRC-SLN formulation showed nearly similar encapsulation efficiency.

Table 2. 4 Entrapment efficiency and drug loading of CRC- TS and CRC- SA

	Lipid (mg)	P 188 (mg)	Curcumin (mg)	DL (%)	EE (%)
CRC- TS	500	250	50	6.36	90.9
CRC- SA	500	250	50	6.48	91.7
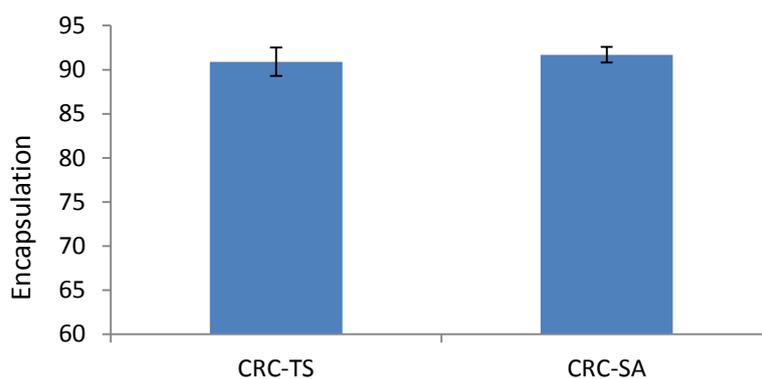
Figure 2. 11 Encapsulation efficiency of curcumin loaded SLN's.

2.4.5 SLN drug release studies

The release studies for CRC loaded SLN formulations were carried out over 120 hours at a controlled temperature of 37°C. Due to the CRC hydrophobic nature the release studies were conducted in 50% v/v ethanol solutions in which the solubility of CRC is 0.693 ± 0.13 mg/ml as suggested by (Kakkar et al., 2011). Figure 2.12 shows both stearic acid and tristearin based CRC-SLNs provide similar release patterns with no statistical difference.
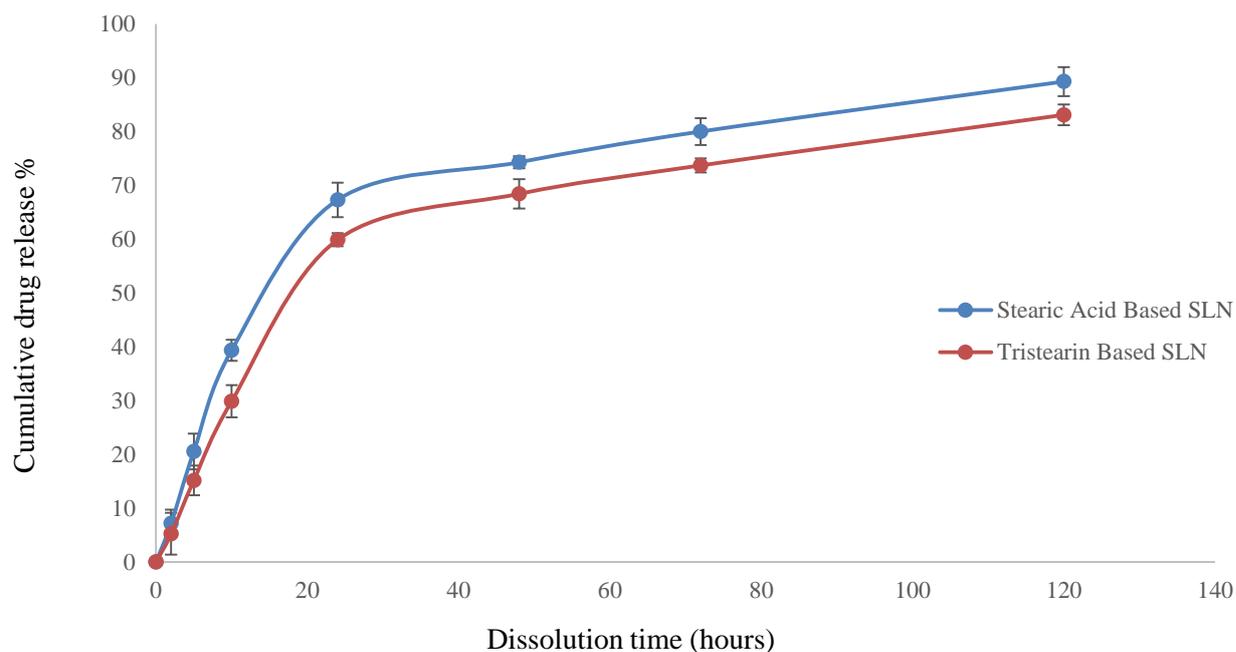
Figure 2. 12 Drug release profile of tristearin and stearic acid based SLN's loaded by curcumin

However, for both lipid core based CRC-SLN an initial burse release (~50%) was observed for the first 24hr. Afterwards the CRC release increased up to 80% over the next 96 hr. The release profiles indicated a two-phase sustained release profile of CRC for both lipid formulations. The release mechanism of CRC is related to the drug distribution within the nanoparticle when the solidification of SLN had taken place during the preparation procedure. The CRC that are actually contained in the outer shell and also on the particle surface is released rapidly while the drug amount that has been actively incorporated into the particle core is released in a prolonged time span (Sun et al., 2013).

2.5 Conclusions

Tristearin and stearic acid based SLN formulations loaded with the anticancer drug CRC were optimized by high pressure homogenization and further characterized using a range of analytical techniques. Both blank and loaded formulations displayed a monomodal size distribution, while the zeta potential also did not deviate significantly, indicating very good stability even after the incorporation of the drug. XRD and DSC analysis confirmed the amorphous nature and drug incorporation into the lipid matrix. The SLN loaded formulations showed high encapsulation efficiencies varying form 92-95%. Finally, the CRC release showed a two-phase sustained release pattern for both lipid formulations.

2.6 References

1. Alam, S., Panda, J. J., & Chauhan, V. S. (2012). Novel dipeptide nanoparticles for effective curcumin delivery. *International journal of nanomedicine*, *7*, 4207.

2. Anand, P., Kunnumakkara, A. B., Newman, R. A., & Aggarwal, B. B. (2007). Bioavailability of curcumin: problems and promises. *Molecular pharmaceutics*, *4*(6), 807-818.

3. Das, M., & Sahoo, S. K. (2012). Folate decorated dual drug loaded nanoparticle: role of curcumin in enhancing therapeutic potential of nutlin-3a by reversing multidrug resistance. *PLoS one*, *7*(3), e32920.

4. Freitas, C., & Muller, R. H. (1999). Correlation between long-term stability of solid lipid nanoparticles (SLN™) and crystallinity of the lipid phase. *European Journal of Pharmaceutics and biopharmaceutics*, *47*(2), 125-132.

5. Giri, B., Gomes, A., Sengupta, R., Banerjee, S., Nautiyal, J., Sarkar, F. H., & Majumdar, A. P. (2009). Curcumin synergizes the growth inhibitory properties of Indian toad (Bufo melanostictus Schneider) skin-derived factor (BM-ANF1) in HCT-116 colon cancer cells. *Anticancer research*, *29*(1), 395-401.

6. Kakkar, V., Singh, S., Singla, D., & Kaur, I. P. (2011). Exploring solid lipid nanoparticles to enhance the oral bioavailability of curcumin. *Molecular nutrition & food research*, *55*(3), 495-503.

7. Khor, T. O., Keum, Y. S., Lin, W., Kim, J. H., Hu, R., Shen, G. & Kong, A. N. T. (2006). Combined inhibitory effects of curcumin and phenethyl isothiocyanate on the

growth of human PC-3 prostate xenografts in immunodeficient mice.*Cancer research*, *66*(2), 613-621.

8. Kong, A. N. T. (Ed.). (2013). *Inflammation, Oxidative Stress, and Cancer: Dietary Approaches for cancer prevention*. CRC Press.

9. Li, W., Khor, T. O., Xu, C., Shen, G., Jeong, W.-S., Yu, S., & Kong, A.-N. (2008). Activation of Nrf2-antioxidant signaling attenuates NF-κB-inflammatory response and elicits apoptosis. Biochemical pharmacology, 76(11), 1485–1489. doi:10.1016/j.bcp.2008.07.017.

10. Liu, J., Gong, T., Wang, C., Zhong, Z., & Zhang, Z. (2007). Solid lipid nanoparticles loaded with insulin by sodium cholate-phosphatidylcholine-based mixed micelles: preparation and characterization. *International journal of pharmaceutics*, *340*(1), 153-162.

11. López-Lázaro, M. (2008). Anticancer and carcinogenic properties of curcumin: considerations for its clinical development as a cancer chemopreventive and chemotherapeutic agent. *Molecular nutrition & food research*, *52*(S1), S103-S127.

12. Mehnert, W., & Mäder, K. (2001). Solid lipid nanoparticles: production, characterization and applications. *Advanced drug delivery reviews*, *47*(2), 165-196.

13. Mulik, R. S., Mönkkönen, J., Juvonen, R. O., Mahadik, K. R., & Paradkar, A. R. (2012). Apoptosis-induced anticancer effect of transferrin-conjugated solid lipid nanoparticles of curcumin. *Cancer nanotechnology*, *3*(1-6), 65-81.

14. Mulik, R. S., Mönkkönen, J., Juvonen, R. O., Mahadik, K. R., & Paradkar, A. R. (2010). Transferrin mediated solid lipid nanoparticles containing curcumin: enhanced *in vitro* anticancer activity by induction of apoptosis. *International journal of pharmaceutics*, *398*(1), 190-203.

15. Padhye, S. G., & Nagarsenker, M. S. (2013). Simvastatin solid lipid nanoparticles for oral delivery: Formulation development and *In vivo* evaluation.*Indian journal of pharmaceutical sciences*, *75*(5), 591.

16. Park, J., Ayyappan, V., Bae, E. K., Lee, C., Kim, B. S., Kim, B. K., ... & Yoon, S. S. (2008). Curcumin in combination with bortezomib synergistically induced apoptosis in human multiple myeloma U266 cells. *Molecular oncology*, *2*(4), 317-326.

17. Potta, S. G., Minemi, S., Nukala, R. K., Peinado, C., Lamprou, D. A., Urquhart, A., & Douroumis, D. (2011). Preparation and characterization of ibuprofen solid lipid nanoparticles with enhanced solubility. *Journal of microencapsulation*, *28*(1), 74-81.

18. Ravindran, J., Prasad, S., & Aggarwal, B. B. (2009). Curcumin and cancer cells: how many ways can curry kill tumour cells selectively?. *The AAPS journal*, *11*(3), 495-510.

19. Reddy, L. H., & Murthy, R. R. (2004). Influence of polymerization technique and experimental variables on the particle properties and release kinetics of methotrexate from poly (butylcyanoacrylate) nanoparticles. *Acta pharmaceutica*, *54*(2), 103-118.

20. Serpe, L., Catalano, M. G., Cavalli, R., Ugazio, E., Bosco, O., Canaparo, R., & Zara, G. P. (2004). Cytotoxicity of anticancer drugs incorporated in solid lipid nanoparticles on HT-29 colorectal cancer cell line. *European Journal of pharmaceutics and biopharmaceutics*, *58*(3), 673-680.

21. Siekmann, B., & Westesen, K. (1994). Thermoanalysis of the recrystallization process of melt-homogenized glyceride nanoparticles. *Colloids and surfaces B: biointerfaces*, *3*(3), 159-175.

22. Sun, J., Bi, C., Chan, H. M., Sun, S., Zhang, Q., & Zheng, Y. (2013). Curcumin-loaded solid lipid nanoparticles have prolonged *in vitro* antitumour activity, cellular uptake and improved *in vivo* bioavailability. *Colloids and Surfaces biointerfaces*, *111*, 367-375.

23. Tiyaboonchai, W., Tungpradit, W., & Plianbangchang, P. (2007). Formulation and characterization of curcuminoids loaded solid lipid nanoparticles. *International journal of pharmaceutics*, *337*(1), 299-306.

24. Yang, K. Y., Lin, L. C., Tseng, T. Y., Wang, S. C., & Tsai, T. H. (2007). Oral bioavailability of curcumin in rat and the herbal analysis from Curcuma longa by LC–MS/MS. *Journal of chromatography B*, *853*(1), 183-189.

25. Yang, L., Chen, L., Meng, B., Suo, J., Wang, H., Xie, H., & Zhang, L. (2006). The effect of curcumin on proliferation and apoptosis in LNCaP prostate cancer cells. *Chinese journal of clinical oncology*, *3*(1), 55-60.

26. Yousefi, A., Esmaeili, F., Rahimian, S., Atyabi, F., & Dinarvand, R. (2009). Preparation and *in vitro* evaluation of a pegylated nano-liposomal formulation containing docetaxel. *Scientica pharmaceutica*, *77*, 453-464.

CHAPTER 3: ANTITUMOUR EFFECTS OF CURCUMIN – LOADED SLN AGAINST HUMAN PROSTATE CANCER CELL LINE

3.1 Introduction

Therapeutic selectivity or preferential killing of cancer cells without significant toxicity to normal cells is one of the most desirable properties of an anti-tumour agent. It is rather encouraging to see that curcumin does exhibit this selectivity (Lazaro et al., 2008). Several pre-clinical data have revealed that curcumin can both inhibit the formation of tumours in animal models of carcinogenesis and act on a variety of molecular targets involved in cancer development. Moreover according to Lazaro et al., 2008, several *in vitro* studies revealed that curcumin is an efficient inducer of apoptosis. Numerous studies shown that Curcumin demonstrates several inhibitory effects on prostate cancer cells (Lei Yang, 2006, Deeb et al., 2008 & Lazaro et al., 2008). It is been reported that curcumin inhibited the phosphorylation of AKt, mammalian target of rapamycin (mTOR), and their downstream substrates in human prostate cancer cells (Wenge Li, 2008). Curcumin can also simultaneously target nuclear factor-kβ (Nf-kβ) signalling pathways by exerting its additive inhibitory effects on cell proliferation and apoptosis of prostate cancer cells (Tin et al., 2006). Deeb et al., (2007) reported that curcumin sensitizes prostate cancer cells to TNF related apoptosis inducing ligand induced apoptosis by inhibiting NF-kβ and its downstream antiapoptotic genes such as Bcl-2 and BcL-xL. Additionally curcumin was found to be inhibiting IL-6 mediated PSA gene expression in LNCaP cells through down-regulation of the expression and activity of androgen receptors (Kong, 2013). Curcumin decreases the level of transcription factor-4 (Tcf-4) leading to the suppression of β-catechin/Tcf-4 transcriptional activity and of the expression of β-catechin target genes and ultimately causing autophagy of the cells (Kong, 2013). According to Kong (2013) curcumin induced apoptosis in LNCaP cells was due to cellular ceramide accumulation and damage to mitochondria in a caspase-independent pathway. Curcumin was also actively been reported to have suppressive effects on the transactivation and expression of androgen receptor and androgen receptor related cofactors (AP-1, NF-kβ) in prostate cancer cell lines (Kong, 2013). In this study curcumin (CRC) encapsulated solid lipid nanoparticles (SLN) were prepared. The anti-tumour effects of these SLN formulations (both loaded and unloaded) were evaluated on human prostate cancer cells. While Blank SLNs (BL-SLN) expectedly did not show any anti-tumour activity, CRC

encapsulated SLNs (CRC-SLN) did show sufficient anti-tumour activity. Both lipid based CRC loaded SLN taken down the cell viability to almost 0% at a CRC concentration of 100 µg/ml. These anti-tumour activities also confirmed curcumin's potency as an anticancer agent. The cellular uptake studies confirmed the internalisation of CRC-SLN, where the CRC-SLNs were seen to be localized in the cytoplasm around the nucleus. Flow cytometric studies confirmed early and late apoptosis inducing ability of CRC-SLNs.

3.2 Materials

Curcumin was purchased from Sigma-Aldrich (Dorset, UK), stearic acid and tristearin was purchased from Sigma-Aldrich. Poloxamer 188 was kindly donated by BASF (Ludwigshafen, Germany). All other chemicals and solvents were of analytical and high-performance liquid chromatography (HPLC) grade. LNCaP cell line was purchased from American Type Culture Collection (ATTC: Manassa, Virginia, USA). Dulbecco's modified Eagle's medium (DMEM), thiazolyl blue tetrazolium bromide (MTT), L-glutamin, Penicillin streptomycin, DAPI (2-4-Amidinopheny6-indolecarbamidine dihydrochloride) and heat inactivated fetal bovin serum (FBS) and trypsin were all purchased from Sigma -Aldrich (UK). PE Annexin V Apoptosis Detection Kit I from BD Biosciences.

3.3 Methods

3.3.1 Preparation of SLN formulations
Please refer to chapter 2, section 2.3.1

3.3.2 Cell viability test
LNCaP prostate cancer cell lines were cultured using DMEM culture medium (supplemented with 10% serum, 1% L-glutamine and 1% penicillin streptomycin) in an incubator maintained at 37ºC and 5% CO2. The culture medium was changed every three days. The cytotoxicity of curcumin loaded SLNs and pure curcumin dissolved in ethanol (10mg/ml) was determined in LNCaP prostate cancer cell line using MTT assay. Cells were seeded in a 24 well flat-bottom plate at cell density of 1×10^6 cells/well and incubated for 24 hours. After 24 hours the SLN formulations were added to the 24 well plates at various concentrations and incubation time. 100µL of MTT solution (5 mg/ml) was added to each well plate at the end of the incubation time and incubated at 37ºC for another 2 hours. The culture medium was discarded, followed by addition of 200µl of acidified isopropanol to dissolve the MTT formazan crystals. 100µL of the dissolved MTT formazan crystals was

then transferred into a 96 well flat-bottom plate and absorbance was read at 492 nm using a microplate reader. Controls include non-treated cells and ethanol (2%) for pure drug cytotoxicity. Curcumin was used at concentrations of 10, 20, 40, 50 and 100 μg/ml. Blank (unloaded) and loaded (50mg of drug) SLN formulation were incubated at SLN concentrations of 0.18, 0.37, 0.73, 1.11, 1.47 mg/ml. Cytotoxicity of Blank and loaded SLN formulations were also tested on LNCaP prostate cancer cell line. The cytotoxicity of pure curcumin drug was also evaluated LNCaP prostate cancer cells for direct anti-proliferative efficacy evaluation with curcumin pure drug.

3.3.3 Cellular uptake by fluorescent microscopy

The cellular uptakes of SLN formulations were determined using a Nikon fluorescent microscope. 20×10^3 cells/well was seeded on cover slips in a 24 well flat-bottom plate. Loaded SLN formulation was incubated with the cells for 24 hrs at various concentrations. The cell medium was discarded from the well after 24 hours incubation time and washed three times with PBS. 1ml of 4% para-formaldehyde was added to the well to fix the cells on the cover slips and left in the dark for 15 minutes. The para-formaldehyde was discarded from the well and cells were washed three times with PBS and then mounted on a glass slide using vectashield mounting medium containing DAPI. The cover slips were sealed on a glass slide with a nail polish and left to dry. Images were acquired using the Nikon ECLIPSE 90i overhead epifluorescent microscope attached to a Nikon digital camera (DS-Qi1Nc) and a computer running Nikon NIS-Elements Advanced Research software. The principal objective used for fluorescent imaging was an oil immersion CFI Plan Apochromat VC 60X N2 (NA1·4, WD 0·13 mm).

3.3.4 Flow cytometric analysis for cellular uptake of SLNs

By using the intrinsic green fluorescence of curcumin, cellular uptake has been quantitavely studies by using fluorescence activated cell sorting (FACS) analysis. 20×10^3 cells/well was seeded on cover slips in a 24 well flat-bottom plate. Cells were then treated with free curcumin and SLN formulations (10 μg/ml) for 24 hours. The cell medium was discarded from the well after 24 hours incubation time and washed three times with PBS. Afterwards the cells were detached from the surface of the well plate by using Trypsin (EDTA). After trypsinization the cells were washed with PBS another three more times and re-suspended in 500 μL of PBS and examined using Accuri C6 (Belgium) flow cytometer. FITC was detected by the FL1 channel.

3.3.5 *In vitro* apoptosis studies

Apoptosis is known to be a form of cell death that plays a vital role during development, normal tissue homeostasis and is deregulated in many diseases, one of which includes cancer. Induction of apoptosis in LNCaP prostate cancer cell lines after drug treatment was studied by flow cytometry. In brief, cells were seeded in a 24 well flat-bottom plate at cell density of 1×10^6 cells/well and incubated for 24 hours. After 24 hours the SLN formulations, both loaded and unloaded and pure CRC were added to the 24 well plates. Untreated cells were used as respective control. After 48 hours, the cells were collected by centrifugation and washed twice with PBS. The pelleted cells were re-suspended in 500 ml of 1X binding buffer, 5 µl PE Annexin V and 5 µl of 7-Amino-Actinomycin (7-AAD) and incubated in dark for 10 min. Samples were analysed on the Accuri C6 flow cytometer for PE and 7AAD expression using a solid state blue laser with a 488 nm excitation spectrum and a detector of FL1 path with filter 530/30 nm. A minimum of 10000 gated events was acquired from the cell population and data analysed using the Accuri C6 software. Cells were considered early apoptotic when PE positive and 7AAD negative. All experiments were performed in triplicates.

3.3.6 Statistical analysis

Results were expressed as means and standard deviation of the mean (n=3). Statistical significance was also determined by T-test analysis for comparison between CRC loaded SLN and blank SLN formulations on LNCaP prostate cancer cell line. Differences were considered as significant when P-value was less than 0.05.

3.4 Results and discussion

3.4.1 Antiproliferative effect of curcumin

The antiproliferative effects of curcumin loaded SLN compared to an alcoholic solution of pure drug and blank SLN formulations were examined. The antiproliferative effect of pure curcumin of on LNCaP prostate cancer cell lines was first examined and compare to the encapsulated SLN drug delivery system.
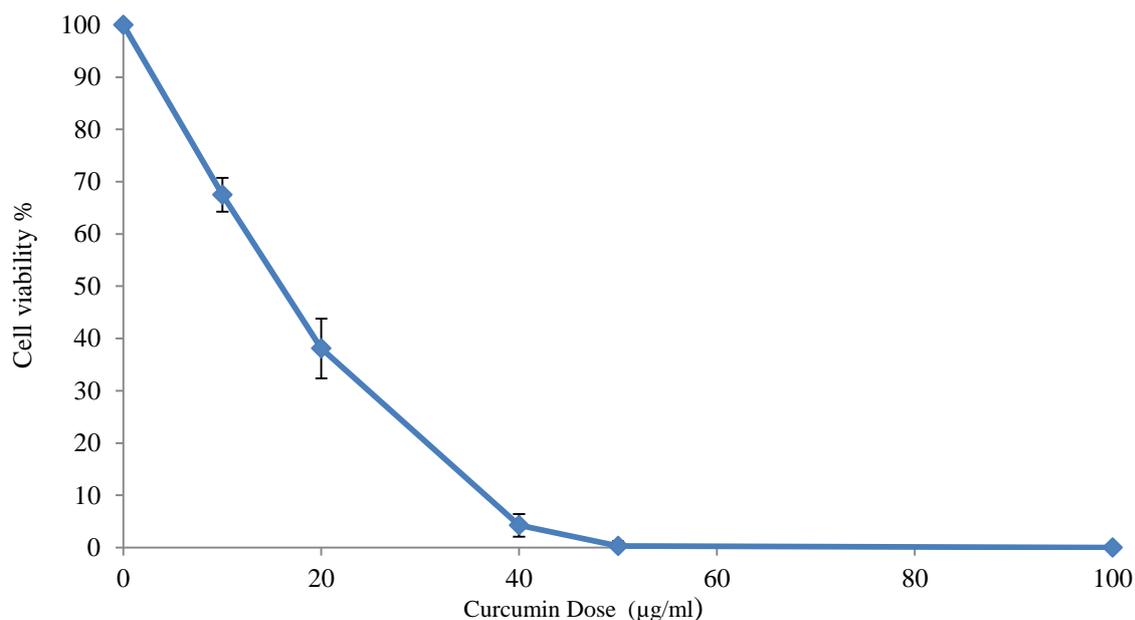
Figure 3. 1 Antiproliferative effects of pure CRC (curcumin) on prostate cancer cells (LNCaP) using the MTT assay for 24 hours incubation time. Data is represented as mean±S.D. (n = 3).

The cytotoxicity studies of pure curcumin showed excellent anti-proliferative activity after 24 hours incubation (Figure 3.1). The LNCaP cell lines viability was reduced to almost 0% at a very low drug concentration of 40 µg/ml. Researchers has confirmed that CRC does have one of the most desirable characteristics of a cancer chemotherapeutic agent. These are known as the therapeutic selectivity or preferential killing of cancer cells by CRC. The process of preferential killing of cancer cells by CRC can undergo without any significant effects to normal cells. According to Yang et al., (2006), curcumin exhibits several inhibitory effects on prostate cancer cells. The cytotoxicity findings, as shown in Figure 3.1, reflect the effect of CRC on LNCaP prostate cancer cell line. These effects can always be regarded advantageous in chemotherapy and it also shows CRC's potent as an anticancer agent for inhibiting prostate cancer cell line growth.

3.4.2 Antiproliferative effect of SLN formulations

As a drug delivery carrier, any cytotoxic effect portrayed by the blank SLN formulations can be considered as a very important feature. Cytotoxicity of empty formulations was evaluated to investigate any significant changes in cell viability upon incubation.
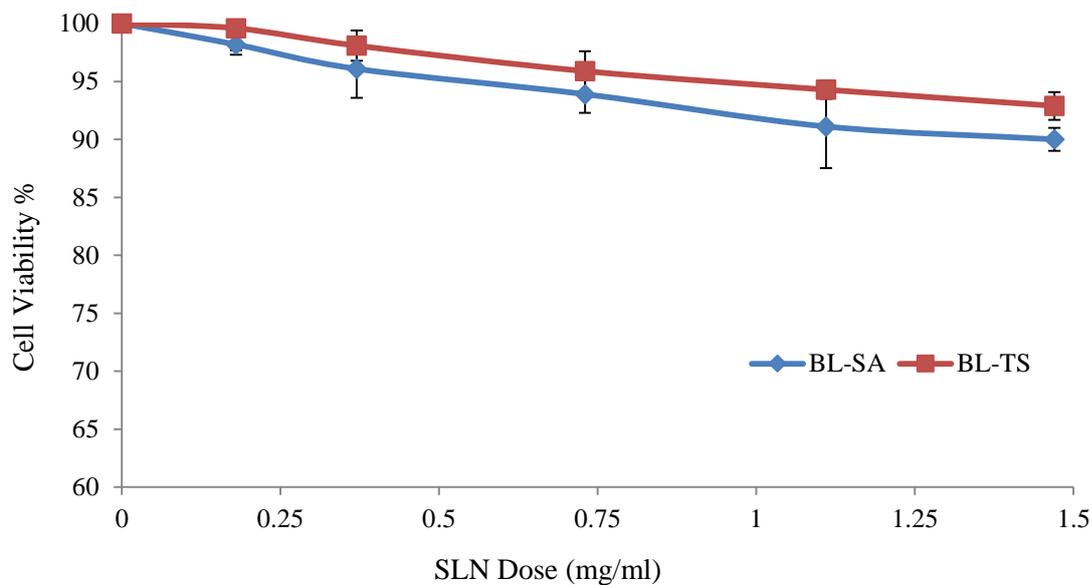
Figure 3. 2 Cytotoxicity of empty SLN formulations (both tristearin and stearic acid based SLNs) ; BL- SA and BL- TS. Data is represented as mean±S.D. (n = 3).
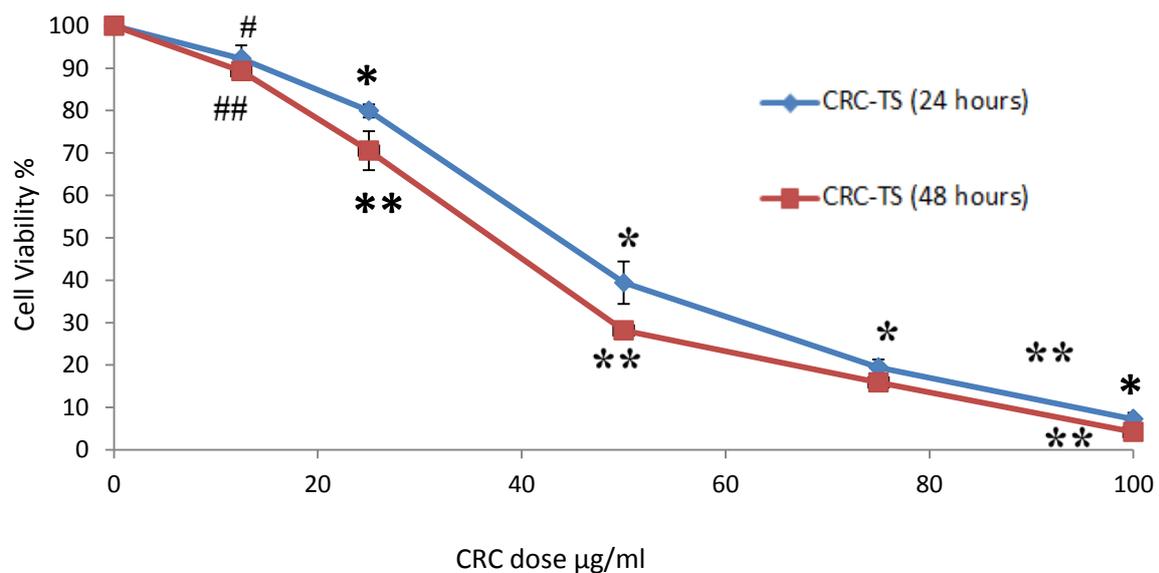
Figure 3. 3 Cytotoxicity of loaded SLN formulations after 24 and 48 hours. Data is represented as mean±S.D. (n = 3). #p=0.0140, *p< 0.0001, CRC-TS (24 hours) vs. BL-TS and #p=0.0043**p< 0.0001, CRC-TS (48 hours) vs. BL-TS

From Figure 3.2, it can be seen that both blank SLN formulations presented negligible cytotoxicity where for blank tristearin (BL-TS) the cell viability was 91.7% and for blank stearic acid (BL-SA) was 90%, respectively.

The effect of increase in curcumin concentration on the antiproliferative action of loaded SLNs was assessed by MTT assay. It was observed that for CRC-TS the antiproliferative effect increased in a dose dependent manner (Figure 3.3). At the lowest dose of 12.5µg/ml CRC concentration a significant reduction of the cell viability (92.25%) was observed (p=0.0140). However, with increasing CRC concentration the difference in cell viability was even more evident and for concentrations of 50µg/ml the cell viability was reduced to 39.42%, which is considered to be highly significant, when compared with blank-tristearin formulation (P<0.001). Further increase in dose to 100µg/ml showed significant reduction to 7.27% (P<0.001). However, while comparing the anticancer activity of pure CRC (Figure 3.1) with CRC-TS (Figure 3.3) it can be observed that free CRC presented significantly higher anticancer activity. These results were in good agreement with those reported in another study by Sun et al., (2013). By increasing the incubation time of CRC-TS the viability of LNCaP cells was further reduced to 4.19% at 100µg/ml after 48 hours incubation, which shows almost a further 50% reduction compared to the 24hr incubation. This time dependent cytotoxic effect of loaded SLN is a proof of sustained release and prolonged inhibitory effect of CRC-SLN (Sun et al., 2013). Since the BL-TS formulations showed negligible effect on the cell viability (Figure 3.2) the antiproliferative effect observed with CRC-TS was attributed to the incorporation of CRC in the lipid nanoparticles.
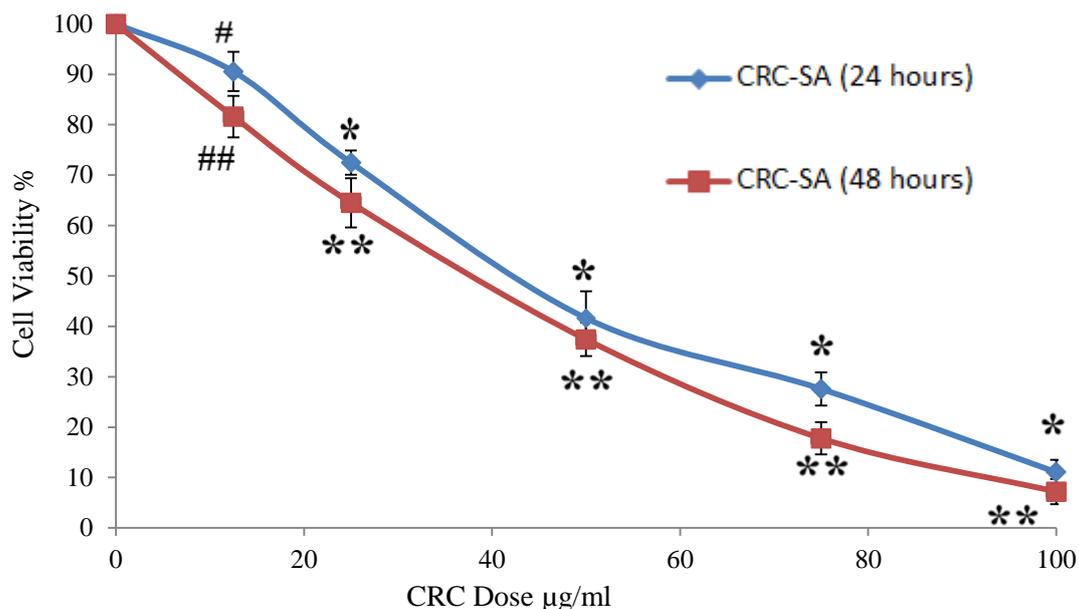
Figure 3. 4 Cytotoxicity of loaded SLN formulations after 24 and 48 hours. Data is represented as mean±S.D. (n = 3). #p=0.0366, *p< 0.0001, CRC-SA (24 hours) vs. BL-SA and ##p=0.0005, **p< 0.0001, CRC-SA(48 hours) vs. BL-SA

Stearic acid based CRC loaded samples displayed similar cytotoxic effect as tristearin loaded SLNs after 24 hours incubation. Increasing curcumin concentration for the CRC-SA showed enhanced cytotoxic effect (Figure 3.4) in a dose dependent manner. At 12.5µg/ml the cell viability was reduced to 90.56% (p=0.0366). As the CRC concentration increased gradually cell viability also started lower down at a regular interval. When the drug concentration increased at 100µg/ml the cell viability was detected down to 11.05%. According to statistical analysis using t-test, at the concentration of 100 µg/ml, CRC-SA exhibited highly significant decrease in cell viability, when compared to blank-stearic acid formulations (P<0.0001). After 48 hours the cytotoxic effect was even more prolific (Figure 3.4) and it can be attributed to the drug sustained release properties from the lipid matrix. As with an increased incubation time more drug is released from the lipid matrix, the cell viability was further reduced to 7.19% at 100µg/ml after 48 hours (p<0.0001). Stearic acid based blank SLN formulations showed negligible decrease in cell viability just like the tristearin based SLN's. This evidently suggests the curcumin is actively initiating the antiproliferative effects that are taking place in LNCaP cell lines.

61

3.4.3 Cellular uptake by fluorescence microscopy

In order to confirm the internalization of the SLN formulation, 10 µg/ml of loaded SLN (both CRC-TS and CRC- SA) were incubated in a prostate cancer cell line (LNCaP) for 24 hours. The qualitative cellular uptake studies carried out with fluorescent microscopy after staining the nucleus of the cells with DAPI while curcumin itself has its intrinsic fluorescence property (Das et al., 2012) and serve as a fluorescence probe to efficiently investigate the uptake of drug loaded SLN's.

Figure 3.5 illustrates the uptake of CRC encapsulated SLNs where after 24 hours of incubation are seen to be localized in the cytoplasm around the nucleus. This high fluorescence intensity that has been observed with CRC loaded SLNs is might be due to the endocytotic pathways, which is known to be a distinct pathway mammalian cells that consists of distinct membrane compartments, which internalize molecules from the plasma membrane and recycle them back to the surface or sort them to degradation. Uptake of nano-particulate materials have been shown to function in this particular cellular uptake pathway. (Alam et al., 2012, Mohanty et al., 2010).
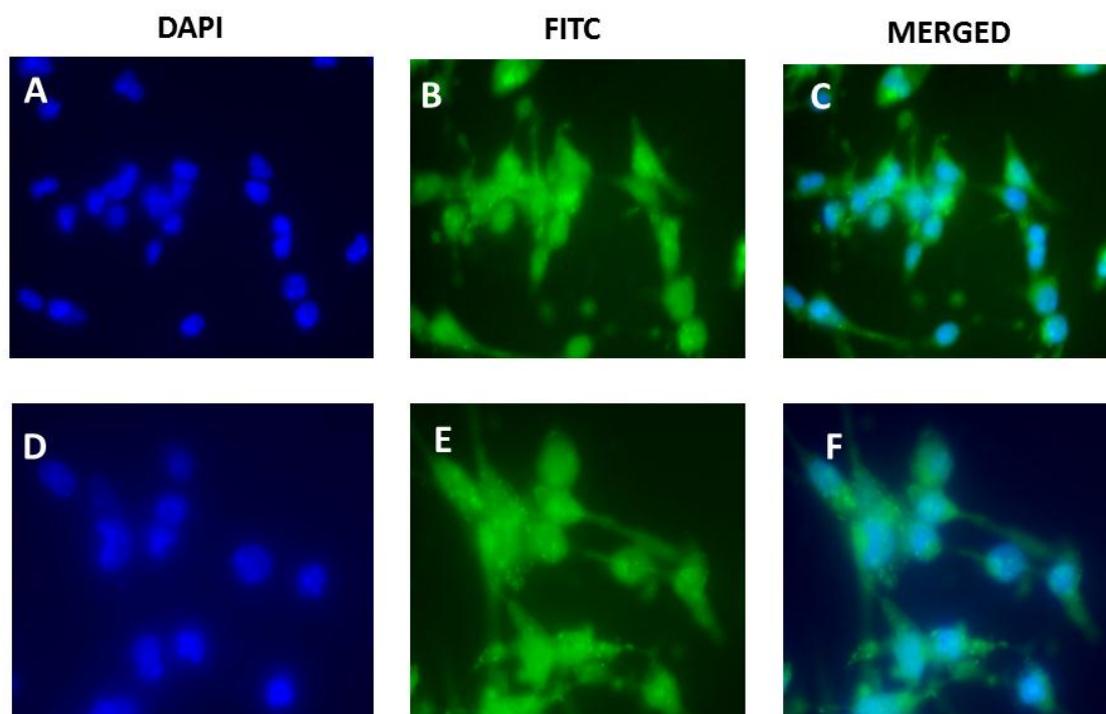
Figure 3. 5 Cellular uptake of curcumin and curcumin loaded SLNs (CRC-SLN). Green colour from FITC represents CRC. Blue colour from DAPI represents nuclei visualization. A-C shows the cellular uptake of CRC-TS and D-F the cellular uptake of CRC- SA.

3.4.4 Flow cytometry analysis for cellular uptake of SLNs

By using the intrinsic green fluorescence of CRC, cellular uptake has been quantitatively examined with fluorescence activated cell sorting (FACS) analysis. The relative extent of cellular uptake of CRC-SLN is presented in figure 3.6 in terms of fluorescence intensity. As seen in figure 3.6, the fluorescent intensity percentage of both tristearin and stearic acid based loaded SLNs appeared to be more than 95%. This high fluorescence intensity relates to the expression of high percentage of cellular uptake. Moreover, while comparing with Blank SLN, no fluorescent intensity was observed. Which confirmed BL-SLN would not be interfering with the fluorescent intensity that was observed with CRC-SLN (Alam et al., 2012).
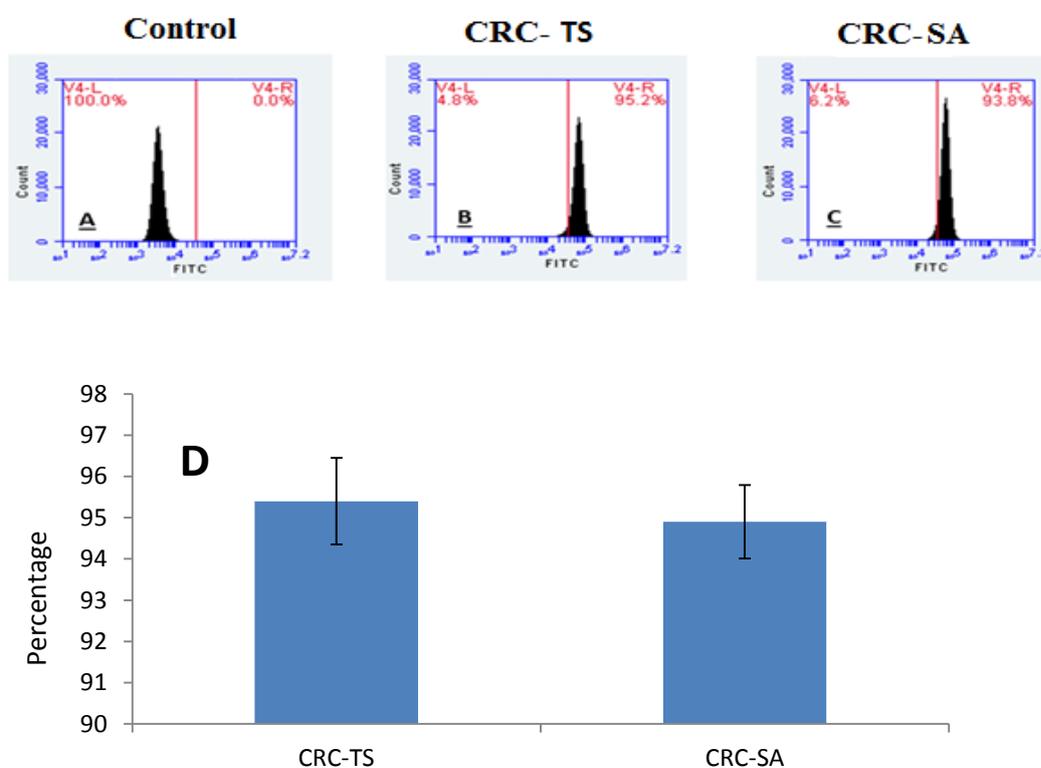
Figure 3. 6 Cellular uptake of CRC-SLNs by flow cytometric analysis. (A) Cellular uptake of control (cells only). (B) Cellular uptake of CRC- TS. (C) Cellular uptake of CRC- SA. (D) bar graphs representing the uptake of curcumin loaded SLNs.

3.4.4 *In vitro* apoptosis studies

The induction of apoptosis by CRC after the treatment with both pure and CRC loaded SLN at different concentration were detected and quantified by flow cytometry. Externalization of phosphatidyl serine (PS) at the outer plasma membrane is an early event in apoptosis, which

is a consequence of loss of plasma membrane asymmetry hence; the PS externalization was detected as an indicator of apoptosis by targeting for the loss of plasma membrane asymmetry by method described earlier (Speth et al., 1988). Apoptosis inducing ability of all formulations were evaluated with PE Annexin V/7aad staining, which binds to cells that express phosphatidylserine on the outer layer of cell membrane, a characteristic feature of cells entering apoptosis (Speth et al., 1988). This allows discrimination of live cells from apoptotic cells (stained with PE Annexin V) and necrotic or late apoptotic pathway (stained with both PE Annexin V and 7AAD). Pure CRC treated cells (15μg/ml) demonstrated that 12% cells were early apoptotic and 24% cells were late apoptotic. In addition as shown in Figure 3.7 CRC-TS and CRC-SA displayed an early and late apoptotic percentage of 35.4%; 40.3% and 20.2%; 34.0% respectively at 50μg/ml. At higher concentration of CRC an increase in late apoptosis percentage is proven to be significant for both lipid based SLNs when compared to unstained cells (p=0.0005 and p<0.0001).
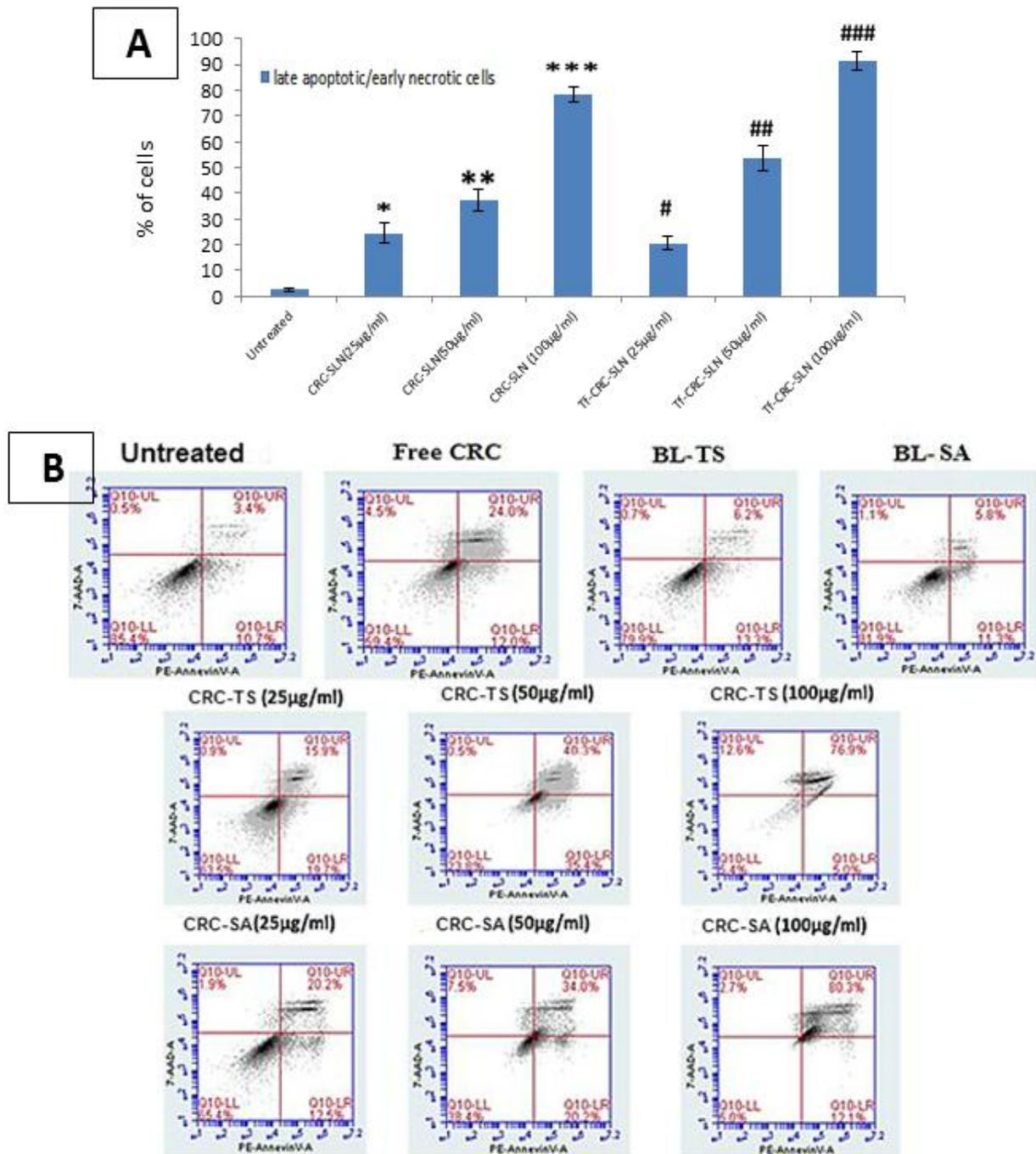
Figure 3. 7 Quantitative apoptotic measurements of LNCaP cells after treatment with BL-SA, pure CRC, CRC-SA and CRC-TS (A) Dose dependent effect on late apoptosis by treatment with a concentration of 25, 50 and 100 μg/ml of CRC-SA and CRC-TS dose for 24 h. Data as mean±S.D. (n = 3). (*) p =0.0005, Control versus CRC-SA and CRC-TS (25μg/ml), (**) p < 0.0001, Control versus CRC-SA and CRC-TS(50μg/ml), (***) p < 0.0001, Control versus CRC-SA and CRC-TS (100μg/ml) (B) Dose dependent effects are expressed as dot plot of PE AnnexinV versus 7-AAD. Dot plot from flow cytometry analysis reveals the four different populations of cells. Top left: necrotic cells; top right: late apoptotic cells; bottom left: live cells; and bottom right: early apoptotic cells.

The effect of blank samples (4mg/ml) was also investigated after 24 hr incubation. The difference of apoptotic inducibility percentage between the blank-SLN treated cells and unstained cells can be considered negligible. Since the controls showed that they have negligible apoptotic effect, this can indicate that the apoptosis induced by all CRC loaded formulations were indeed because of curcumin.

3.5 Conclusions

In this study curcumin was encapsulated in tristearin and stearic acid based SLNs and evaluated as an anticancer drug delivery system against LNCaP prostate cancer cells. The cytotoxicity studies of blank and SLN encapsulated CRC showed promising results for further development of an effective CRC loaded SLN formulation. Both CRC loaded SLNs showed similar cell viability which was reduced to almost 5% at 100µg/ml. It was shown that bulk CRC reduced cell viability to 4% at a very low concentration (40 µg/ml), while the CRC encapsulated SLN showed effective reduction of cell viability at higher CRC concentrations. This behaviour is related to the sustained release pattern of CRC from SLN. Cellular uptake studies showed CRC-SLN internalisation within the cytoplasm around the nucleus of the cells. Sufficient therapeutic potential was indicated by both lipids based CRC-SLNs as both these CRC-SLNs showed prominent apoptosis upon incubation on the cells. Another important observation from the dose dependent apoptosis study of CRC-SLN was detection of distinctly more late apoptotic cells than early apoptotic cells which can be attributed to the diffusion and accumulation of CRC at high concentration directly at the sight of action causing more necrosis. The effective *in vitro* anticancer activity of both CRC-SLN formulations suggests that can be used for future *in vivo* studies.

3.6 References

1. Alam, S., Panda, J. J., & Chauhan, V. S. (2012). Novel dipeptide nanoparticles for effective curcumin delivery. *International journal of nanomedicine*, *7(5)*, 4207.

2. Das, M., & Sahoo, S. K. (2012). Folate decorated dual drug loaded nanoparticle: role of curcumin in enhancing therapeutic potential of nutlin-3a by reversing multidrug resistance. *PLoS One*, *7*(3), e32920.

3. Freitas, C., & Müller, R. H. (1999). Correlation between long-term stability of solid lipid nanoparticles (SLN™) and crystallinity of the lipid phase. *European journal of pharmaceutics and biopharmaceutics*, *47*(2), 125-132.

4. Kakkar, V., Singh, S., Singla, D., & Kaur, I. P. (2011). Exploring solid lipid nanoparticles to enhance the oral bioavailability of curcumin. *Molecular nutrition & food research*, *55*(3), 495-503.

5. Khor, T. O., Keum, Y. S., Lin, W., Kim, J. H., Hu, R., Shen, G., ... & Kong, A. N. T. (2006). Combined inhibitory effects of curcumin and phenethyl isothiocyanate on the growth of human PC-3 prostate xenografts in immunodeficient mice. *Cancer research*, *66*(2), 613-621.

6. Kong, A. N. T. (Ed.). (2013). *Inflammation, oxidative stress, and cancer: Dietary approaches for cancer prevention*. CRC Press.

7. Li, W., Khor, T. O., Xu, C., Shen, G., Jeong, W.-S., Yu, S., & Kong, A.-N. (2008). Activation of Nrf2-antioxidant signaling attenuates NF-κB-inflammatory response and elicits apoptosis. *Biochemical pharmacology, 76(11), 1485–1489*

8. Liu, J., Gong, T., Wang, C., Zhong, Z., & Zhang, Z. (2007). Solid lipid nanoparticles loaded with insulin by sodium cholate-phosphatidylcholine-based mixed micelles: preparation and characterization. *International journal of pharmaceutics*, *340*(1), 153-162.

9. López-Lázaro, M. (2008). Anticancer and carcinogenic properties of curcumin: considerations for its clinical development as a cancer chemopreventive and chemotherapeutic agent. *Molecular nutrition & food research*, *52*(S1), S103-S127.

10. Mehnert, W., & Mäder, K. (2001). Solid lipid nanoparticles: production, characterization and applications. *Advanced drug delivery reviews*, *47*(2), 165-196.

11. Mohanty, C., & Sahoo, S. K. (2010). The *in vitro* stability and *in vivo* pharmacokinetics of curcumin prepared as an aqueous nanoparticulate formulation. *Biomaterials*, *31*(25), 6597-6611.

12. Mulik, R. S., Mönkkönen, J., Juvonen, R. O., Mahadik, K. R., & Paradkar, A. R. (2012). Apoptosis-induced anticancer effect of transferrin-conjugated solid lipid nanoparticles of curcumin. *Cancer nanotechnology*, *3*(1-6), 65-81.

13. Mulik, R. S., Mönkkönen, J., Juvonen, R. O., Mahadik, K. R., & Paradkar, A. R. (2010). Transferrin mediated solid lipid nanoparticles containing curcumin: enhanced *in vitro* anticancer activity by induction of apoptosis. *International journal of pharmaceutics*, *398*(1), 190-203.

14. Reddyt, L. H., & Murthy, R. R. (2004). Influence of polymerization technique and experimental variables on the particle properties and release kinetics of methotrexate from poly (butylcyanoacrylate) nanoparticles. *Acta pharmaceutica*,*54*(2), 103-118.

15. Serpe, L., Catalano, M. G., Cavalli, R., Ugazio, E., Bosco, O., Canaparo, R., & Zara, G. P. (2004). Cytotoxicity of anticancer drugs incorporated in solid lipid nanoparticles on HT-29 colorectal cancer cell line. *European journal of pharmaceutics and biopharmaceutics*, *58*(3), 673-680.

16. Siekmann, B., & Westesen, K. (1994). Thermoanalysis of the recrystallization process of melt-homogenized glyceride nanoparticles. *Colloids and surfaces B: biointerfaces*, *3*(3), 159-175.

17. Speth, P. A. J., Van Hoesel, Q. G. C. M., & Haanen, C. (1988). Clinical pharmacokinetics of doxorubicin. *Clinical pharmacokinetics*, *15*(1), 15-31.

18. Sun, J., Bi, C., Chan, H. M., Sun, S., Zhang, Q., & Zheng, Y. (2013). Curcumin-loaded solid lipid nanoparticles have prolonged *in vitro* antitumour activity, cellular uptake and improved *in vivo* bioavailability. *Colloids and surfaces b: biointerfaces*, *111*, 367-375.

19. Tiyaboonchai, W., Tungpradit, W., & Plianbangchang, P. (2007). Formulation and characterization of curcuminoids loaded solid lipid nanoparticles. *International Journal of Pharmaceutics*, *337*(1), 299-306.

20. Yang, K. Y., Lin, L. C., Tseng, T. Y., Wang, S. C., & Tsai, T. H. (2007). Oral bioavailability of curcumin in rat and the herbal analysis from Curcuma longa by LC–MS/MS. *Journal of chromatography B*, *853*(1), 183-189.

21. Yang, L., Chen, L., Meng, B., Suo, J., Wang, H., Xie, H.,& Zhang, L. (2006). The effect of curcumin on proliferation and apoptosis in LNCaP prostate cancer cells. *Chinese journal of clinical oncology*, *3*(1), 55-60.

22. Yousefi, A., Esmaeili, F., Rahimian, S., Atyabi, F., & Dinarvand, R. (2009). Preparation and *in vitro* evaluation of a pegylated nano-liposomal formulation containing docetaxel. *Scientia Pharmaceutica*, *77(21)*, 453-464.

CHAPTER 4: RETINOIC ACID DELIVERY TO LNCAP HUMAN PROSTATE CANCER CELLS USING SOLID LIPID NANOPARTICLES

4.1 Introduction

Solid lipid nanoparticles (SLN) have attracted increasing attention as promising colloidal carrier systems, especially for lipophilic drugs (Chen et al., 2001; Mehnert et al., 2001; Müller et al., 2004; Castelli et al., 2005). SLN are spheres or platelets in the submicron size range (mainly between 150 and 300 nm). These are made up from lipids, which are solid at room and body temperature and dispersed in an aqueous medium (Müller et al., 2011 and Battaglia and Gallarate., 2012). SLNs are composed of a high melting point lipid as a solid core, which is coated by surfactants. Therefore, lipophilic drugs can be efficiently incorporated in the lipid core of SLNs. SLNs are consisted of a solid core rather than a fluid core such as liposomes and emulsions, which facilitates prolonged and controlled release of drugs (Mehnert et al., 2001). SLN incorporated drugs are protected against chemical degradation (Lim et al., 2002). SLNs are easier to scale up compared with other drug delivery systems such as polymeric nanoparticles or liposomes (Mueller et al., 2000). The advantages of SLNs have driven numerous studies with various applications, particularly for parenteral administration. Typical SLN parenteral applications include intra-articular to intravenous peroral administration (Muller et al., 2000). Studies performed by Gasco et al., revealed that intravenously administered SLN have led to prolonged drug plasma levels. Moreover, a much lower uptake by liver and spleen macrophages are also observed due to low surface hydrophobicity of SLNs avoiding the absorption of any blood proteins (Gasco et al., 1993 and Goppert and Muller, 2005).

Retinoic acid (RTA) is a promising anticancer agent, which has been investigated in chemoprevention and treatment of cancer (Orlandi et al., 2002 & Carneiro et al., 2012). The anticancer properties of RTA are achieved by binding to retinoic acid receptors or retinoid X receptors present on the nuclear membrane of cancer cells, leading to the induction of growth inhibition, differentiation or apoptosis in these cells (Fang et al., 2002). RTA has already been used in clinical trials where RTA was given to cancer patients by oral administration, though the RTA concentration in blood circulation gradually decreases after long-term oral treatment. This phenomenon might occur due to the induced cytochrome P-450-dependent metabolism of RTA (Muindi et al., 1992). The poor aqueous solubility of RTA can be a

major drawback for its parenteral administration. However, the incorporation of RTA in lipid-based carriers such as SLNs can be an attractive mean to overcome the solubility limitations. The aim of this study was to develop stable RTA-SLN formulations with improved cellular uptake and anticancer efficiency in prostate LNCaP cancer cells.

4.2 Materials

Retinoic acid was purchased from TCI (UK). Stearic acid (SA), tristearin (TS) and trilaurin (TL) were purchased from Sigma-Aldrich. Precirol® ATO 5 (PR) was purchased from Gattefosse. Poloxamer 188 (P188) was kindly donated by BASF (Ludwigshafen, Germany). All the other chemicals and solvents were of analytical and high-performance liquid chromatography (HPLC) grade. LNCaP cell line was purchased from American Type Culture Collection (ATTC, Manassa, Virginia, USA). Dulbecco's modified Eagle's medium (DMEM), thiazolyl blue tetrazolium bromide (MTT), L-glutamin, Penicillin streptomycin and heat inactivated fetal bovin serum (FBS) and trypsin was purchased from Sigma -Aldrich (UK). PE Annexin V Apoptosis Detection Kit I from BD Biosciences, UK.

4.3 Methods

4.3.1 Preparation of SLN

Please refer to chapter 2, section 2.3.1

4.3.2 Particle size analysis and zeta potential

Please refer to chapter 2, section 2.3.2

4.3.3 Atomic force microscopy

For AFM experiments, 3µL of RTA loaded and unloaded SLN were deposited onto a freshly cleaved mica surface ((G250-2 mica sheets 1" x 1" x 0.006"; Agar Scientific Ltd, Essex, UK), and left to dry for 1 h before AFM imaging. The images were obtained by scanning the mica surface, in air, under ambient conditions using a PeakForce QNM Scanning Probe Microscope (Digital Instruments, Santa Barbara, CA, USA; Bruker Nanoscope analysis software Version 1.40). The AFM measurements were obtained using ScanAsyst-air probes, and the spring constant (0.67 N/m; nominal 0.4 N/m) and deflection sensitivity were calibrated, but not the tip radius (a nominal value of 2 nm was used). Surface roughness (Ra) values were determined by entering surface scanning data into a digital levelling algorithm (Bruker Image Analysis Nanoscope Analysis software V 1.40). AFM images were collected from two different samples by random spot surface sampling (at least five areas).

4.3.4 Lyophilisation of SLNs

Please refer to chapter 2, section 2.3.3

4.3.5 X-ray diffraction

Please refer to chapter 2, section 2.3.4

4.3.6 Differential scanning calorimetry (DSC)

Please refer to chapter 2, section 2.3.5

4.3.7 Determination of encapsulation efficiency

The drug loading (DL) and encapsulation efficiency (EE) was estimated according to Potta et al., (2011). In brief, 1 ml of SLN nanosuspension was centrifuged at 40,000 rpm, for 30 min at 25°C. The pellets of RTA loaded SLN were then dissolved in acetonitrile and the absorbance of the dissolved pellet were measured after appropriate dilutions. The DL and encapsulation efficiency (EE%) were calculated by using Equations (1) and (2).

$$Drug\ loading\ = \frac{Amount\ of\ RTA\ in\ SLNs}{amount\ of\ SLNs} \times 100\ \ (1)$$

$$Encapsulation\ efficiency\ = \frac{Drug\ loading}{Theoretical\ drug\ loading} \times 100\ \ (2)$$

4.3.8 Drug release properties of RTA-SLNs

SLN dispersion (1ml) was transferred into a cellulose dialysis bag (molecular weight cut-off: 10,000), which was then suspended in a beaker containing a mixture of double-distilled water and ethanol (50:50, v/v) as the dissolution medium (Liu et al., 2007). The beaker was then placed in a shaker bath with a set temperature of 37°C. At various time intervals, the whole content of the beaker was emptied and replaced with another 20 ml of dissolution medium. Drug content was analysed using UV at λ$_{max}$ of 340 nm.

4.3.9 Cell viability test

LNCaP prostate cancer cell lines were cultured in DMEM (Sigma, UK) medium supplemented with 10% serum (Gibco, UK), 1X L-glutamine/penicillin streptomycin (Sigma, UK) at 37ºC and 5% CO2. The culture medium was changed every three days. The cytotoxicity of RTA loaded SLNs and pure RTA (dissolved in ethanol) was determined in LNCaP prostate cancer cell line using MTT assay. Cells were seeded in a 24 well flat-bottom plate at cell density of 1×10^6 cells/well in 1ml DMEM and incubated for 24 hr. The SLN

formulations, (empty, loaded), pure RTA and ethanol were then added into the 24 well plates at various concentrations for different incubation times (24, 48 hr). Pure RTA were solubilized in ethanol (10mg/ml) and incubated at RTA concentrations of 10, 20, 50, 100, 200 µg/ml. At the end of the incubation time 100 µL of MTT solution (5 mg/ml) was added to each well and incubated at 37 ºC for another 2 hours. The culture medium was then discarded and 200 µl of acidified isopropanol added to dissolve the MTT formazan crystals. A total of 100 µL of the dissolved MTT formazan crystals was transferred into a 96 well flat-bottom plate and absorbance read at 492 nm using a microplate reader. Controls included are non-treated cells and ethanol (2%) for the pure drug cytotoxicity assay. Blank (unloaded) and loaded SLN formulation were incubated and the cytotoxicity of blank and loaded SLN formulations were also tested on LNCaP cells. Concentrations of blank SLN were kept between 0.18, 0.37, 0.73, 1.11, 1.47 and 2.94 mg/ml while loaded formulations had drug concentration of 12.5, 25, 50, 75, 100 and 200 µg/ml.

4.3.10 Cellular uptake by fluorescent microscopy

Samples for microscopic analysis were prepared via seeding 2×10^4 cells/well on cover slips in a 24 well flat-bottom plate. Empty rhodamine (10µg/10mg of lipid) stained SLN formulation was incubated with the cells for 24 hr at various concentrations. The cell medium was discarded from the well after 24 hr incubation time and washed three times with PBS. 1 ml of 4% para-formaldehyde was added to the well to fix the cells on the cover slips and left in the dark for 15 minutes. The para-formaldehyde was discarded from the well and cells were washed three times with PBS and then mounted on a glass slide using vectashield mounting medium containing DAPI. The cover slips were sealed on a glass slide with a nail polish and left to dry. Images were acquired using the Nikon ECLIPSE 90i overhead epifluorescent microscope attached to a Nikon digital camera (DS-Qi1Nc) and a computer running Nikon NIS-Elements Advanced Research software. The principal objective used for fluorescent imaging was an oil immersion CFI Plan Apochromat VC 60X N2 (NA1·4, WD 0·13 mm).

4.3.11 *In vitro* apoptosis studies

Apoptosis is a form of cell death that plays an important role during development, normal tissue homeostasis and is deregulated in many diseases, including cancer. The effect of apoptosis in LNCaP prostate cancer cell lines was studied by flow cytometry. The early stages of apoptosis were detected following staining with a PE Annexin V Apoptosis Detection Kit I containing 7AAD as vital stain (BD, UK). The cells were seeded in a 24 well flat-bottom plate at cell density of 1×10^6 cells/well and incubated for 24 hr. and SLN formulations, (empty, loaded) and pure RTA (25 ug/ml) were added to the 24 well plates. Untreated cells were used as negative control. After 48 hr, cells were stained according to manufacturer protocol. Samples were analysed on the Accuri C6 flow cytometer for PE and 7AAD expression using a solid state blue laser with a 488 nm excitation spectrum and a detector of FL1 path with filter 530/30 nm. A minimum of 10000-gated events was acquired from the cell population and data analysed using the Accuri C6 software. Cells were considered early apoptotic when PE positive and 7AAD negative; late apoptotic/early necrotic when PE positive and 7AAD positive. All experiments were performed in triplicates and repeated three times.

4.3.12 Statistical analysis

Please refer to chapter 3, section 3.3.6

4.4 Results and discussion

4.4.1 Particle size distribution and zeta potential

The particle size and zeta potential of blank SLN's prepared by various lipids was investigated by using the same lipid/surfactant ratios as shown in Table 4.1. As previously discussed in chapter 2, lipid and surfactant amount was kept to 500mg and 250mg due to the unstable characteristics of the SLN dispersion upon alteration of lipid and surfactant amount. Higher amount of lipid concentration can affect the particle size, which in turn destabilises the dispersion. Moreover, increasing the surfactant amount can cause rapid particle surface deformation (Freitas et al., 1999). Laser diffraction analysis showed monomodal particle size distribution for all dispersions with sizes varying from 140 – 150nm and polydispersity indexes less than 0.22. It is obvious he lipid nature did not affect the obtained SLN particle sizes. Similarly the zeta potential varied between -13 to -19mV which resulted is an indication of long term stability as the higher zeta potential values indicate high electric charge on the surface of the SLNs, which induces strong repellent forces among particles to prevent aggregation of the SLN dispersion (Yousefi et al., 2009). Indeed SLN dispersions were stable over six months with a slight increase on the particle size varying from 10 – 20nm (table 4.3).

RTA loaded SLNs of the same lipids were then prepared by high-pressure homogenisation at temperatures above the lipid melting point. Initially, SLNs were loaded with 50mg RTA as, an increased amount of RTA resulted in rapid flocculation which was not suitable for particle size or zeta potential experiments. During the process optimization it was observed that RTA-SLN prepared with TL and PR were very unstable followed by drug precipitation within a few hours even at low drug loadings and thus further evaluation of RTA-SLNs with these two lipids was not possible. The loaded SLN dispersions prepared by TS and SA showed far better stability and were further evaluated. RTA-SLNs prepared by using TS as the core lipid showed an average particle size of 255.9nm and zeta potential of -0.05 mV but appeared to be unstable during long term stability. After six months, RTA recrystallization was observed and a second particle size peak at 3.3μm appeared as shown in Figure 4.2.

In contrast RTA–SLNs prepared by using SA as the core lipid showed monomodal narrow particle size distribution with a z-average diameter of 232.3±3.1nm and -8.55±1.71 mV zeta potential. As shown in Table 4.2 for the RTA loaded SLNs a significant particle size increase was observed compared to the empty dispersions of the same lipids. This increase can be attributed to drug incorporation in the lipid nano-spheres. In addition, RTA can cause

significant increase in the viscosity resulting in an increase in particle size (Padhye *et al.*, 2013).

Table 4. 1 Blank SLN dispersions made by TS, SA, PR and TL (n=3)

SLNs	Lipid	Lipid (mg)	P188 (mg)	Particle size (nm, ±SD)	Zeta potential (mV, ±SD)	PI (±SD)
BL- TS	Tristearin	500	250	148.4 ±3.1	-19.20 ±1.61	0.11 ±0.03
BL- SA	Stearic Acid	500	250	145.1 ±2.7	-18.74 ±1.77	0.10 ±0.02
BL- PR	Precirol	500	250	143.4 ±1.2	-15.47 ±0.13	0.08 ±0.03
BL- TL	Trilaurin	500	250	149.2 ±5.5	-13.32 ±0.23	0.07 ±0.01

Table 4. 2 RTA loaded SLN dispersion made by SA and TS (n=3)

SLNs	Lipid	Lipid (mg)	P188 (mg)	RTA (mg)	Particle size (nm, ±SD)	Zeta potential (mV, ±SD)	PI (±SD)
RTA- TS	Tristearin	500	250	50	255.9 ±2.7	-0.06 ± 0.01	0.30± 0.09
RTA- SA	Stearic acid	500	250	50	232.3 ±3.1	-8.55 ±1.71	0.21±0.05

Table 4. 3 Stability of SLN dispersions after 1, 3 and 6 months.

	Months	Particle size (nm)		Zeta Potential (mV)	
		Empty	Loaded	Empty	Loaded
RTA-SA	1	147 ±0.9	233.2 ±1.9	-18.55 ±1.3	-8.19 ±1.1
	3	151.1 ±3.6	237.3 ±2.7	-18.11 ±1.2	-7.88 ±1.5
	6	154.8 ±1.1	240.7 ±3.1	-18.01 ±0.1	-7.81±0.6
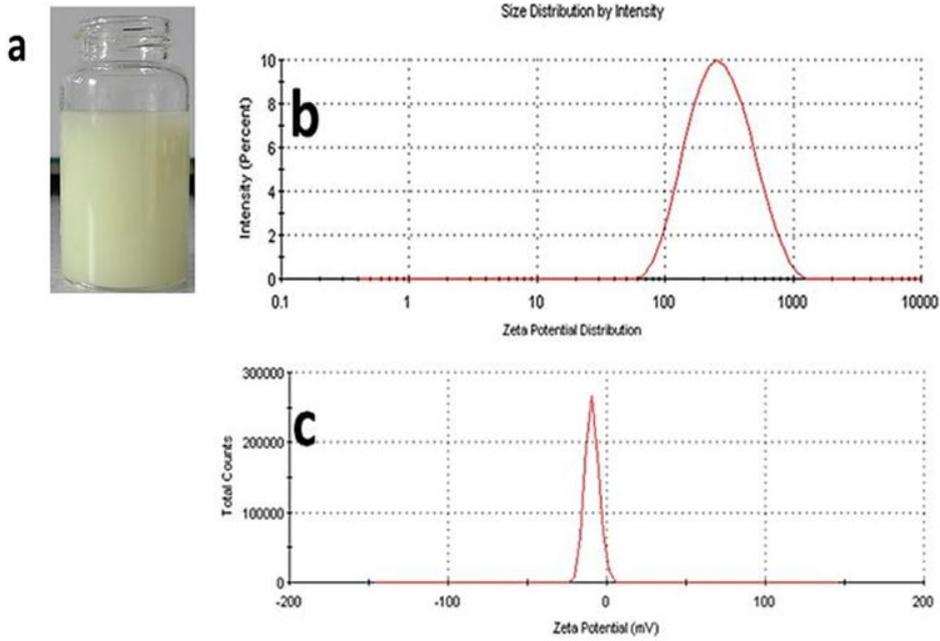
Figure 4. 1 (a) RTA-SA SLN dispersion. (b) Particle size distribution of RTA-SA (nm) (c) Zeta potential (mV) of RTA-SA.
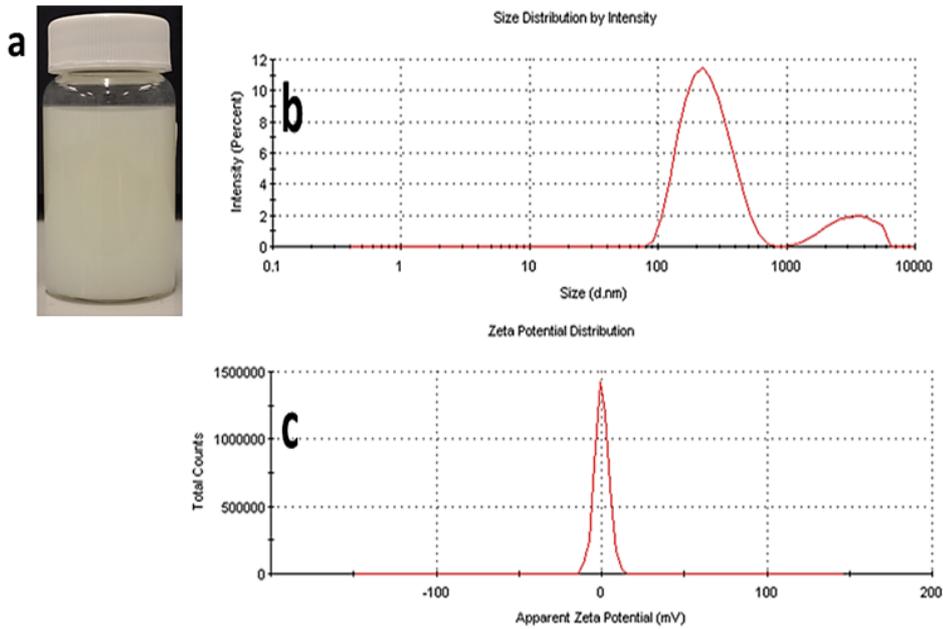
Figure 4. 2 (a) RTA-TS SLN dispersion. (b) Particle size distribution of RTA-TS (nm). (c) Zeta potential (mV) of RTA-TS

4.4.2 AFM morphology of SLNs

AFM analysis identified SLNproperties at high resolution across a topographic image to measure the particle size. The overall particle diameter (estimated from the width of the peak at the baseline in section height profiles), for both empty and loaded SLN dispersions were estimated, as shown in Figure 4.3. AFM analysis revealed spherical shaped nanoparticles with particle sizes of 117.8 ±11.0 nm and 169.8 ±21.0 nm for empty and loaded SLNs respectively. The results obtained from the AFM imaging are similar to those from the laser diffraction measurements but with slightly smaller particle diameters. Again the reason for the observed smaller particle sizes is that SLNs were absorbed on the mica surface and underwent a drying process, which might have attributed to the size deformation (Jung et al., 2006). Moreover, in AFM studies there is a slight flattening of the SLNs which might also be responsible in giving away slight difference between the diameter and the height of nanoparticles (Dubes et al., 2003).
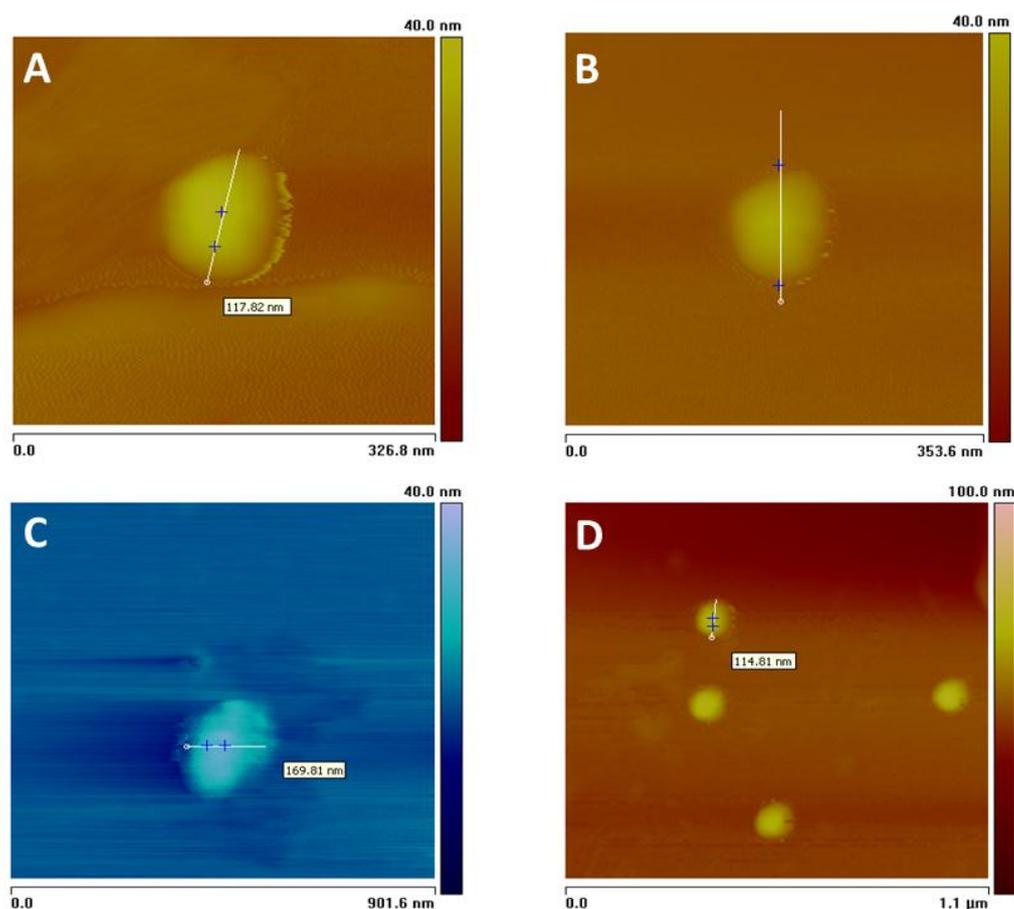
Figure 4. 3 AFM images of blank-SLN (A, B) and RTA loaded SLN (C, D)

4.4.3 Physicochemical characterization

The physical state of bulk materials, empty SLN and RTA-SLN was evaluated by XRD analysis. The empty and drug loaded dispersions were freeze dried prior to the X-ray analysis. As shown in Figure 4.4 the diffractograms of bulk SA and RTA showed characteristic sharp peaks at 6.63°, 11.1°, 21.55°, 24.15° and 5.19°, 13.52°, 14.71°, 15.56°, 20°, 20.8°, 22.81°, 24.98°, 24.98°, 26.15°, 27.23° 2θ values respectively which indicated the crystalline nature of both materials. Similarly P188 presented intensity peaks at 19.17°, 23.36° 2θ values. In Figure 4.5 it is evident that the less ordered crystals of SA are present for both empty and loaded SLNs where the majority of the intensity peaks has disappeared. Likewise no RTA intensity peaks could be observed for the drug loaded SLNs suggesting that RTA is entrapped within the lipid core in an amorphous form (Mulik & Monkkonen, 2010).
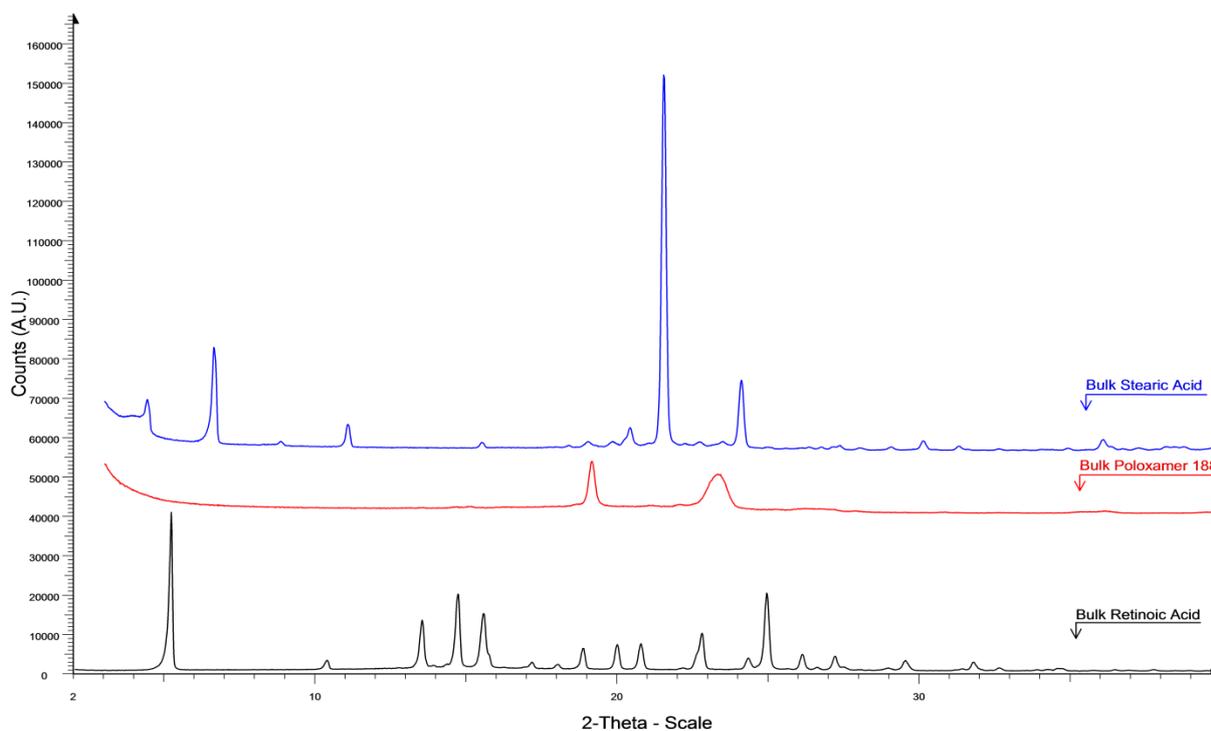
Figure 4. 4 XRD diffractogram of bulk stearic acid, poloxamer 188 and retinoic acid.
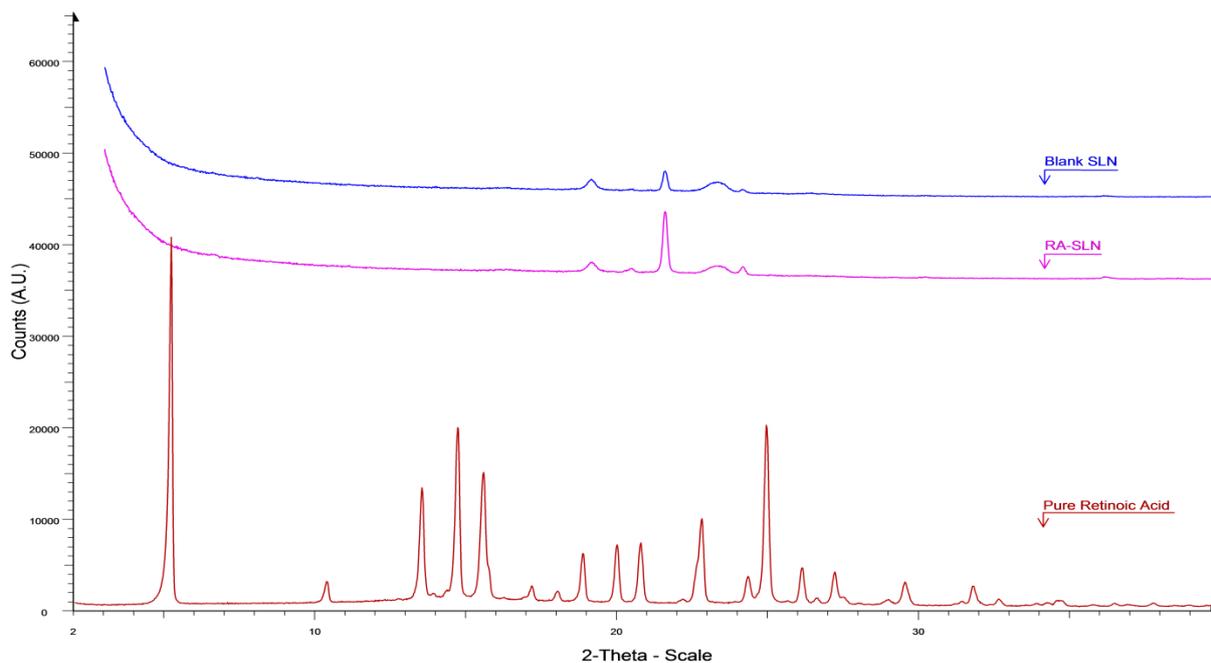
Figure 4. 5 XRD diffractograms of blank SLN, RTA-SLN and retinoic acid.

DSC thermal analysis of bulk SA, P88, RTA empty and loaded SLNs carried out to further investigate the physical state of the colloidal lipid matrices. The bulk SA, P188 and RTA presented melting endothermic peaks at 69.82°C, 51.81°C and 167.80°C respectively. The SLN formulations showed two distinct melting endothermic peaks at 66.49°C and 49°C, which are attributed to the lipid and surfactant respectively. The melting endotherms of empty SLNs appeared broad, and less sharp compared to the bulk substances indicating an increased number of lattice defects (Siekmann et al., 1994). In addition, the melting peaks for both empty and loaded SLNs were shifted at lower temperatures indicating possible surfactant - lipid interactions (Padhye et al., 2013). For the RTA-SLN the melting endotherm of RTA could not be observed suggesting that the drug is in amorphous state. However, RTA could have been completely solubilised in the lipid matrix due to the melting of drug in lipid (Padhye et al., 2013). In another study Mulik et al. (2012) proposed that these findings indicate the entrapment of RTA within the nanoparticles in a molecular dispersion form.
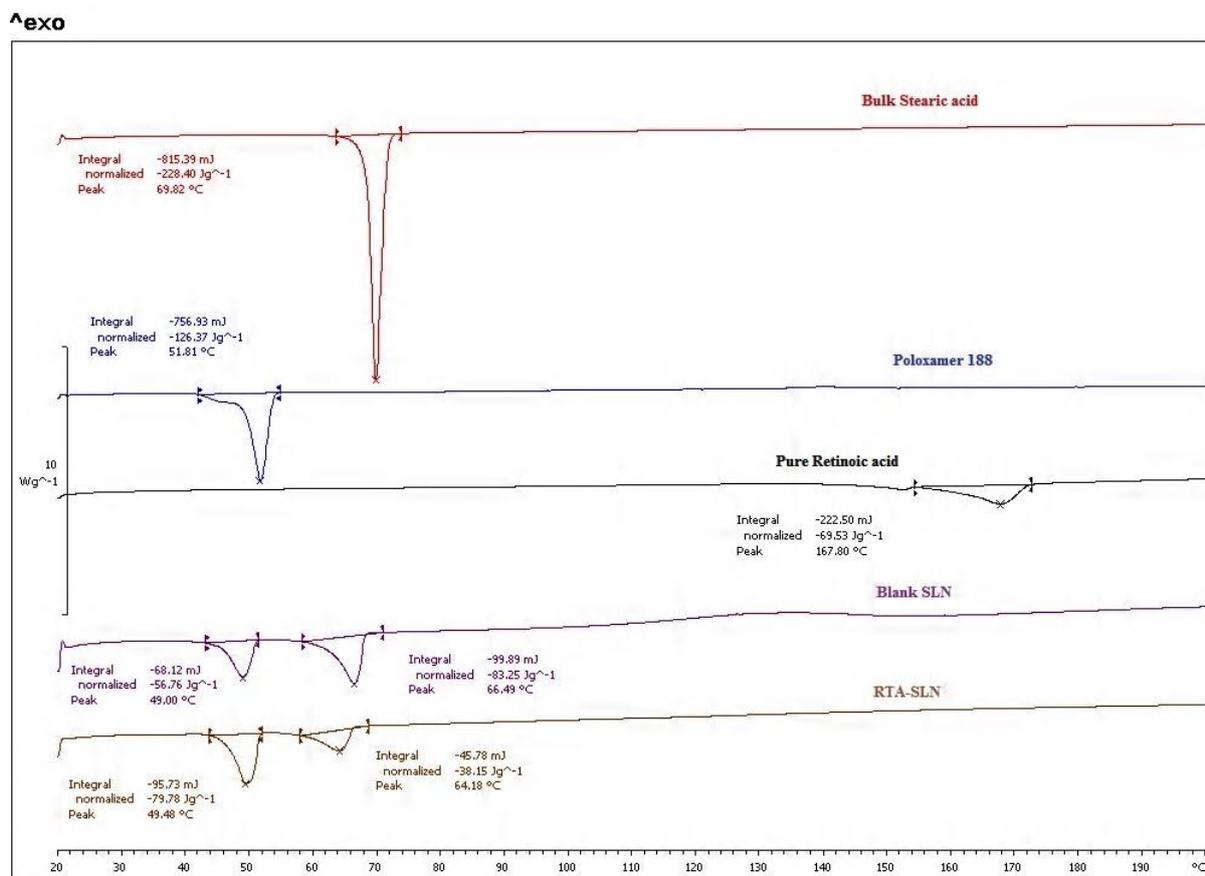
Figure 4. 6 DSC thermographs of RTA, bulk stearic acid, P188, BL-SLN and RTA-SLN

4.4.4 Determination of EE and DL

RTA-SLNs prepared either with SA or TS as the core lipid demonstrated EE of 90% suggesting very high drug entrapment in the nanoparticles. As RTA is very hydrophobic the stability of the drug within the lipid matrix is considered to be the key factor behind drug encapsulation within the SLN (Chinsriwongkul et al., 2011). According to Tiyaboonchai et al., (2007) addition of surfactant in SLN dispersions plays a key role in enhancing the drug loading efficiency. In the developed SLN dispersions P188 was used as a surfactant, where the estimated DL observed was 6.2 %. Nevertheless the DL was not very high as RTA started precipitating immediately when loading was increased.

4.4.5 Drug release studies

As shown in Figure 4.7, RTA-SLN formulations presented a biphasic *in vitro* drug release pattern. A burst release was observed for the first 10 hr where almost 40% drug was released followed by sustained release for five days. The initial burst release characteristics indicates

that some drug molecules were adsorbed onto the particle surface, while the sustained release pattern suggests drug diffusion from the core of the lipid matrix (Sun et al., 2013). According to Nayak et al., (2010) the drug release patterns from the lipid core depends greatly on the crystallinity of the lipid matrix. As shown from the XRD analysis, RTA loaded SLN diffractograms showed less ordered crystals as a majority, as a result less ordered lipid matrix helps drug to elute out more rapidly.
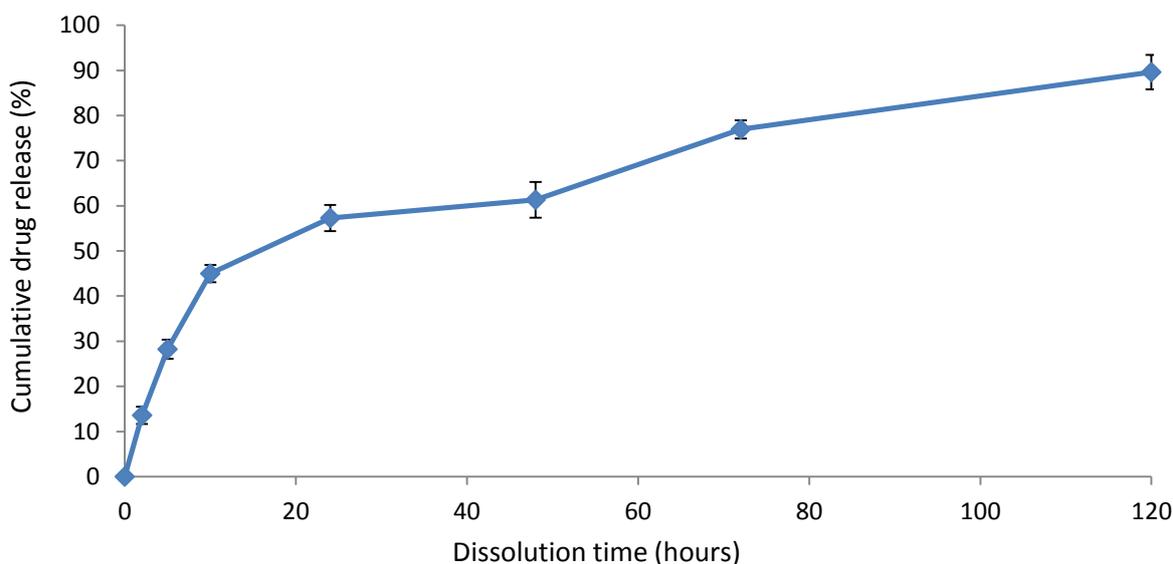
Figure 4. 7 Drug release profile of stearic acid based SLNs loaded by RTA.

4.4.6 Cell viability of RTA and SLN formulations

The cytotoxicity of bulk RTA, empty and RTA loaded SLN was evaluated in LNCaP prostate cancer cells by using an MTT assay. The RTA cyctotoxicity was extrapolated by comparison of alcoholic solution and loaded SLNs treatment. According to Serpe et al., (2004), SLN can enter cancer cells, which should facilitate the anticancer activity of the drug when encapsulated in the lipid core.

RTA a potent anticancer agent showed strong cytotoxicity on LNCaP cell lines at the concentration of 20 µg/ml, where the cell viability was reduced at 59.3% after 24 hr incubation (Figure 4.8). The RTA cytotoxicity increased with the drug concentration and at 50 µg/ml the viability was reduced to 46.75% while further increase at 200µg/ml resulted in 9.53% cell viability. The observation is in agreement with previous data on the effect of RTA on prostate cancer cells (McCormick et al., 1999).
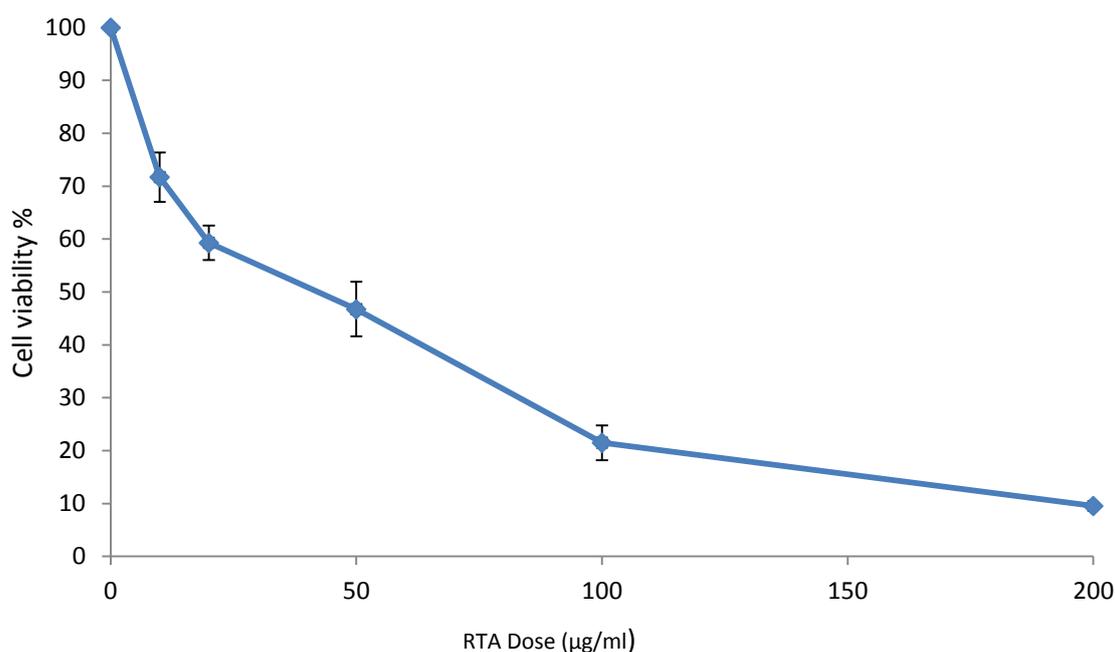
Figure 4. 8 Antiproliferative effects of pure RTA on prostate cancer cells (LNCaP) using the MTT assay for 24 hr incubation time.

As shown in Figure 4.9 the cytotoxicity of empty SLNs with SA as the core lipid was evaluated in order to confirm any significant loss in cell viability. The results showed negligible cytotoxicity with 90% cell viability at 3mg/ml of SLN dispersions.
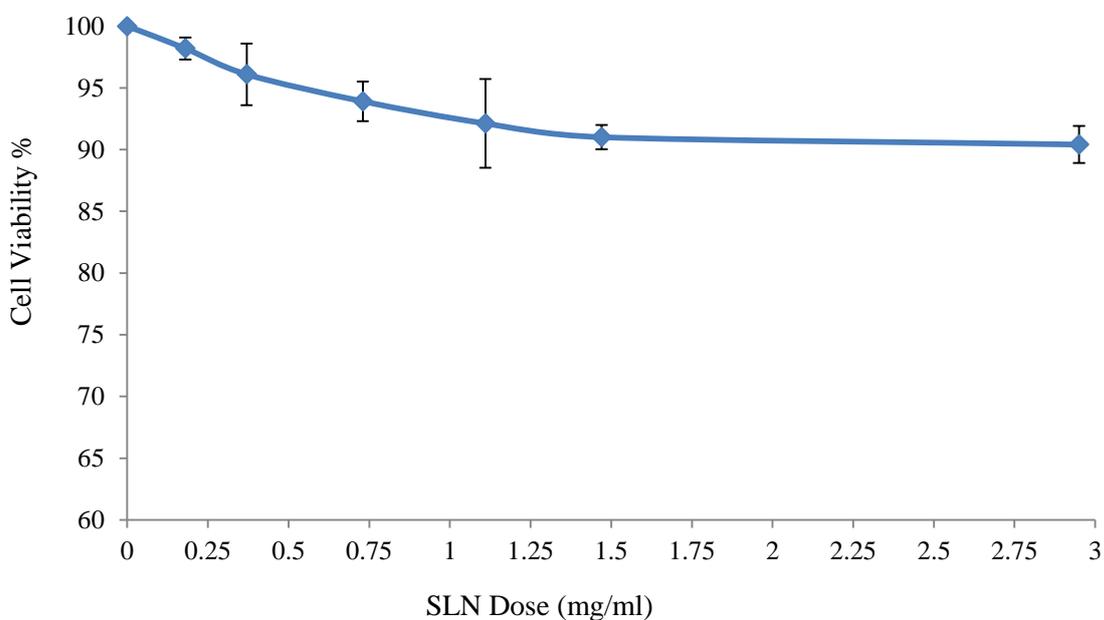
Figure 4. 9 Cell viability of Stearic acid based blank SLN (BL- SLN), after 24 hours of incubation.

The effect of increase in RTA concentration on cell viability was assessed by MTT assay (Figure 4.10). It was observed that with RTA-SLN the toxic effect was dose dependent. At the lowest drug concentration tested of 12.5µg/ml cell viability had decreased to 88.64% while remaining significantly higher in control cells treated with SLN formulation only (p<0.05). With an increasing drug concentration the cytotoxic effect got even more pronounce. At 100µg/ml drug concentration significant difference in cell viability was observed between RTA-SLN and blank SLN formulations, as the cell viability was taken down to 46.84% (P<0.001).With an even RTA concentration of 200µg/ml the cell viability was 35.17%. The effect of treatment time on the cytotoxicity of RTA-SLN was also investigated. After 48h treatment RTA-SLN was significantly more effective than after 24h treatment. As the cell viability was 19.75 % at a RTA concentration of 200µg/ml. The time dependant increase in the cytotoxic effect suggests that more drug is released from the lipid matrix indicating sustained release effect of RTA-SLN. These findings also show that free RTA (Figure 4.10) is significantly more anti-proliferative than RTA-SLN. In case of blank SLN, since it doesn't necessarily possess any significant effect on cell viability, the confirmation of RTA's effect on the LNCaP prostate cancer cell was confirmed.
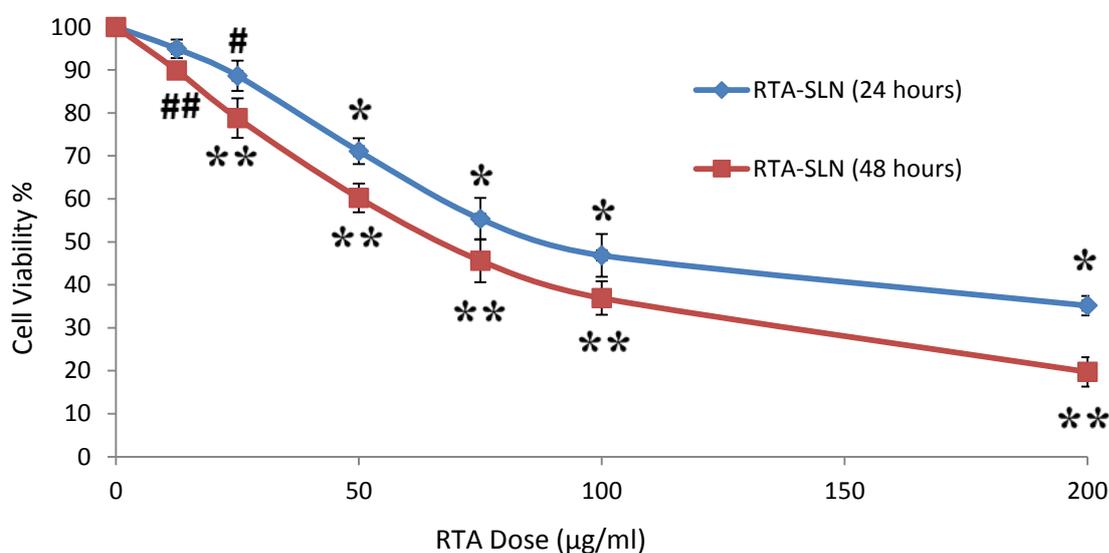
Figure 4. 10 Cell viability of Stearic acid based RTA loaded SLN (RTA-SLN), after 24 and 48 hr incubation. Data is represented as mean±S.D. (n = 3). #p<0.05, *p< 0.0001, RTA-SLN (24 hr) vs. BL-SLN and ##p<0.05, **p< 0.0001, RTA-SLN (48 hr) vs. BL-SLN

4.4.7 Cellular internalisation and *in vitro* apoptosis

SLNs are known to enter cells via endocytosis. In order to confirm the internalization of the SLN formulation, rhodamine containing SLN was incubated with prostate cancer cell line (LNCaP) and cellular uptake visualised via fluorescent microscopy after staining the nucleus of the cells with DAPI. Internalization of SLN formulation was observed after 24 hrs. SLN particles were localised in the cytoplasm around the cell nucleus as illustrated in Figure 4.11
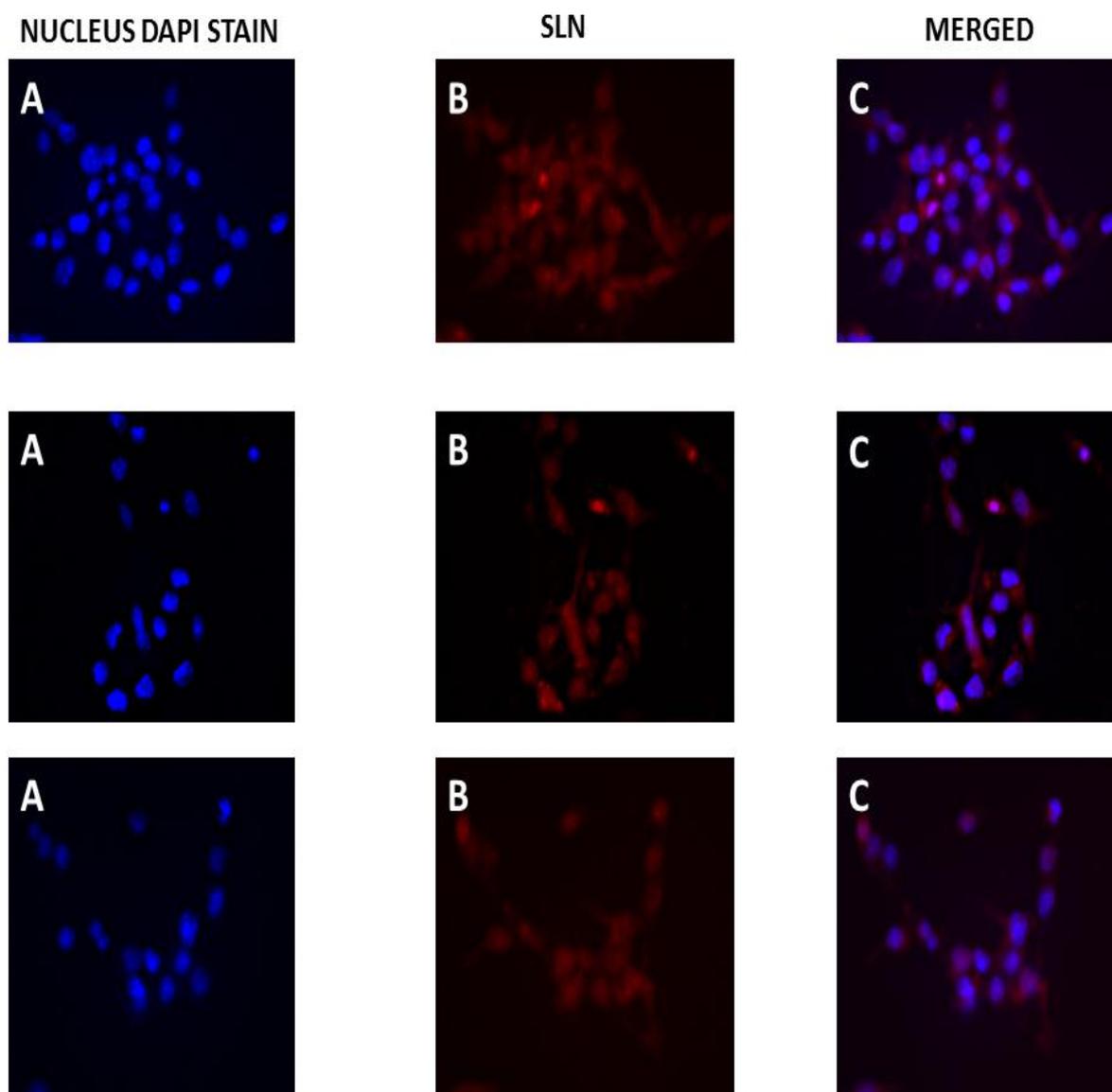
Figure 4.11 Fluorescent images of the cellular uptake of empty formulated SLN localisation in the cytoplasm of the cell. The nucleus of the cell was stained blue with DAPI and SLN formulation was labelled with rhodamine, red.

The induction of apoptosis by RTA both pure and within SLN at different concentration was detected and quantified by flow cytometry (Figure 4.12). Cells treated with pure RTA (25µg/ml) showed that 24.3% of the whole population was early apoptotic while 20% was

late apoptotic/ early necrotic. Similarly, when treated with RTA-SLN at 25µg/ml 27.4% were early apoptotic and 17.7% were late apoptotic/ early necrotic. These results suggest that like pure RTA, RTA loaded SLN's also induced apoptosis. At higher concentration of both treatments an increase in late apoptotic/early necrotic cells percentage were observed (Figure 4.12).

The increase in the percentage of late apoptotic/early necrotic cells following treatment clearly linked RTA and RTA loaded SLNs which appeared to be significantly higher when compared to untreated cells ($p < 0.05$). This increasing population of late apoptotic/early necrotic cells with higher concentration confirmed that enhanced cytotoxicity of RTA-SLN's was dose dependant. Experiments with control (blank SLN treated cells) and untreated cells showed negligible effects in terms of inducing the apoptotic pathways, as no significant alteration were observed in both early apoptotic and late apoptotic/early necrotic cell populations.
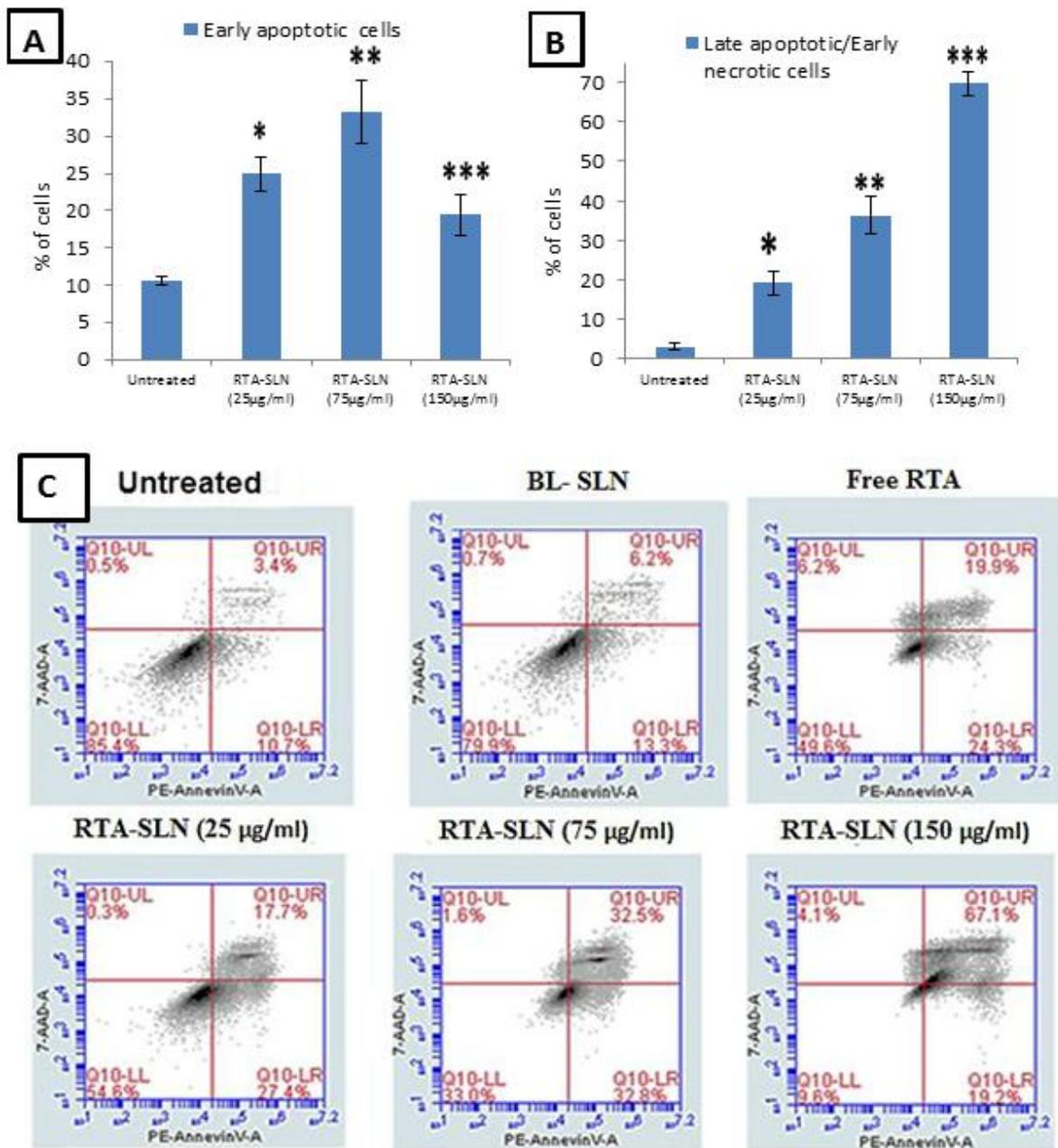
Figure 4. 2 Quantitative apoptotic measurement in LNCaP cells after treatment with BL-SLN (blank SLN), pure retinoic acid and RTA-SLN (RTA loaded SLN). (A) Dose dependent effect on early apoptosis by treatment with a concentration of 25, 75 and 150μg/ml of RTA-SLN dose for 48 h determined by flow cytometry analysis. (B) Dose dependent effect on late apoptosis by treatment with a concentration of 25, 75 and 150μg/ml of RTA-SLN dose for 48 h determined by flow cytometry analysis. The results are expressed as bar chart. Data as mean±S.D. (n = 3). (*) p< 0.05, Control versus RTA-SLN (25μg/ml), (**) p<0.05, Control versus RTA-SLN (75μg/ml), (***) p<0.05, Control versus RTA-SLN (150μg/ml) (C) Dose dependent effects are expressed as dot plot of PE AnnexinV versus 7-AAD. Top left: necrotic cells; top right: late apoptotic cells/early necrotic cells; bottom left: live cells; and bottom right: early apoptotic cells.

87

4.5 Conclusions

In the current study SLN dispersions were prepared by HPH and loaded with the anticancer agent RTA. Drug loaded SLNs presented good stability only when SA was used as core lipid. The dispersions showed high EE with biphasic release where the initial burst release was followed by a sustained pattern. The anticancer activity of RTA-SLNs was assessed in LNCaP prostate cancer cells and showed 19.75% at a RTA concentration of 200 µg/ml after 48 hours incubation. Moreover, fluorescent microscopy images confirmed the internalisation of SLNs inside the cytoplasm of the cell. *In vitro* apoptosis analysis revealed that upon treating the cells by RTA-SLN, 67.1% of the cells were late apoptotic/early necrotic at 150µg/ml RTA concentration. Overall the optimized RTA – SLN dispersions appeared to be a promising drug delivery system and can be used for further cancer treatment.

4.6 References

1. Battaglia, L., & Gallarate, M. (2012). Lipid nanoparticles: state of the art, new preparation methods and challenges in drug delivery. *Expert opinion on drug delivery*, *9*(5), 497-508.

2. Carneiro, G., Silva, E. L., Pacheco, L. A., de Souza-Fagundes, E. M., Corrêa, N. C. R., de Goes, A. M., & Ferreira, L. A. M. (2012). Formation of ion pairing as an alternative to improve encapsulation and anticancer activity of all-trans retinoic acid loaded in solid lipid nanoparticles. *International journal of nanomedicine*, *7*, 6011.

3. Castelli, F., Puglia, C., Sarpietro, M. G., Rizza, L., & Bonina, F. (2005). Characterization of indomethacin-loaded lipid nanoparticles by differential scanning calorimetry. *International journal of pharmaceutics*, *304*(1), 231-238.

4. Chen, D. B., Yang, T. Z., Lu, W. L., Zhang, Q. (2001). *In vitro* and *in vivo* study of two types of long-circulating solid lipid nanoparticles containing paclitaxel. *Chemical and pharmaceutical bulletin*, *49*(11), 1444-1447.

5. Chinsriwongkul, A., Chareanputtakhun, P., Ngawhirunpat, T., Rojanarata, T., Sila-on, W., Ruktanonchai, U., & Opanasopit, P. (2012). Nanostructured lipid carriers (NLC) for parenteral delivery of an anticancer drug. *Aaps pharmscitech*, *13*(1), 150-158.

6. Fang, J., Chen, S. J., Tong, J. H., & Wang, Z. G. (2002). Treatment of Acute Promyelocytic Leukemia with ATRA and As2O3: A Model of Molecular. *Cancer biology & therapy*, *1*(6), 614-620.

7. Gasco, M. R. (1993). *U.S. Patent No. 5,250,236*. Washington, DC: U.S. Patent and Trademark Office.

8. Göppert, T. M., & Müller, R. H. (2005). Adsorption kinetics of plasma proteins on solid lipid nanoparticles for drug targeting. *International journal of pharmaceutics*, *302*(1), 172-186.

9. Jung, H., Kim, J., Park, J., Lee, S., Lee, H., Kuboi, R., & Kawai, T. (2006). Atomic force microscopy observation of highly arrayed phospholipid bilayer vesicle on a gold surface. *Journal of bioscience and bioengineering*, *102*(1), 28-33.

10. Li, W. W., Li, V. W., Hutnik, M., & Chiou, A. S. (2011). Tumour angiogenesis as a target for dietary cancer prevention. *Journal of oncology*, *2012*.

11. Lim, S. J., & Kim, C. K. (2002). Formulation parameters determining the physicochemical characteristics of solid lipid nanoparticles loaded with all-trans retinoic acid. *International journal of pharmaceutics*, *243*(1), 135-146.

12. Liu, J., Gong, T., Wang, C., Zhong, Z., & Zhang, Z. (2007). Solid lipid nanoparticles loaded with insulin by sodium cholate-phosphatidylcholine-based mixed micelles: preparation and characterization. *International journal of pharmaceutics*, *340*(1), 153-162.

13. Maden, M. (2007). Retinoic acid in the development, regeneration and maintenance of the nervous system. *Nature reviews neuroscience*, *8*(10), 755-765.

14. McCormick, D. L., Rao, K. V. N., Steele, V. E., Lubet, R. A., Kelloff, G. J., & Bosland, M. C. (1999). Chemoprevention of rat prostate carcinogenesis by 9-cis-retinoic acid. *Cancer research*, *59*(3), 521-524.

15. Mehnert, W., & Mäder, K. (2001). Solid lipid nanoparticles: production, characterization and applications. *Advanced drug delivery reviews*, *47*(2), 165-196.

16. Mueller, R. H., Maeder, K., & Gohla, S. (2000). Solid lipid nanoparticles (SLN) for controlled drug delivery–a review of the state of the art. *European journal of pharmaceutics and biopharmaceutics*, *50*(1), 161-177.

17. Muindi, J., Frankel, S., Miller, W. J., Jakubowski, A., Scheinberg, D. A., Young, C., . Warrell, R. J. (1992). Continuous treatment with all-trans retinoic acid causes a progressive reduction in plasma drug concentrations: implications for relapse and

retinoid" resistance" in patients with acute promyelocytic leukemia [published erratum appears in Blood 1992 Aug 1; 80 (3): 855]. *Blood*, *79*(2), 299-303.

18. Mulik, R. S., Mönkkönen, J., Juvonen, R. O., Mahadik, K. R., Paradkar, A. R. (2012). Apoptosis-induced anticancer effect of transferrin-conjugated solid lipid nanoparticles of curcumin. *Cancer nanotechnology*, *3*(1-6), 65-81.

19. Muller, R. H., & Keck, C. M. (2004). Challenges and solutions for the delivery of biotech drugs–a review of drug nanocrystal technology and lipid nanoparticles. *Journal of biotechnology*, *113*(1), 151-170.

20. Müller, R.H., Shegokar, R., Keck, C.M., 2011. 20 years of lipid nanoparticles (SLN and NLC): present state of development and industrial applications. *Current drug Discovery Technologies 8*(3), 207–227.

21. Nayak, A. P., Tiyaboonchai, W., Patankar, S., Madhusudhan, B., & Souto, E. B. (2010). Curcuminoids-loaded lipid nanoparticles: novel approach towards malaria treatment. *Colloids and Surfaces B: Biointerfaces*, *81*(1), 263-273.

22. Orlandi, M., Mantovani, B., Ammar, K., Avitabile, E., Dal Monte, P., & Bartolini, G. (2002). Retinoids and cancer: antitumoural effects of ATRA, 9-cis RA and the new retinoid IIF on the HL-60 leukemic cell line. *Medical principles and practice: international journal of the Kuwait University, Health science centre*, *12*(3), 164-169.

23. Padhye, S. G., & Nagarsenker, M. S. (2013). Simvastatin solid lipid nanoparticles for oral delivery: Formulation development and *In vivo* evaluation.*Indian journal of pharmaceutical sciences*, *75*(5), 591.

24. Potta, S. G., Minemi, S., Nukala, R. K., Peinado, C., Lamprou, D. A., Urquhart, A., & Douroumis, D. (2011). Preparation and characterization of ibuprofen solid lipid nanoparticles with enhanced solubility. *Journal of microencapsulation*,*28*(1), 74-81.

25. Serpe, L., Catalano, M. G., Cavalli, R., Ugazio, E., Bosco, O., Canaparo, R., ... & Zara, G. P. (2004). Cytotoxicity of anticancer drugs incorporated in solid lipid nanoparticles on HT-29 colorectal cancer cell line. *European journal of pharmaceutics and biopharmaceutics*, *58*(3), 673-680.

26. Siekmann, B., Westesen, K. (1994). Thermoanalysis of the recrystallization process of melt-homogenized glyceride nanoparticles. *Colloids and surfaces B: Biointerfaces*, *3*(3), 159-175.

27. Speth, P. A. J., Van Hoesel, Q. G. C. M., & Haanen, C. (1988). Clinical pharmacokinetics of doxorubicin. *Clinical pharmacokinetics*, *15*(1), 15-31.

28. Sun, J., Bi, C., Chan, H. M., Sun, S., Zhang, Q., & Zheng, Y. (2013). Curcumin-loaded solid lipid nanoparticles have prolonged *in vitro* antitumour activity, cellular uptake and improved *in vivo* bioavailability. *Colloids and surfaces b: biointerfaces*, *111*, 367-375.

29. Tiyaboonchai, W., Tungpradit, W., & Plianbangchang, P. (2007). Formulation and characterization of curcuminoids loaded solid lipid nanoparticles. *International journal of pharmaceutics*, *337*(1), 299-306.

30. Yang, M., He, S., Fan, Y., Wang, Y., Ge, Z., Shan, L., ... & Gao, C. (2014). Microenvironmental pH-modified solid dispersions to enhance the dissolution and bioavailability of poorly water-soluble weakly basic GT0918, a developing anti-prostate cancer drug: Preparation, characterization and evaluation *in vivo*. *International journal of pharmaceutics, 475*(1), 97-109.

31. Yang, X., Liu, Y., Liu, C., & Zhang, N. (2012). Biodegradable solid lipid nanoparticle flocculates for pulmonary delivery of insulin. *Journal of biomedical nanotechnology, 8*(5), 834-842.

32. Yousefi, A., Esmaeili, F., Rahimian, S., Atyabi, F., & Dinarvand, R. (2009). Preparation and *in vitro* evaluation of a pegylated nano-liposomal formulation containing docetaxel. *Scientia Pharmaceutica*, *77(21)*, 453-464.

CHAPTER 5: FORMULATION AND DELIVERY OF CURCUMIN LOADED NANOSTRUCTURED LIPID CARRIERS (NLC) WITH ANTI-TUMOUR ACTIVITY ON LNCAP PROSTATE CANCER CELLS

5.1 Introduction

Curcumin, a yellow-coloured phenolic substance derived from the rhizome of the spice herb *Curcuma longa,* widely known as turmeric, has a broad spectrum of biological and pharmacological activity. Clinical trials have shown that curcumin has antioxidant, anti-inflammatory, anti-bacterial, anti-fungal, and anti-carcinogenic activity. Further, the cardio protective and neuro protective effects of curcumin are also well documented (Thiyagarajan et al*.,* 2004). The most compelling and key rationale for the therapeutic use of curcumin is its good safety profile. To date, no studies in either animals or humans have demonstrated any toxicity associated with the use of curcumin, even at high doses (Shankar *et al.,* 1980). Unfortunately the potential use of CRC is severely limited by its poor water solubility and short biological half-life, which results in low bioavailability irrespective of the route of administration (Newman *et al.,* 2007). Several approaches have been investigated to increase the bioavailability of curcumin, including nanoparticles, liposomes, micelles, and phospholipid complexes. SLNs have been intensively studied as a drug delivery system for CRC for several routes of administration, such as peroral, parenteral, dermal, and topical delivery (Souto et al*.,* 2007). However, several aspects of SLN are proven to be rather disadvantageous for the delivery of CRC. One of them is the possible drug expulsion from the solid lipid core due to the highly crystalline nature of the SLN matrix. Moreover, drug loading capacity can also be drastically reduced due to highly ordered crystalline arrangement (Souto et al*.,* 2007). To overcome these problems possessed by SLN, use of blends of lipids that do not form a highly ordered crystalline arrangement is needed. NLCs are the second generation lipid nano carriers composed of solid lipid matrix that are incorporated with liquid lipids (Zauner et al*.,* 2001). NLCs have the ability to strongly immobilize drugs and prevent the particles from coalescing by virtue of the solid matrix as compared to emulsions (Souto et al*.,* 2007). In addition, the mobility of the incorporated drug molecules is also drastically reduced in the solid phase. Furthermore, the liquid oil droplets in the solid matrix increase the drug loading capacity as compared to NLCs. NLCs also have the advantages over polymeric

nanoparticles including low toxicity, biodegradability, drug protection, controlled release, and avoidance of organic solvents during production (Iqbal et al*.,* 2012). NLCs have been intensively studied as delivery carriers of hydrophobic drugs such as CRC. Several studies have been performed to evaluate the potential use of NLC for parenteral administration of CRC. Effectivity of CRC-NLC in central nervous system after systemic administration were also evaluated which gave rather satisfactory results (Puglia et al*.,* 2012). In these studies CRC loaded NLC were prepared by using high pressure homogenisation. These CRC-NLCs were characterized by size, zeta potential, polydispersity index and Scanning electron microscopy. Moreover, entrapment efficiency and drug loading of these CRC-NLCs were also evaluated. Release pattern of CRC from NLC was investigated. The anti-tumour effects of NLC formulations (both unloaded and loaded) were investigated on LNCaP human prostate cancer cells. As expected, blank NLC showed negligible effects on cell viability studies while CRC-NLC showed sufficient anti-tumour activity. The cell viability was taken down to almost 0% at 100µg/ml of CRC concentration after 48 hours of incubation. These anti-tumour activity confirmed CRCs efficiency as an anticancer agent. Cellular uptake by fluorescent microscopy and fluorescence activated cell sorting analysis (FACS) confirmed the localization of CRC in the cytoplasm around the nucleus. The induction of apoptosis by CRC-NLC was investigated by using flow cytometry. Where like pure curcumin, NLC loaded with CRC also followed same apoptotic pathway which confirmed CRC does retain its efficiency as an anticancer agent even after encapsulating it inside NLC.Tumour inhibition effects of pure CRC and NLC-CRC on nude mice bearing LNCaP prostate cancer xerograph's were evaluated.

5.2. Materials

Curcumin was purchased from Sigma-Aldrich (Dorset, UK), stearic acid, tristearin and oleic acid and tween 80 was purchased from Sigma-Aldrich. Poloxamer 188 was kindly donated by BASF (Ludwigshafen, Germany). All other chemicals and solvents were of analytical and high-performance liquid chromatography (HPLC) grade. LNCaP cell line was purchased from American Type Culture Collection (ATTC: Manassa, Virginia, USA). Dulbecco's modified Eagle's medium (DMEM), thiazolyl blue tetrazolium bromide (MTT), L-glutamin, Penicillin streptomycin and heat inactivated fetal bovin serum (FBS) and trypsin were all purchased from Sigma -Aldrich (UK). PE Annexin V Apoptosis Detection Kit I from BD Biosciences.

5.3 Methods

5.3.1 Preparation of NLC formulations

NLCs were prepared by high pressure homogenization. The lipid phase, consisting of stearic acid and oleic acid was coarsely emulsified in water phase by a high speed dispersion device. The pre-emulsion was then further processed with a high pressure homogenizer.

In brief, NLC comprising of appropriate amounts of lipid (both solid and liquid lipids), poloxamer 188, tween80 and/or no drug (CRC) were weighed out (Table 5.1). The volume of water to make these formulations were kept at 30 ml. Samples composed of either empty lipids or loaded with curcumin, were initially heated to a temperature above the melting point of the lipid. In case of curcumin encapsulated NLC, curcumin is separately dissolved in ethanol (3ml) and then it's mixed with the molten lipid. In this process curcumin gets dissolved in the molten lipid. The drug containing melt lipid was dispersed in a hot surfactant solution and homogenized with an UltraTurrax T25 (IKA®- WERKE GMBH, Staufen, Germany) homogenizer to form a pre-emulsion. The produced coarse dispersion was then transferred and homogenized in Micro DeBee (South Easton, MA, USA) high pressure homogenizer at 15,000 PSI for 7 minutes at 70^0C. The hot nanodispersions were left to cool down and allow lipid to crystallize by forming lipid nanoparticles with a solid matrix.

Table 5. 1 Compositions of BL-NLC and CRC-NLC

Formulations	Tristearin (mg)	Oleic Acid (mg)	Poloxamer 188 (mg)	Tween 80	CRC (mg)	Water (ml)
BL-NLC	400	250	150	100	90	30
CRC-NLC	400	250	150	100	90	30

5.3.2 Particle size analysis and zeta potential

Please refer to chapter 2, section 2.3.1

5.3.3 Determination of encapsulation efficiency

Please refer to chapter 2, section 2.3.6

5.3.4 Drug release properties of CRC-NLCs

Please refer to chapter 2, section 2.3.7

5.3.5 Cell viability Test

LNCaP prostate cancer cell lines were cultured using DMEM culture medium (supplemented with 10% serum, 1% L-glutamine and 1% penicillin streptomycin) in an incubator maintained at 37ºC and 5% CO_2. The culture medium was changed every three days. The cytotoxicity of curcumin loaded NLCs and pure curcumin (drug dissolved in ethanol) was determined in LNCaP prostate cancer cell line using MTT assay. Cells were seeded in a 24 well flat-bottom plate at cell density of 1×10^6 cells/well and incubated for 24 hours. After 24 hours the NLC formulations were added to the 24 well plates at various concentrations and incubation time. 100μL of MTT solution (5 mg/ml) was added to each well plate at the end of the incubation time and incubated at 37ºC for another 2 hours. The culture medium was discarded, followed by addition of 200μl of acidified isopropanol to dissolve the MTT formazan crystals. 100μL of the dissolved MTT formazan crystals was then transferred into a 96 well flat-bottom plate and absorbance was read at 492 nm using a microplate reader. Controls include non-treated cells and fixed volume of ethanol for the pure drug cytotoxicity assay. Curcumin was used at concentrations of 10, 20, 40, 50 and 100 μg/ml. Blank (unloaded) and loaded (90mg of drug) NLC formulation were incubated at NLC concentrations of 0.1, 0.2, 0.4, 0.6 and 0.9 mg/ml. Cytotoxicity of Blank and loaded NLC formulations were also tested on LNCaP prostate cancer cell line. The cytotoxicity of pure curcumin drug was also evaluated LNCaP prostate cancer cells for direct anti-proliferative efficacy evaluation with curcumin pure drug.

5.3.6 Cellular uptake by fluorescent microscopy

Please refer to chapter 3, section 3.3.3

5.3.7 Flow cytometric analysis for cellular uptake of NLCs

Please refer to chapter 3, section 3.3.4

5.3.8 *In vitro* apoptosis studies

Please refer to chapter 3, section 3.3.5

5.3.9 Treatment of mice bearing human prostate cancer xenografts

In vivo studies were carried out following treatment protocol previously reported by Yan et al., (2012) with slight modification. House and feed purchased female nude mice aged 6-8 weeks under standard conditions kept in a 12 hours light/ 24 hours dark cycle. LNCaP prostate cancer cell line was cultured in a complete culture medium DMEM. Prostate cancer xenograft was established by injecting 2×10^6 LNCaP cells (in 100μl of PBS) into the fat pad

of mouse mammary glands. Tumour allowed to grow for 3 days without any treatments and monitor the tumour volume daily by measuring two perpendicular tumour diameters with a calliper [tumour volume [mm3] = (length [mm]) x (width [mm])^2 x 0.52]. Afterwards the mice with the prostate cancer xenograft were divided into four groups (n=6/group) according to the treatment received: The blank control, CRC solution, Blank NLC and CRC encapsulated NLC. For CRC based treatments, 20 mg/kg of CRC was administered. The treatments were administered by injecting intravenously via mice tail (two injections per week with injection volume of 200µl for 4 weeks). Then tumour size measurements and animal weight were taken twice a week.

5.3.10 Statistical analysis of tumour regression

Please refer to chapter 3, section 3.3.6

5.4 Results and discussion

5.4.1 Size distribution and zeta potential

Preparation of BL-NLC and CRC-NLC was successfully achieved by using of high pressure homogenisation process. All components used for the fabrication of NLC were generally recognised as safe (GRAS) approved (Table 5.1). Particle size and zeta potential of BL-NLC and CRC-NLC were measured immediately after preparation and also for a period of 6 months after storage at 4^0C (Table 5.2). As shown in Figure 5.1 the particle analysis showed that the sizes of BL-NLC and CRC-NLC were in the range of 110-150 nm. The inclusion of CRC in NLCs slightly increased the particle size to approximately 36 nm. Nevertheless, Figure 5.2 shows a narrow, monomodal particle size distribution for both empty and drug loaded NLCs. Moreover, the small size range of NLC (110-150 nm) assured its acceptability for its usage as a parenteral drug delivery system. The size of nanoparticles can play a vital role in determining the bio-accessibility of the entrapped molecules (Jun et al., 2011) while the, decrease of the vesicle size results in increase of the drug bioavailability and prevents embolism (Verma et al., 2003). The polydispersity index (PI) of investigated NLCs showed values less than 0.3, indicating homogenous populations. Regarding zeta potential, all formulations displayed a negative surface charge ranging from -40 mV to -45 mV. In general, nanoparticles are considered to be stable dispersion when the absolute value of zeta potential is above -30 mV due to the electric repulsion between the particles (Puglia et al., 2012). The highly negative zeta potential of the developed NLC formulations resulted in stable nanodispersions while a small decrease in zeta potential values was observed for CRC-NLCs

(-42.8 ±0.6) with respect to BL-NLC (-44.1 ±1.4). This result could be explained by assuming a partial absorption of drug onto nanoparticle surface and consequent masking of the surfactant negative charges (Puglia et al., 2012).

Table 5. 2 Particle size and zeta potential of NLC formulations (n=3).

	Months	**Particle size (nm)**	**Zeta Potential (mV)**
Blank NLC	1	113.7 ±1.2	-44.1 ±1.4
	3	115.0 ±0.8	-44.1 ±0.3
	6	118.3 ±1.3	-42.9 ±0.9
CRC-NLC	1	146.5 ±1.1	-42.8 ±0.6
	3	147.7 ±1.7	-41.1 ±1.0
	6	149.6 ±2.4	-40.6 ±0.7

		Size (d.nm):	% Intensity:	St Dev (d.nm):
Z-Average (d.nm): 114.2	Peak 1:	146.1	100.0	49.63
Pdl: 0.209	Peak 2:	0.000	0.0	0.000
Intercept: 0.936	Peak 3:	0.000	0.0	0.000
Result quality : Good				

Size Distribution by Intensity

		Size (d.nm):	% Intensity:	St Dev (d.nm):
Z-Average (d.nm): 145.7	Peak 1:	178.8	100.0	83.82
Pdl: 0.170	Peak 2:	0.000	0.0	0.000
Intercept: 0.952	Peak 3:	0.000	0.0	0.000
Result quality : Good				

Size Distribution by Intensity
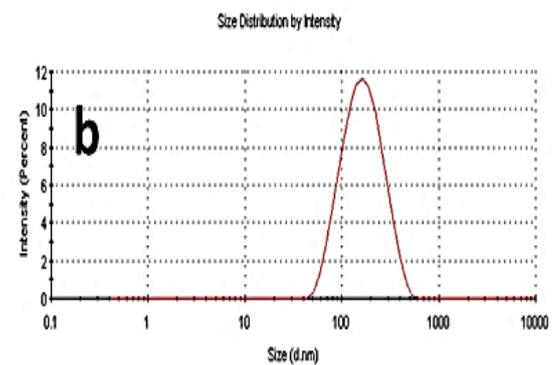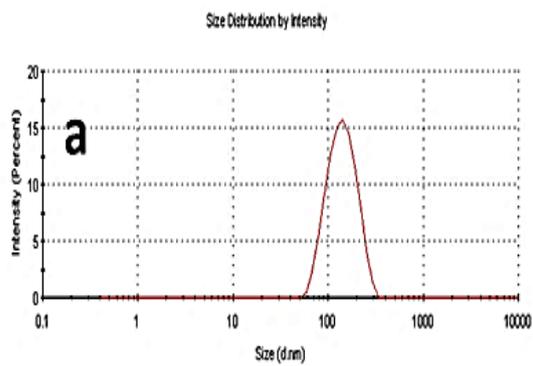
		Mean (mV)	Area (%)	St Dev (mV)
Zeta Potential (mV): -45.5	Peak 1:	-45.5	100.0	5.01
Zeta Deviation (mV): 5.01	Peak 2:	0.00	0.0	0.00
Conductivity (mS/cm): 0.00434	Peak 3:	0.00	0.0	0.00
Result quality : Good				

Zeta Potential Distribution

		Mean (mV)	Area (%)	St Dev (mV)
Zeta Potential (mV): -43.3	Peak 1:	-43.3	100.0	6.20
Zeta Deviation (mV): 6.20	Peak 2:	0.00	0.0	0.00
Conductivity (mS/cm): 0.00738	Peak 3:	0.00	0.0	0.00
Result quality : Good				

Zeta Potential Distribution
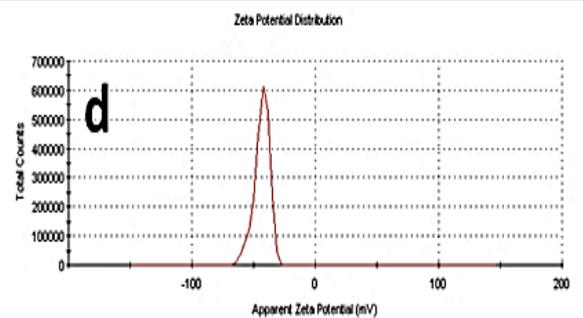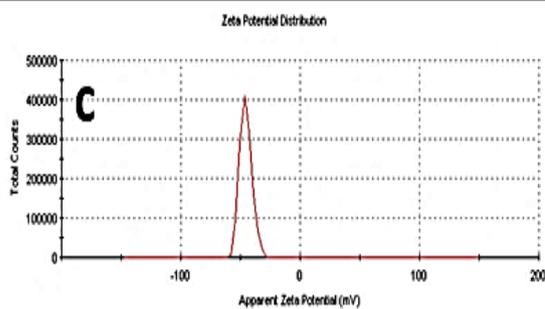
Figure 5. 1 (a) Particle size distribution of BL-NLC (nm). (b) Particle size distribution of CRC-NLC (nm). (c) Zeta potential (mV) of BL-NLC. (d) Zeta potential (mV) of CRC-NLC

5.4.2 Determination of encapsulation efficiency and drug loading

CRC-NLC formulations exhibited good drug loading and high entrapment efficiency. The drug loading of CRC-SLN formulation was 9.29%. Moreover, high values of entrapment efficiency (92.9%) of the CRC-NLC formulation indicated the efficiency of the hot homogenization method for lipophilic compounds and also demonstrate that there was no noteworthy loss of drug(s) during the procedure. These results are in agreement with the previous study as they have demonstrated nearly similar drug loading capacities of NLC formulations. (Fang et al., 2012). High entrapment efficiency and drug loading of these CRC-NLC formulations were achieved due to the lipophilic nature of CRC. Moreover, less ordered crystal lattice of NLCs also facilitated high drug loading, since less ordered crystals favoured the accommodation of drugs inside the lipid matrix (Nayak et al., 2010).

5.4.3 Drug release profile of CRC in NLC formulations

A key issue investigated in this study was the feasibility of using NLC to deliver CRC. The ability of NLC to deliver CRC was examined by determining the drug release, as shown in Figure 5.2 The release study carried over 120 hr at a controlled temperature of 37°C. The NLC and due to the CRC hydrophobic nature the release studies were conducted in 50% v/v ethanol solutions in which the solubility of CRC is 0.693 ± 0.13 mg/ml as suggested by (Kakkar et al., 2011).
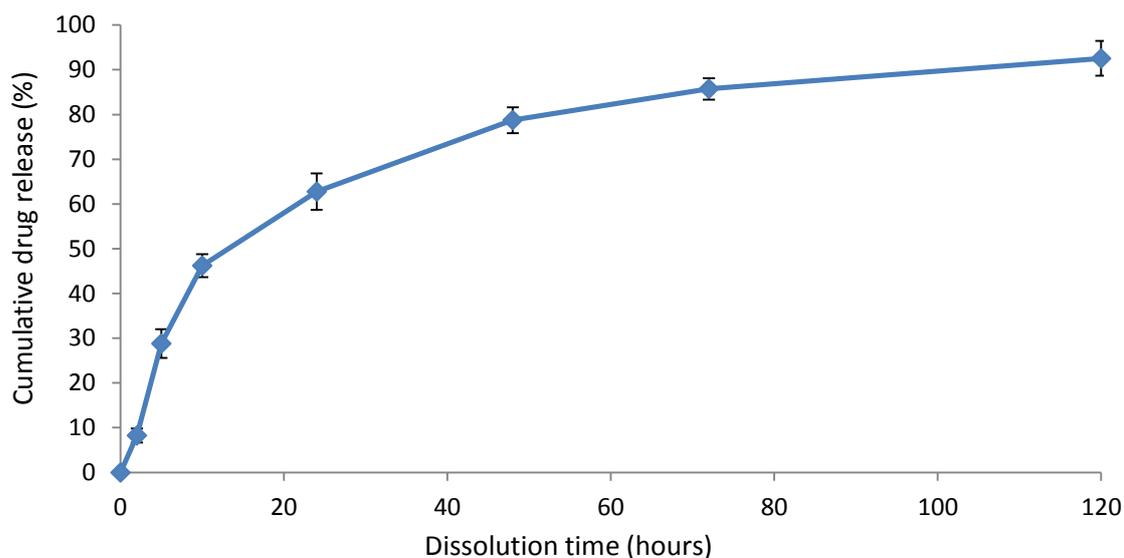
Figure 5. 2 *In vitro* release profiles of curcumin from CRC-NLC

CRC release pattern seems to be characterized by two different rends. An initial burst effect for the first 10 hours and a sustained drug release from NLC for the remaining time of monitoring. The percentage of cumulative release after 48 hours was 78.75%. Afterwards this value went up to 92.54% over the next 72 hours. The result is consistent with the findings of other researchers regarding CRC release from lipid nanoparticles (Nayak et al., 2010). Although, the components used to formulate CRC loaded lipid nanoparticles were different to the ones used in present work, the results obtained seem to have a common explanation: the burst effect can be attributed to the absorbed drug on the surface of NLC, while the sustained release is likely due to the time required for the drug to diffuse into the release medium from the NLC (Castelli et al., 2005). Interestingly both curcumin encapsulated SLN (Figure. 2.12) and NLC showed similar release pattern, although a blend of liquid and solid lipid should have contribute towards a faster release of CRC. Possible reason behind that is the usage of the dialysis bags and 50:50 alcoholic medium to evaluate release profiles. As this method can only be used to provide an indicative release pattern rather than the actual amount of released drug (Kakkar et al., 2011).

5.4.4 Antiproliferative effect of curcumin

To assess the cytotoxicity of CRC loaded NLC formulations, its tumour killing activity was determined against LNCaP prostate cancer cells by MTT assay. CRC loaded NLC formulations antiproliferative activity was evaluated in order to assess whether the efficacy of CRC was retained following the encapsulation into a lipid matrix. The antiproliferative effect of pure CRC on LNCaP prostate cancer cell line was first examined and compared to the CRC-NLC drug delivery system.

As previously discussed in Chapter 3 (Figure 3.1)bulk CRC exhibited excellent anti-proliferative activity after 24 hours incubation. According to researchers CRC tend to possess some of the most desired characteristics of a cancer therapeutic agent and preferential killing or therapeutic selectivity is one of it main features. In other words, CRC can undergo the preferential killing of cancer cells without significant effects to the normal cells(Liu et al., 2013). *In vitro* cytotoxicity activities of CRC on LNCaP prostate cancer showed significant anti-proliferative activity which is an indication of CRC's potency against this cancer cell line.

5.4.5 Antiproliferative effect of NLC formulations

Cytotoxicity of blank NLC formulations is considered to be an important aspect in terms of using it as a potent drug delivery system and negligible cytotoxicity of lipid nanoparticles is a prerequisite for cancer applications. Blank NLC formulations were tested on LNCaP prostate cancer cells to evaluate their effect on the cytotoxicity of LNCaP prostate cancer cell.
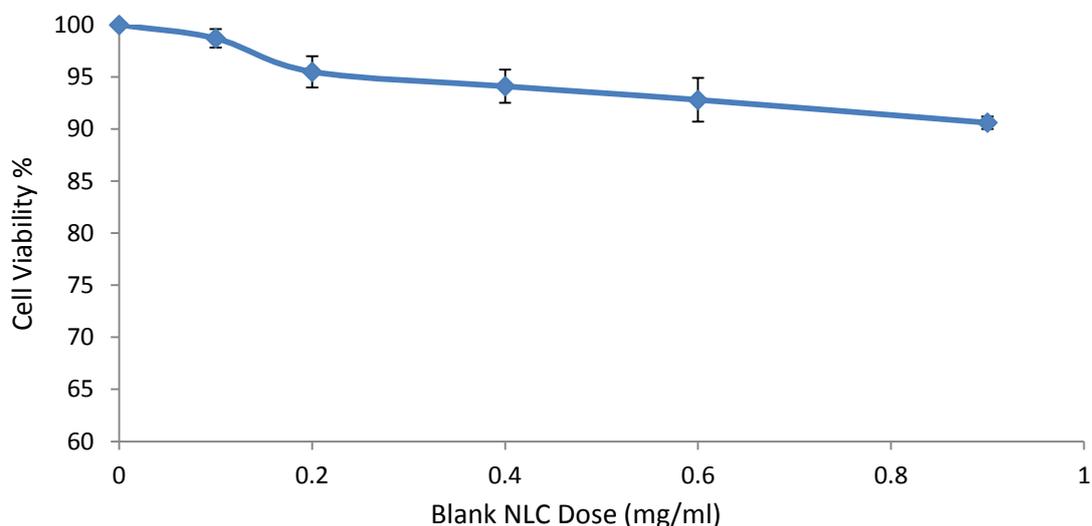
Figure 5. 3 Cytotoxicity of blank NLC formulation. Data is represented as mean±S.D. (n= 3).

As observed in Figure 5.3, blank NLC formulations have no effect on the cytotoxicity of the LNCaP prostate cancer cell. The cell viability was 90.6% after 24 hour of incubation at high NLC concentration (0.9mg/ml), which can be considered negligible (Mulik et al., 2010).
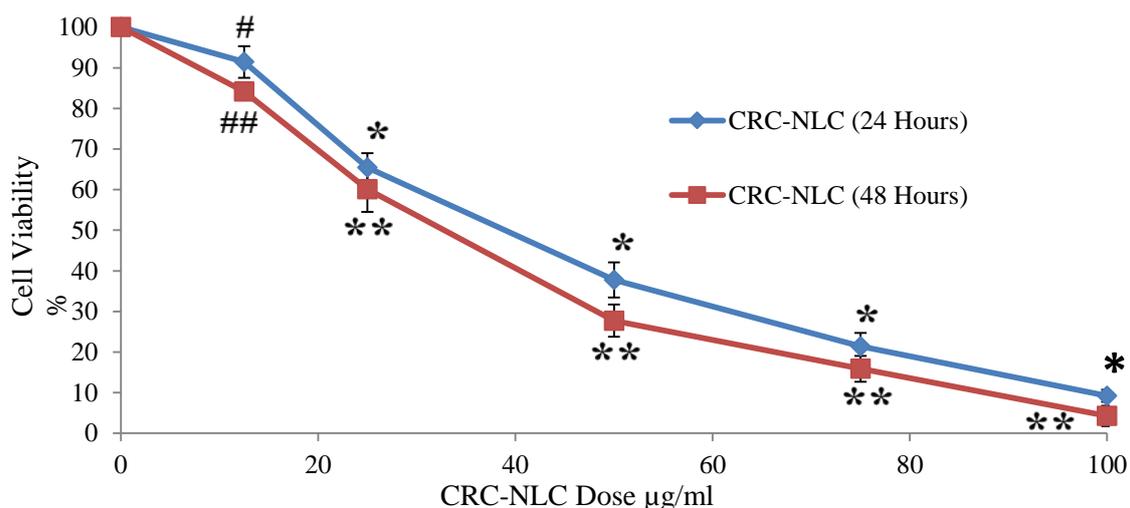
Figure 5. 4 Cytotoxicity of CRC loaded NLC formulation after 24 and 48 hours. Data is represented as mean±S.D. (n= 3). #p=0.0323, *p< 0.0001, CRC-NLC (24 hours) vs. BL-NLC and ##p=0.0003, **p< 0.0001, CRC-NLC (48 hours) vs. BL-NLC

101

The antiproliferative effect of CRC-NLC formulations was evaluated by the MTT assay. As shown in Figure 5.4 the increase of CRC concentration showed an effect on the viability of prostate cancer cells. At the lowest dose of 12.5μg/ml CRC concentration the cell viability was decreased down to 91.43%. At higher CRC concentrations of 50μg/ml and 75μg/ml the anti-proliferative activity of CRC-NLC was even more pronounce, as the cell viability was reduced to 37.78% and 21.39% respectively. At a dose of 100μg/ml the cell viability was further reduced to 9.2%, which is considered to be very significant when compared with blank NLC formulation (P<0.0001). This data's provided a clear indication that the antiproliferative effect of CRC-NLC is exerted on LNCaP prostate cancer cell line in a dose dependent manner. However, from the release studies of CRC-NLC, a sustained release pattern of CRC has been observed. To further evaluate this finding, a 48 hour study has also been conducted on LNCaP prostate cancer cells. As anticipated, after 48 hours of drug incubation the anti-proliferative effect was even more pronounce. By increasing the incubation time at 100μg/ml CRC concentration the cell viability was almost 0%. These results were in good agreement with those reported in another study by Ji *et al.,* (2007). This time dependent cytotoxic effect of CRC-NLC formulation is a clear indication of CRC's sustained release from NLC and also a prolonged inhibitory effect of CRC-NLC. These inhibitory effects of CRC-NLC is also proven to be slightly more efficient when compared with SLN based CRC loaded dispersions. As shown in Figure 3.3 CRC-SLN lowers down cell viability to 7.1% after 48 hour incubation, while at same concentration cell viability of CRC-NLC is 4.2%. A possible reason behind this difference is because of the solid and liquid lipid blend on NLC, which initiated a faster drug release and also improved the encapsulation efficiency of CRC (Zauner et al*.,* 2001). As, the blank NLC without any CRC had no effect on the cytotoxicity of LNCaP prostate cancer cells, it indicated that the cytotoxicity toward the prostate cancer cell was mainly a consequence of the CRC molecules.

5.4.6 Cellular Uptake by Fluorescence Microscopy

One of the advantages of CRC is its intrinsic fluorescence, which can be detected directly to quantify its cellular uptake. Fluorescence microscopy was used to investigate cellular uptake of CRC-NLCs. For a better understanding of the internalisation of the CRC-NLC inside the cell several parameters such as laser power, offset, sensitivity and gain constant were harmonized during cell imaging. According to Mohanty et al*.,* (2010) NLCs are known to enter the cells via endocytotic pathways. In order to confirm internalisation of these CRC-NLCs, 10 μg/ml of of CRC-NLC were incubated in LNCaP prostate cancer cell for 24 hours.

Upon incubation qualitative cellular uptake studies were performed. The nucleus of the cell was stained with DAPI, a DNA selective fluorescent probe (Suzuki et al., 1997) prior to the experiment, and after fixation the images were recorded. The superimposed images as shown in Figure 5.4, clearly indicates green (CRC-NLC) and blue (nucleus) areas, confirming the internalisation of CRC-NLC within the cytoplasm of the around the nucleus.
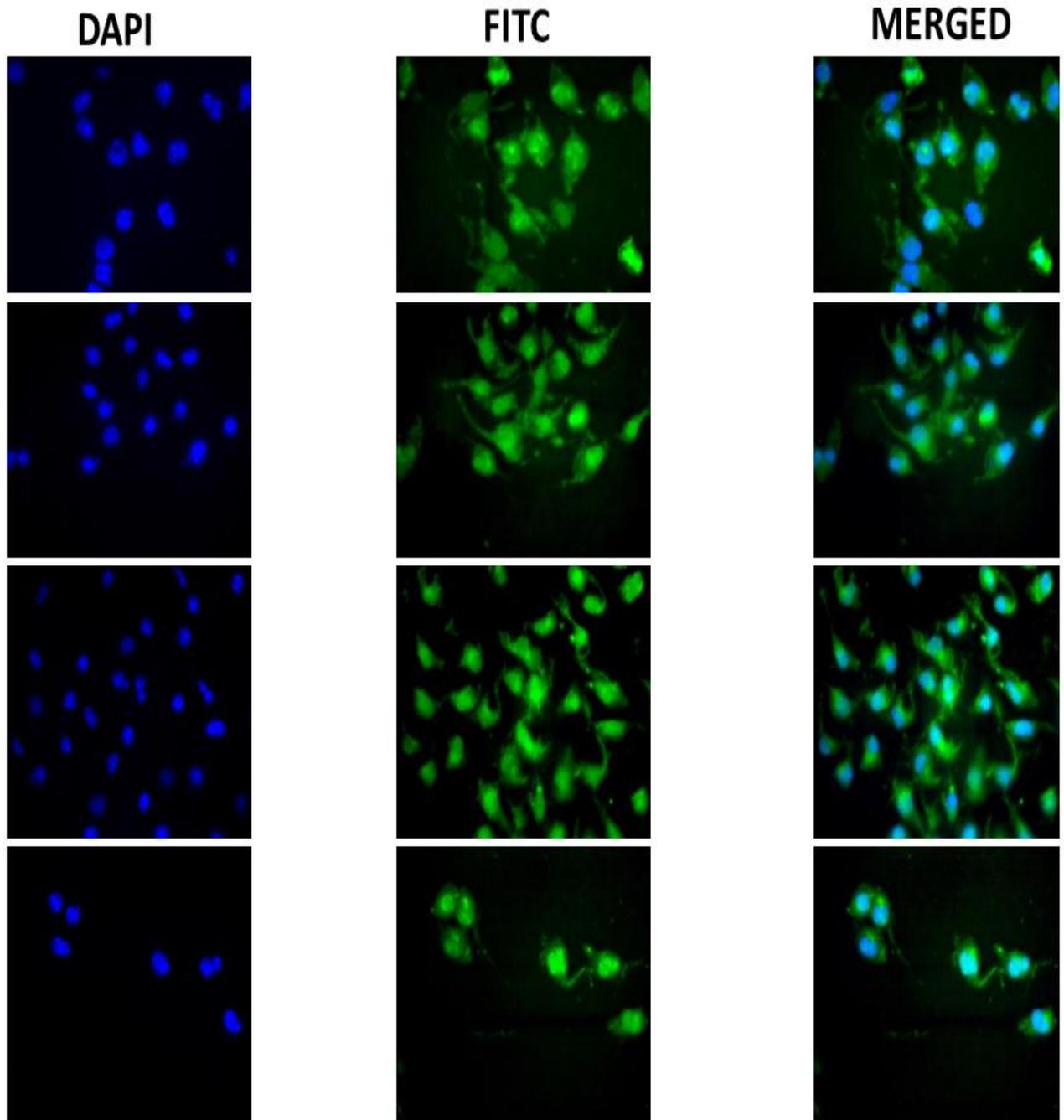
Figure 5. 5 Cellular uptake of curcumin and curcumin loaded NLCs (CRC-NLC). Green colour from FITC represents CRC. Blue colour from DAPI represents nuclei visualization.

5.4.7 Flow cytometry analysis for cellular uptake of NLCs

Flow cytometric histograms presented in Figure 5.8 show CRC accumulation on LNCaP prostate cancer cell lines after 24 hour incubation of CRC-NLC on LNCaP cells (cellular uptake was quantitavely analyse). The signal intensity was quantitavely measured for the cells. High fluorescence intensity relates to the expression of high percentage of cellular uptake. The results presented in histogram (Figure 5.6) revealed signal intensity of 96.2% for CRC-NLC. In order to investigate whether, BL-NLC does produce any autofluorescence and whether it is interfering with the fluorescent intensity produced by CRC-NLC, blank NLCs were also analysed. As seen from Figure 5.6, no fluorescent intensity was observed. Moreover, CRC-NLC showed similar cellular uptake characteristics as CRC-SLN (Figure 3.6). Both CRC-SLN and CRC-NLC showed signal intensity of above 90%, which is an indication that just like SLN, NLC is also being up-taken by the cells via similar endocytotic pathways (Mohanty et al., 2010). These data collected from flow cytometric quantitative cellular uptake of CRC-NLC were in agreement with the recorded fluorescent microscopy images.
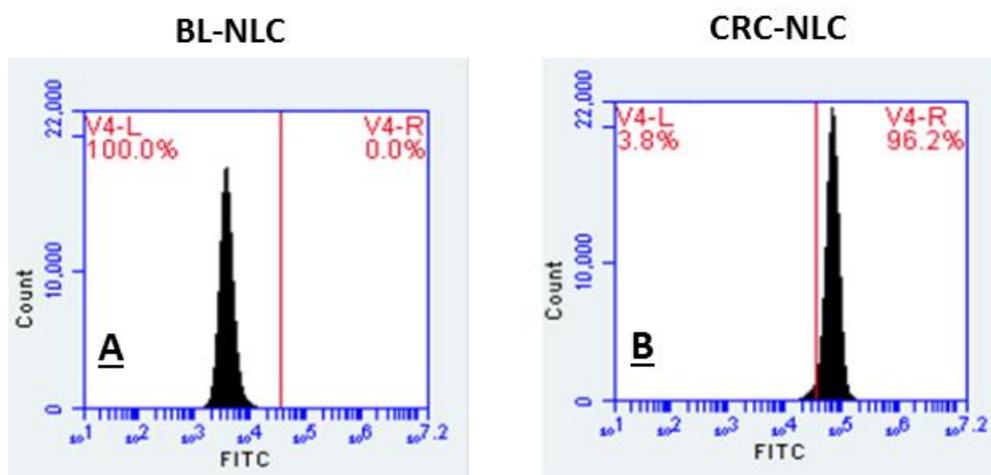
Figure 5. 6 Cellular uptake of CRC-NLC by flow cytometric analysis. (A) Cellular uptake of BL-NLC (B) Cellular uptake of CRC- NLC

5.4.8 *In vitro* apoptosis study

Apoptosis is known to be a physiologically programmed cell death which occurs during cellular development. Apoptosis is differentiated from necrosis in a point of view that it is a programmed cell death. During apoptosis phosphadylcholine (PS; located on the cytoplasmic side of a normal cell bilayer) is translocated from the inner to the outer leaflet of the plasma membrane, which exposes PS to the external cellular environments (Speth et al. 1988). Both

treated and untreated cells were stained with PE Annexin V and 7AAD. PE Annexin V staining can identify apoptosis at an earlier stage since it has high affinity for PS. 7AAD is used with PE Annexin V, which allows identification of early apoptotic cells (7AAD negative, PE Annexin V positive). Cells that are viable with intact membranes exclude 7AAD, and dead and damaged cells are permeable to 7AAD.
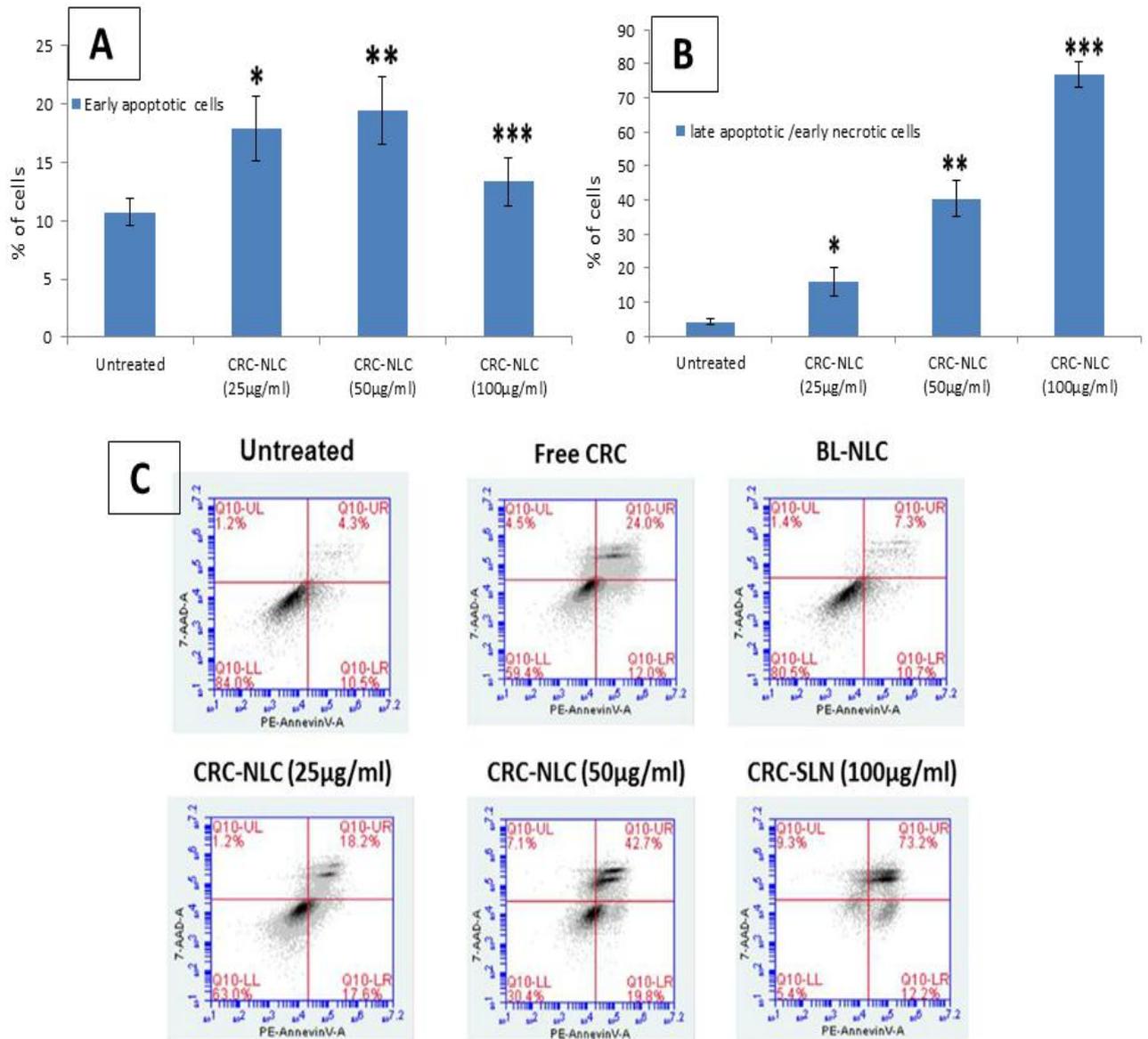
Figure 5. 7 Quantitative apoptotic measurement in LNCaP cells after treatment with BL-NLC (blank-NLC), pure curcumin and CRC-NLC (CRC loaded NLC). (A) Dose dependent effect on early apoptosis by treatment with a concentration of 25, 50 and 100μg/ml of CRC-NLC dose for 24 h determined by flow cytometry analysis. (B) Dose dependent effect on late apoptosis by treatment with a concentration of 25, 50 and 100μg/ml of CRC-NLC dose for 24 h determined by flow cytometry analysis. The results are expressed as bar chart. Data as mean±S.D. (n = 3). (*) p< 0.05, Control versus CRC-NLC (25μg/ml), (**) p<0.05, Control versus CRC-NLC (50μg/ml), (***) p<0.05, Control versus CRC-NLC (100μg/ml) (C) Dose dependent effects are expressed as dot plot of PE AnnexinV versus 7-AAD. Top left: necrotic cells; top right: late apoptotic cells/early necrotic cells; bottom left: live cells; and bottom right: early apoptotic cells.

As shown in Figure 5.7 the induction of apoptosis by CRC after the treatment on cells was detected and quantified by flow cytometry. Pure CRC (15µg/ml) showed 12% early apoptotic and 24% late apoptotic/early necrotic cells. The apoptotic cells were detected in cells treated with CRC-NLC formulations. CRC-NLC treated cells showed 17.6% and 18.2% of early apoptotic (PE Annexin V^+7AAD^-) and late apoptotic/early necrotic (PE Annexin V^+7AAD^+) populations, respectively at 25µg/ml of CRC concentration. This confirmed like pure CRC, NLC loaded with CRC also induces apoptotic pathways. At higher concentration of 50µg/ml and 100µg/ml, a significant increase in apoptotic cells were observed.. The percentage of early apoptotic (PE AnnexinV$^+7AAD^-$) and late apoptotic/early necrotic (PE AnnexinV$^+7AAD^+$) populations in cells treated with CRC-NLC at 50µg/ml CRC dose was19.8% and 42.7%. Moreover, when compared with CRC-SLN formulations (Figure 3.6), CRC-NLC was proven to be following similar apoptotic pathways as SLN based formulations. The percentage of early apoptotic (PE AnnexinV$^+7AAD^-$) and late apoptotic/early necrotic (PE AnnexinV$^+7AAD^+$) populations in cells treated with CRC-SLN at 50µg/ml was 20.2% and 34.0%. Although CRC-NLC showed higher apoptotic cells percentage for reasons discussed previously, this is also an indication that both CRC-SLN and CRC-NLCs are efficient in inducing cellular apoptosis. Experiment with controls (untreated and BL-NLC) showed that they have negligible apoptotic effect which is an indication that the apoptosis induced by the CRC-NLC formulations were indeed because of CRC.

5.4.9 *In vivo* anti-tumour effect of CRC and CRC loaded NLC formulations on mice bearing LNCaP prostate cancer tumour tissue weight

To assess whether CRC loaded NLC foster anti-tumour activity *in vivo*, the CRC-NLC, alongside with pure CRC and blank NLC formulations were injected in mice xenografts of LNCaP prostate cancer tumour at the dose of 20mg/kg. The inoculation of prostate cancer cells in mice took place with a cell density of 1×10^6. And cells were allowed to grow for 6 consecutive days before the commencement of treatments with different formulations
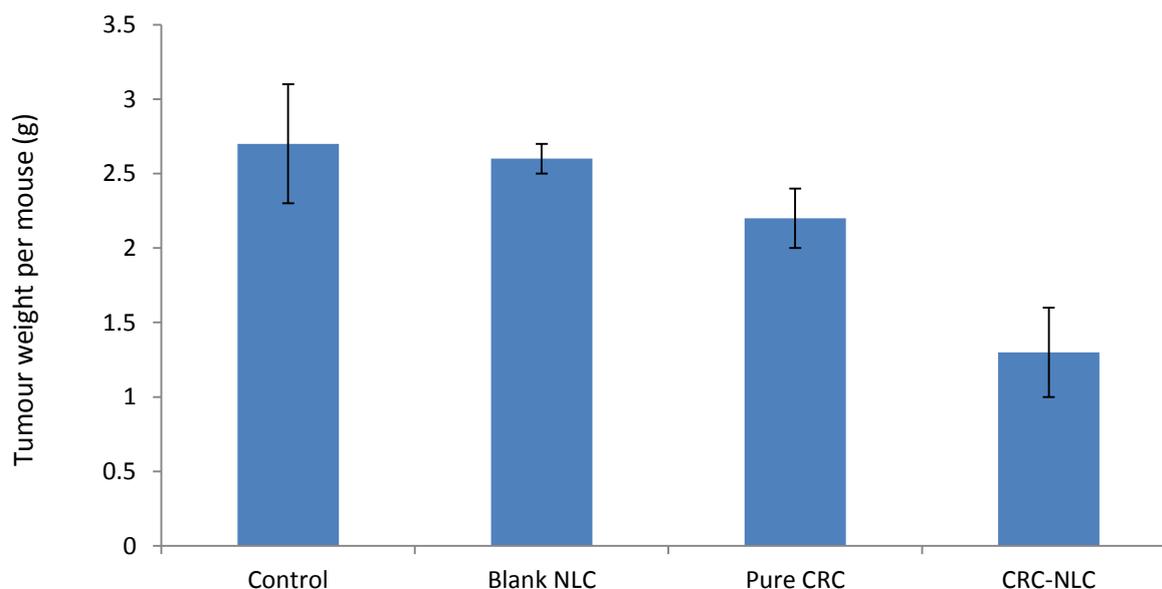
Figure 5. 8 Comparative therapeutic effects of control, blank NLC, pure CRC, CRC-NLC on tumour suppression of LNCaP prostate cancer.

In order to evaluate statistical significant difference between each group of NLC formulations unpaired t-test was used and revealed the difference of anti-tumour efficacy between each formulation. Figure 5.8 shows the anti-tumour activity of CRC compared to the control and blank NLC group and the data are expressed in terms of mean tumour tissue weight in each group. Upon administration of CRC on mice bearing LNCaP prostate cancer tumour, the tumour was reduced by 19%, when compared to the control treatment. Moreover, an unpaired t-test of these two groups showed significant difference, where the P value equals 0.021. An even greater anti-tumour effect was observed when treating the mice bearing tumour with CRC-NLC formulations. Upon treatment for 4 weeks with CRC encapsulated NLC formulations, a tumour size reduction of 52% and 50% was observed compared to the control group and blank NLC group respectively. Unpaired t-test showed that the therapeutic efficacy of the CRC loaded NLC formulations were significantly higher when compared to control group and blank NLC group ($P<0.0001$). The anti-tumour efficacy of pure CRC and CRC-NLC were also evaluated and the results obtained upon treatment for 4 weeks indicated that *in vivo* anti-melanoma efficacy of CRC-NLC group was significantly higher than that off CRC alone at the same CRC dose level ($P<0.0001$). The tumour weight comparison of bulk CRC with the CRC loaded NLC showed that the tumour weight was reduced to 40% for the latter animal group. This clearly indicates the advantage of the NLC encapsulated CRC for the delivery of CRC and cancer treatment.

5.4.10 Effect of CRC and CRC encapsulated SLN formulations on tumour growth regression in terms of tumour volume

Pure CRC and CRC-NLC formulations showed anticancer activity in, *in vivo* models and their therapeutic efficacy was evaluated in terms of tumour volume. As shown in Figure 5.8, the treatment with bulk CRC and loaded NLCs resulted in significant tumour regression of LNCaP prostate cancer xenograft tumours when compared with control and blank NLC treated mice. The results of tumour volume changes as a function of time with CRC loaded NLC are shown in Figure 5.9. In LNCaP prostate tumour models, the average tumour volumes after 4 weeks of therapy were as follows: 1410.2 mm^3 for control, 1374.14 mm^3 for blank NLC, 1153.13 mm^3 for pure CRC and 776.39 mm^3 for CRC loaded NLC. NLC encapsulated CRC had significant growth suppressive effects compared with control and blank NLC (P<0.0001). Moreover as shown in Figure 5.11, CRC –NLC also had greater anti-tumour efficacy when compared to pure CRC (P<0.0001). Another important observation was the tumour suppressive characteristics of the blank NLC formulations. As shown in Figure 5.9, blank NLC did not depict any significant decrease in tumour growth suppression, similar to control treatment (P=0.1292).
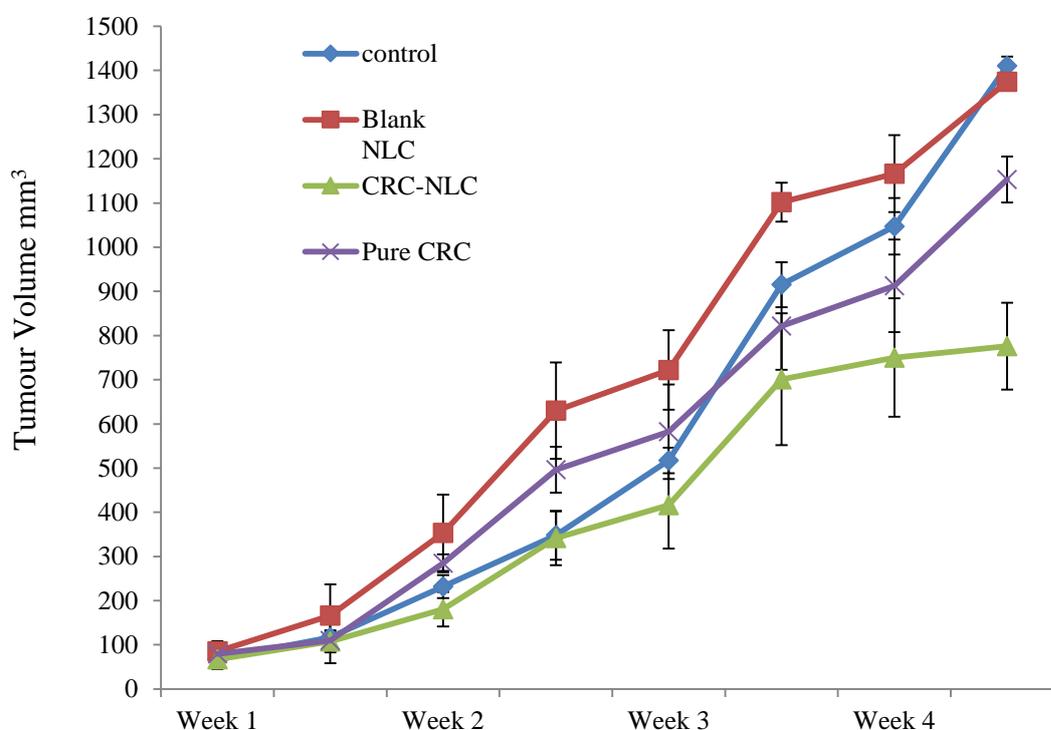
Figure 5. 9 Therapeutic effect of control, blank NLC, pure CRC and CRC-NLC on mice bearing tumour.

The therapeutic efficacy of bulk CRC and CRC-NLC formulations are depicted in Figure 5.10, as a summary graph of their tumour regression efficacy. Statistical analysis using ANOVA shows that there is a significant difference in the therapeutic efficiency between the treatments administered in the tumour bearing mice (P = 0.000). The results obtained by this particular *in vivo* study, proved that CRC loaded NLC formulations are capable of providing greater anti-tumour effect than that of pure CRC solution. Moreover, since blank NLC did not show any visible tumour regressive behaviour, the anti-tumour effects observed were attribute to the efficacy and incorporation of CRC. Observations of mice weight were also conducted during the treatment for 4 weeks and no weight changes were observed during the course of therapy in any of the mice receiving the treatment. Observations shown in Figure 5.11 demonstrate formulations to be well tolerated by the mice with no signs of toxicity or significant weight loss.
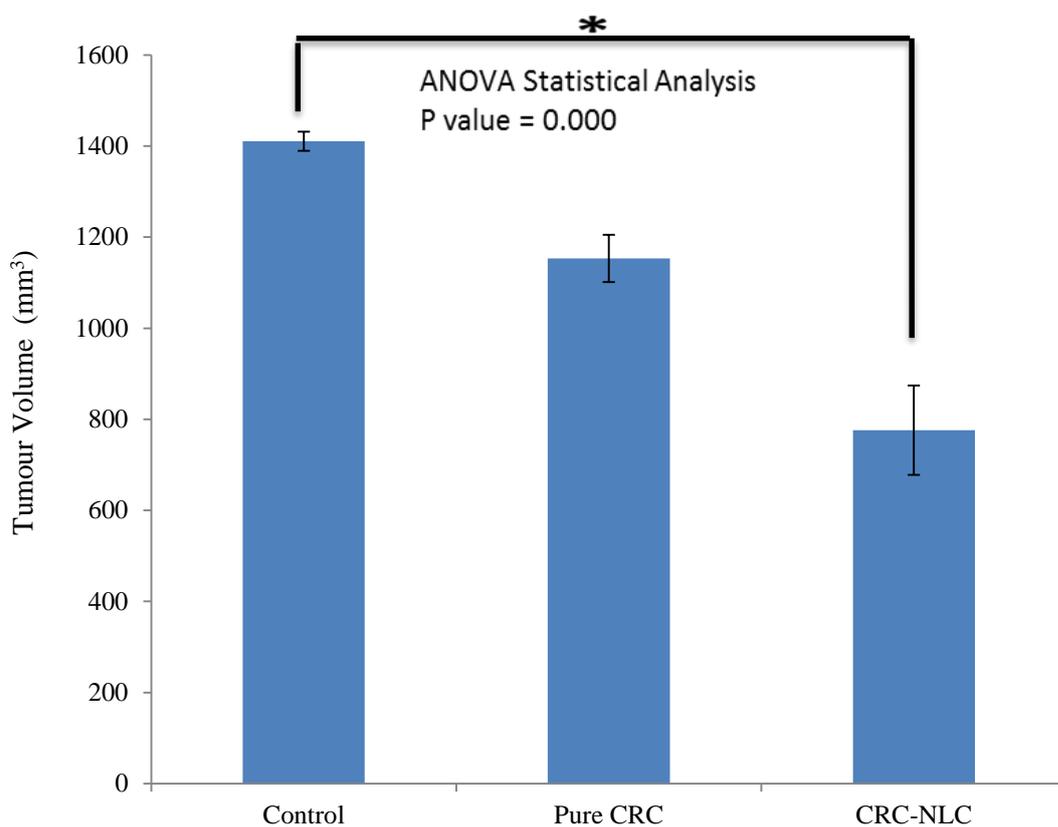
Figure 5. 0 Difference in therapeutic efficiency of control, pure CRC and CRC-NLC formulations in mice bearing tumour.
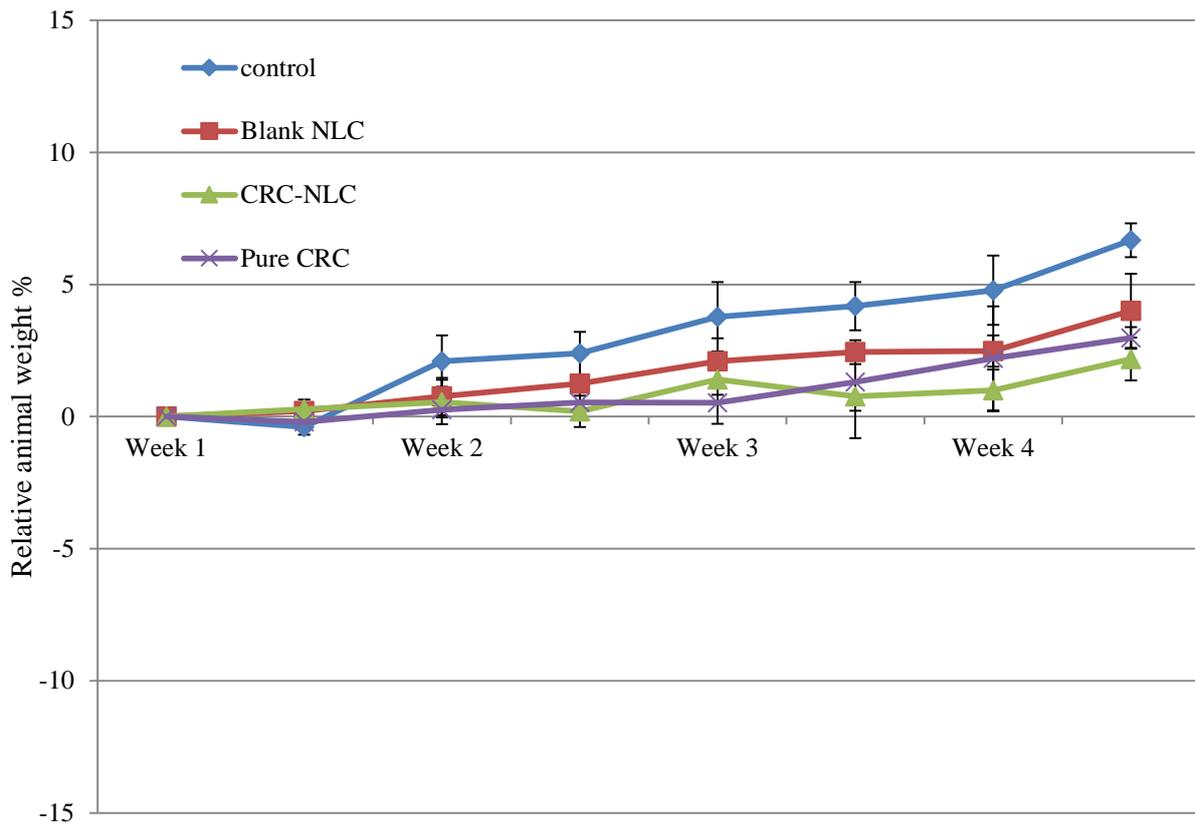
Figure 5. 11 Treatment tolerance by mice bearing tumour over the treatment study period of four weeks.

The malignancy is highly resistant to chemotherapy; moreover in addition to that the bioavailability of CRC is known to be poor at the same time, although, CRC is known to be highly potent in initiating protection against cancer in experimental animals induced by a variety of chemical carcinogens (Huang et al., 1988). Moreover CRC has the capability of inhibiting cell growth, activation of signal transduction, and transforming activities in both androgen-dependent and androgen-independent prostate cancer cells. On top of that, CRC is also known to exert strong antioxidant and anti-inflammatory activities by suppressing both constitutive and inducible nuclear factor- ƙB (NF-ƙB) (Hour et al., 2002). . Encapsulating CRC in NLC can somewhat eradicate the bioavailability related problems of CRC in intravenous administration, which can assist exerting maximum anti-tumour effects of CRC when administered in tumour site. According to researchers, encapsulating CRC in nanostructured lipid carriers can initiate higher plasma concentration of CRC, which might be a result of the small size of nanoparticles; which also in turn helps keeping the formulation in the circulation for an extended period (Madane et al., 2014). Prolonged time at circulation

helps giving away a sustained release of drug from the nanoparticles, which might have led to greater anti-tumour effect when compared to pure CRC formulation (Duan et a., 2010). CRC and CRC loaded NLC treatments has successfully slowed tumour growth and prolonged mice survival but did not eliminate tumour growth, similar findings were reported by Chen et al, (2012), when administering CRC via lipid nanoparticle based vehicle.

5.5 Conclusions

In the study, CRC loaded NLC formulations were successfully fabricated by using high pressure hot homogenization processing. Prepared NLC showed very narrow size distribution with negative zeta potential values at -40 mV, which resulted in particles long term stability. *In vitro* release studies, indicated sustained release with a very high encapsulation efficiency of CRC within the lipid matrix. In addition, the potency of CRC-NLC as an anticancer agent was evaluated by *in vitro* fluorescent microscopy, FACS flow cytometry and *in vitro* cell viability assay. Cell viability assays revealed significant cell growth inhibition after treating the cells with CRC-NLC, where at a CRC concentration of 100 µg/ml the cell viability was taken down to 4.28%. FACS flow cytometry studies confirmed CRC-NLCs apoptosis inducing abilities, as at 100 µg/ml CRC concentration the percentage of cells on late apoptotic/early necrotic cells were 76.9%. *In vivo*, animal studies of CRC-NLC dispersion revealed a significantly higher anti-cancer efficiency on LNCaP prostate cancer xenografts compared to unloaded NLCs and bulk CRC. CRC-NLC demonstrated significant tumour suppression which is very promising for potential applications in prostate cancer treatment.

5.6 References

1. Anand, P., Kunnumakkara, A. B., Newman, R. A., & Aggarwal, B. B. (2007). Bioavailability of curcumin: problems and promises. *Molecular pharmaceutics*,*4*(6), 807-818.

2. Castelli, F., Puglia, C., Sarpietro, M. G., Rizza, L., & Bonina, F. (2005). Characterization of indomethacin-loaded lipid nanoparticles by differential scanning calorimetry. *International journal of pharmaceutics*, *304*(1), 231-238.

3. Chen, Y., Wu, Q., Zhang, Z., Yuan, L., Liu, X., & Zhou, L. (2012). Preparation of curcumin-loaded liposomes and evaluation of their skin permeation and pharmacodynamics. *Molecules*, *17*(5), 5972-5987.

4. Duan, J., Zhang, Y., Han, S., Chen, Y., Li, B., Liao, M., ... & Huang, B. (2010). Synthesis and in vitro/in vivo anti-cancer evaluation of curcumin-loaded chitosan/poly (butyl cyanoacrylate) nanoparticles. *International journal of pharmaceutics*, *400*(1), 211-220.

5. Fang, M., Jin, Y., Bao, W., Gao, H., Xu, M., Wang, D., ... & Liu, L. (2012). *In vitro* characterization and *in vivo* evaluation of nanostructured lipid curcumin carriers for intragastric administration. *International journal of nanomedicine*, *7*, 5395.

6. Hour, T. C., Chen, J., Huang, C. Y., Guan, J. Y., Lu, S. H., & Pu, Y. S. (2002). Curcumin enhances cytotoxicity of chemotherapeutic agents in prostate cancer cells by inducing p21WAF1/CIP1 and C/EBPβ expressions and suppressing NF-κB activation. *The prostate*, *51*(3), 211-218.

7. Huang, M. T., Smart, R. C., Wong, C. Q., & Conney, A. H. (1988). Inhibitory effect of curcumin, chlorogenic acid, caffeic acid, and ferulic acid on tumor promotion in mouse skin by 12-O-tetradecanoylphorbol-13-acetate. *Cancer research*, *48*(21), 5941-5946.

8. Iqbal, M. A., Md, S., Sahni, J. K., Baboota, S., Dang, S., & Ali, J. (2012). Nanostructured lipid carriers system: recent advances in drug delivery. *Journal of drug targeting*, *20*(10), 813-830.

9. Jun, J. Y., Nguyen, H. H., Chun, H. S., Kang, B. C., & Ko, S. (2011). Preparation of size-controlled bovine serum albumin (BSA) nanoparticles by a modified desolvation method. *Food chemistry*, *127*(4), 1892-1898.

10. Kakkar, V., Singh, S., Singla, D., & Kaur, I. P. (2011). Exploring solid lipid nanoparticles to enhance the oral bioavailability of curcumin. *Molecular nutrition & food research*, *55*(3), 495-503.

11. Khor, T. O., Keum, Y. S., Lin, W., Kim, J. H., Hu, R., Shen, G., ... & Kong, A. N. T. (2006). Combined inhibitory effects of curcumin and phenethyl isothiocyanate on the growth of human PC-3 prostate xenografts in immunodeficient mice.*Cancer Research*, *66*(2), 613-621.

12. Liu, J., Chen, S., Lv, L., Song, L., Guo, S., & Huang, S. (2013). Recent progress in studying curcumin and its nano-preparations for cancer therapy. *Current pharmaceutical design, 19(11)*, 1974-1993.

13. Liu, J., Gong, T., Wang, C., Zhong, Z., & Zhang, Z. (2007). Solid lipid nanoparticles loaded with insulin by sodium cholate-phosphatidylcholine-based mixed micelles: preparation and characterization.*International journal of pharmaceutics*, *340*(1), 153-162.

14. Madane, R. G., & Mahajan, H. S. (2014). Curcumin-loaded nanostructured lipid carriers (NLCs) for nasal administration: design, characterization, and in vivo study. *Drug delivery*, (0), 1-9.

15. Mehnert, W., & Mäder, K. (2001). Solid lipid nanoparticles: production, characterization and applications. *Advanced drug delivery reviews*, *47*(2), 165-196.

16. Mohanty, C., & Sahoo, S. K. (2010). The *in vitro* stability and *in vivo* pharmacokinetics of curcumin prepared as an aqueous nanoparticulate formulation. *Biomaterials*, *31*(25), 6597-6611.

17. MuÈller, R. H., MaÈder, K., & Gohla, S. (2000). Solid lipid nanoparticles (SLN) for controlled drug delivery–a review of the state of the art. *European journal of pharmaceutics and biopharmaceutics*, *50*(1), 161-177.

18. Mulik, R. S., Mönkkönen, J., Juvonen, R. O., Mahadik, K. R., & Paradkar, A. R. (2010). Transferrin mediated solid lipid nanoparticles containing curcumin: enhanced *in vitro* anticancer activity by induction of apoptosis. *International journal of pharmaceutics*, *398*(1), 190-203.

19. Müller, R. H., Petersen, R. D., Hommoss, A., & Pardeike, J. (2007). Nanostructured lipid carriers (NLC) in cosmetic dermal products. *Advanced Drug Delivery Reviews*, *59*(6), 522-530.

20. Nayak, A. P., Tiyaboonchai, W., Patankar, S., Madhusudhan, B., & Souto, E. B. (2010). Curcuminoids-loaded lipid nanoparticles: novel approach towards malaria treatment. *Colloids and Surfaces B: Biointerfaces*, *81*(1), 263-273.

21. Puglia, C., Frasca, G., Musumeci, T., Rizza, L., Puglisi, G., Bonina, F., & Chiechio, S. (2012). Curcumin loaded NLC induces histone hypoacetylation in the CNS after intraperitoneal administration in mice. *European Journal of Pharmaceutics and Biopharmaceutics*, *81*(2), 288-293.

22. Shankar, T. B., Shantha, N. V., Ramesh, H. P., Murthy, I. A., & Murthy, V. S. (1980). Toxicity studies on turmeric (Curcuma longa): acute toxicity studies in rats, guineapigs and monkeys. *Indian journal of experimental biology*, *18*(1), 73-75.

23. Siekmann, B., & Westesen, K. (1992). Submicron-sized parenteral carrier systems based on solid lipids. Pharmacological letters *1*(3), 123-126.

24. Souto EB, & Muller RH. (2007). Nanoparticulate drug delivery systems . *Informa Healthcare*, 213-233.

25. Souto, E. B., & Muller, R. H. (2007). Lipid nanoparticles (solid lipid nanoparticles and nanostructured lipid carriers) for cosmetic, dermal, and transdermal applications. *Drugs and pharmaceutical sciences*,*166*, 213.

26. Suzuki, T., Fujikura, K., Higashiyama, T., & Takata, K. (1997). DNA staining for fluorescence and laser confocal microscopy. *Journal of Histochemistry & cytochemistry*, *45*(1), 49-53.

27. Thiyagarajan, M., & Sharma, S. S. (2004). Neuroprotective effect of curcumin in middle cerebral artery occlusion induced focal cerebral ischemia in rats. *Life sciences*, *74*(8), 969-985.

28. Verma, D. D., Verma, S., Blume, G., & Fahr, A. (2003). Particle size of liposomes influences dermal delivery of substances into skin. *International journal of pharmaceutics*, *258*(1), 141-151.

29. Yang, L., Chen, L., Meng, B., Suo, J., Wang, H., Xie, H., & Zhang, L. (2006). The effect of curcumin on proliferation and apoptosis in LNCaP prostate cancer cells. *Chinese journal of clinical oncology*, *3*(1), 55-60.

30. Zauner, W., Farrow, N. A., & Haines, A. M. (2001). *In vitro* uptake of polystyrene microspheres: effect of particle size, cell line and cell density. *Journal of controlled release*, *71*(1), 39-51.

CHAPTER 6: EFFICACY OF TRANSFERRIN CONJUGATED AND UNCONJUGATED CURCUMIN LOADED SOLID LIPID NANOPARTICLES IN LNCAP HUMAN PROSTATE CANCER CELL LINE *IN VITRO & IN VIVO*

6.1 Introduction

Prostate cancer is the most common form of cancer in men and is the second leading cause of cancer mortality in men over the age of 40 years in the United States (Melhed et al., 2002). The induction of human prostate cancer is a multistage process, involving progression from small latent carcinomas of low histological grade to high grade metastatic cancer. Over the past decade, substantial improvements in diagnosis and staging of the disease have been made with the combined use of digital rectal examination, measurement of serum PSA (prostate specific antigen) levels and transrectal ultrasound (Caplan et al., 2002). Almost 90% of the men diagnosed with prostate cancer in North America are present with localized disease. Therefore, an early intervention to treat the disease with a less invasive local treatment could be more appropriate for such patients. In addition, local therapy could be useful in patients who develop recurrence after radical prostatectomy to reduce the risk of local and/or metastatic progression of the disease (Caplan et al., 2002). Curcumin is an anticancer agent with a wide spectrum of anti-tumour activity. Curcumin has a wide range of therapeutic efficacy such as, antioxidant, anti-inflammatory, antimicrobial, wound healing, cancer chemo-preventive, and potentially chemotherapeutic properties. Several investigations on curcumin (CRC) have already demonstrated the strong therapeutic potential of CRC against cancers of various origins such as, skin, prostate, ovarian, colon, breast, brain, blood, liver, and pancreas being completely harmless to normal healthy cells at the same time in total contrast to chemotherapy (Aggarwal et al., 2003). Curcumin can exert its anticancer effects in many mechanisms which is not yet fully known, Although, several investigation taken place in the past have proposed a few mechanisms such as, cell cycle inhibition, signal transduction modulation resulting in gene expression alterations, and apoptosis .It has been demonstrated recently that cell cycle inhibition and induction of apoptosis are the main underlying mechanisms involved in anticancer activity of CRC (Aggarwal et al., 2003). Generation of reactive oxygen species (ROS) and inhibition of NFkB being the main

pathways involved in the induction of apoptosis. Moreover, it has been scientifically proved that curcumin imparts its anticancer effect by acting against all three stages of carcinogenesis (i.e., initiation, progression, and promotion) affecting specific signalling cascade target. Despite of tremendous therapeutic potential of curcumin against cancer including low bioavailability, short half-life, and photo-degradation are the major limiting factors of curcumin its overall therapeutic efficacy (Mulik et al., 2012) In this study curcumin encapsulated solid lipid nanoparticles (CRC-SLN) were formulated. Solid lipid nanoparticles are known to overcome the limitations that are possessed by CRC, as discussed in chapter two and three. However, to increase the therapeutic efficacy of CRC a tumour specific therapy has been advocated. In this regards solid lipid nanoparticles are conjugated to tumour specific ligand. As a ligand transferrin (Tf) has been extensively investigated for drug targeting to tumours because most tumour cells over express Tf receptors (Sahoo et al., 2004). Overexpression of Tf receptor in malignant tissues compared with normal tissues because of the higher iron demand of malignant cells for fast growth and division is well known resulting in the shift of scientific attention towards Tf-mediated drug and gene delivery systems in the past few years for cancer targeting. For example, Tf-conjugated PLGA nanoparticles containing paclitaxel for enhanced anti-proliferative activity, Tf–PEG liposomes for intracellular delivery and targeting to solid tumours, Tf-conjugated gold nanoparticles for cancer cell imaging and therapy, Tf-conjugated PEG– albumin nanoparticles for brain targeting, Tf receptor-targeted lipid nanoparticles for delivery of an antisense oligodeoxyribonucleotide against Bcl-2, Tf-conjugated curcumin-loaded super paramagnetic iron oxide nanoparticles against leukemia etc (Mulik et al., 2012). The main objective of the present study was to formulate stable conjugated and unconjugated solid lipid nanoparticles loaded with CRC. (CRC-SLN & Tf-CRC-SLN). Tf-CRC-SLN was formulated for the targeted delivery of LNCaP prostate cancer cell line and evaluates its enhanced anticancer effect *in vitro* & *in vivo*.

6.2 Materials

Curcumin, transferrin, stearic acid, was purchased from Sigma-Aldrich. Poloxamer 188 was kindly donated by BASF (Ludwigshafen, Germany). 1-ethyl-3-[3-dimethylaminopropy] carbodiimide hydrochloride (EDC) was purchased from Sigma-Aldrich. Bradford assay reagent was purchased from Bio-Rad. All other chemicals and solvents were of analytical and high-performance liquid chromatography (HPLC) grade. LNCaP cell line was purchased

from American Type Culture Collection (ATTC: Manassa, Virginia, USA). Dulbecco's modified Eagle's medium (DMEM), thiazolyl blue tetrazolium bromide (MTT), L-glutamin, Penicillin streptomycin and heat inactivated fetal bovin serum (FBS) and trypsin were all purchased from Sigma -Aldrich (UK). PE Annexin V Apoptosis Detection Kit I from BD Biosciences.

6.3 Methods

6.3.1 SLN preparation
Please refer to chapter 2, section 2.3.1

6.3.2 Bio-conjugation of Tf
Transferrin was coupled on the surface of the SLNs by using 1-ethyl-3-carbodiimide (EDC), as described before by Greg et al., 1996 (Figure 6.1). Firstly, transferrin (10mg/ml) protein was dissolved In PBS, pH 7.2 and an aliquot added to the reaction lipid mixture. Afterwards EDC (10mg per ml of lipid/protein mixture) was added. EDC was then solubilised by using a vortex mixture. The mixture was then left for reaction for 2 hours at room temperature. At the end of the reaction, excess EDC and transferrin was excluded from the transferrin conjugated SLN suspension by size exclusion technique using Sepharose CL-4B column. Bradford assay was utilised to verify bounded and unbounded transferrin (Tf).

6.3.3 Methodology of Transferrin assay quantification
Transferrin is a globular glycoprotein with molecular weight of 80kDa and high aqueous solubility. The average amount of transferrin conjugated to SLNs was quantified by Bradford assay which is a commonly used procedure for determination of protein concentrations in solutions and depends on the change in absorbance of Coomassie Blue G-250 upon binding of the protein. The calorimetric assay, as the concentration of the protein increases, results in colour changes which becomes darker. The protein concentration in a sample (e.g. Tf-conjugated SLN) is determined in comparison to protein standard solutions known. Bovine Serum Albumin (BSA) was utilised as protein standard with concentration range of 0.0, 0.125, 0.5, 1.0 and 2.0mg. 100μl of each standard was pipetted in glass tube and 5ml of the Bradford reagent was added. The mixture was vortex and allowed to stand at room temperature for 5 minutes before reading at 595nm using UV spectrophotometer. For blank 100μl of deionised water was pipetted and 5ml of Bradford reagent was added followed by vortex and UV reading. For TF-conjugated SLN, 100μl of SLN sample was pipetted and the

same procedure as the BSA standard was followed. All tests were carried out in triplicate and a linear regression calibration curve was obtained for BSA standards. Amount of transferrin conjugated on SLN surface was determined using the BSA calibration curve.

6.3.4 Particle size analysis and zeta potential

Please refer to chapter 2, section 2.3.2

6.3.5 Determination of encapsulation efficiency

Please refer to chapter 2, section 2.3.6

6.3.6 Cell viability test

Please refer to chapter 3, section 3.3.2

6.3.7 Cellular uptake by fluorescent microscopy

Please refer to chapter 3, section 3.3.3

6.3.8 Flow cytometric analysis for cellular uptake of conjugated and unconjugated SLNs

Please refer to chapter 3, section 3.3.4

6.3.9 *In vitro* apoptosis studies

Please refer to chapter3, section 3.3.5

6.3.10 Treatment of mice bearing human prostate cancer xenografts

In-vivo studies were undertaken in collaboration with Pasteur Institute, Greece. House and feed purchased female nude mice aged 6-8 weeks under standard conditions kept in a 12 hours light/ 24 hours dark cycle. LNCaP prostate cancer cell line was cultured in a complete culture medium DMEM. Prostate cancer xenograft was established by injecting 2×10^6 LNCaP cells (in 100μl of PBS) into the fat pad of mouse mammary glands. Tumour allowed to grow for 3 days without any treatments and monitor the tumour volume daily by measuring two perpendicular tumour diameters with a calliper [tumour volume [mm3] = (length [mm]) x (width [mm])^2 x 0.52]. Afterwards the mice with the prostate cancer xenograft were divided into four groups (n=6/group) according to the treatment received: The blank control, CRC solution, Blank SLN CRC encapsulated SLN (CRC-SLN) and Tf conjugated CRC loaded SLN (Tf-CRC-SLN). For CRC based treatments, 20 mg/kg of CRC was administered. The treatments were administered by injecting intravenously via mice tail

(two injections per week with injection volume of 200µl for 4 weeks). Then tumour size measurements and animal weight were taken twice a week.

6.3.11 Statistical analysis of tumour regression

Please refer to chapter 3, section 3.3.6

6.4 Results and discussion

6.4.1 Analysis of SLN formulation of both conjugated and un-conjugated

The SLN formulations (both loaded and unloaded) were prepared by using different lipids and surfactants. After successful high-pressure homogenization SLNs were conjugated with transferrin and characterized by size and zeta potential. The physical properties of SLN in terms of size and zeta potential before and after transferrin conjugation are given in Table 6.1. All SLN dispersions showed very good polydispersity of less than 0.2 suggesting narrow size distribution, which in turn can also be considered as a homogenous distribution (Yashwant *et al.,* 2007). SLNs showed very good stability over a period of six months with slight increase in particle size varying from 5–7nm. The average particle sizes of empty (unloaded) SLNs before and after the conjugation were 145.1nm and 153.3nm respectively. While for the loaded formulations it was 218.5nm and 231.4nm for CRC-SLN and Tf-CRC-SLN respectively. Zeta potential of BL-SLN and CRC-SLN was -18.74 mV and -8.11 mV respectively, while BL-Tf-SLN and Tf-CRC-SLN showed zeta potential of -18.35 and -8.36. The zeta potential of all formulations demonstrated negligible increase, which also indicates very good dispersion stability However, the zeta potential was found to be decreased when the SLN formulations (both conjugated and un-conjugated) were loaded with CRC (Table 6.1). As known from previous studies, SLN stability is partially related to its packing materials (Freitas, 1998). In this study CRC was encapsulated inside the solid lipid core which in turn might have slightly decreased the zeta potential value of CRC-SLN. Although, the decrease zeta potential is considered to be an indication of possible particle aggregation; at this particular instance this difference can be considered negligible since, the zeta potential of all loaded formulations showed slight increase over a period of six months. This is an indication of satisfactory electrochemical and physical stability (Sun et al., 2013). The transferrin (Tf) conjugation led to particle size increase of approximately 7nm. Similarly, the Tf conjugation on CRC loaded SLN resulted in particle size increase from 218.5nm to

231.4nm. The particle size increase can be easily explained by the size of Tf molecule on the surface of SLN particles.

Table 6. 1 Particle size and zeta potential of SLN formulations (n= 3)

	Months	Particle size (nm)		Zeta Potential (mV)	
		Empty	**Loaded**	**Empty**	**Loaded**
Unconjugated SLN (blank)	1	145.1 ±2.7	218.5 ±3.7	-18.74 ±1.6	-8.11 ±0.1
	3	147.8 ±3.5	221.3 ±1.9	-18.38 ±2.4	-7.95 ±0.5
	6	149.1 ±1.1	223.7 ±2.0	-17.95 ±0.31	-7.93±0.3
Tf -SLN (blank)	1	153.3 ±0.9	231.4 ±2.5	-18.35 ±1.3	-8.36 ±0.1
	3	155.1 ±3.6	233.1 ±2.6	-18.11 ±1.2	-8.10 ±0.5
	6	158.8 ±3.3	233.6 ±1.4	-18.01 ±0.1	-8.09 ±0.2

The process of conjugating Tf on SLN surface was similar to the one proposed by Greg, 1996 (Figure 6.1). The amount of the conjugated Tf on SLNs was quantitated by Bradford assay, as previous studies suggested (Mulik *et al.,* 2010). Upon conjugation of SLN, gel filtration chromatography has been used to for the separation of protein bounded to SLN. Upon collection of several SLN fractions from gel filtration chromatography, Bradford assay analysis was performed; which gave away two different curves (Figure 6.2).
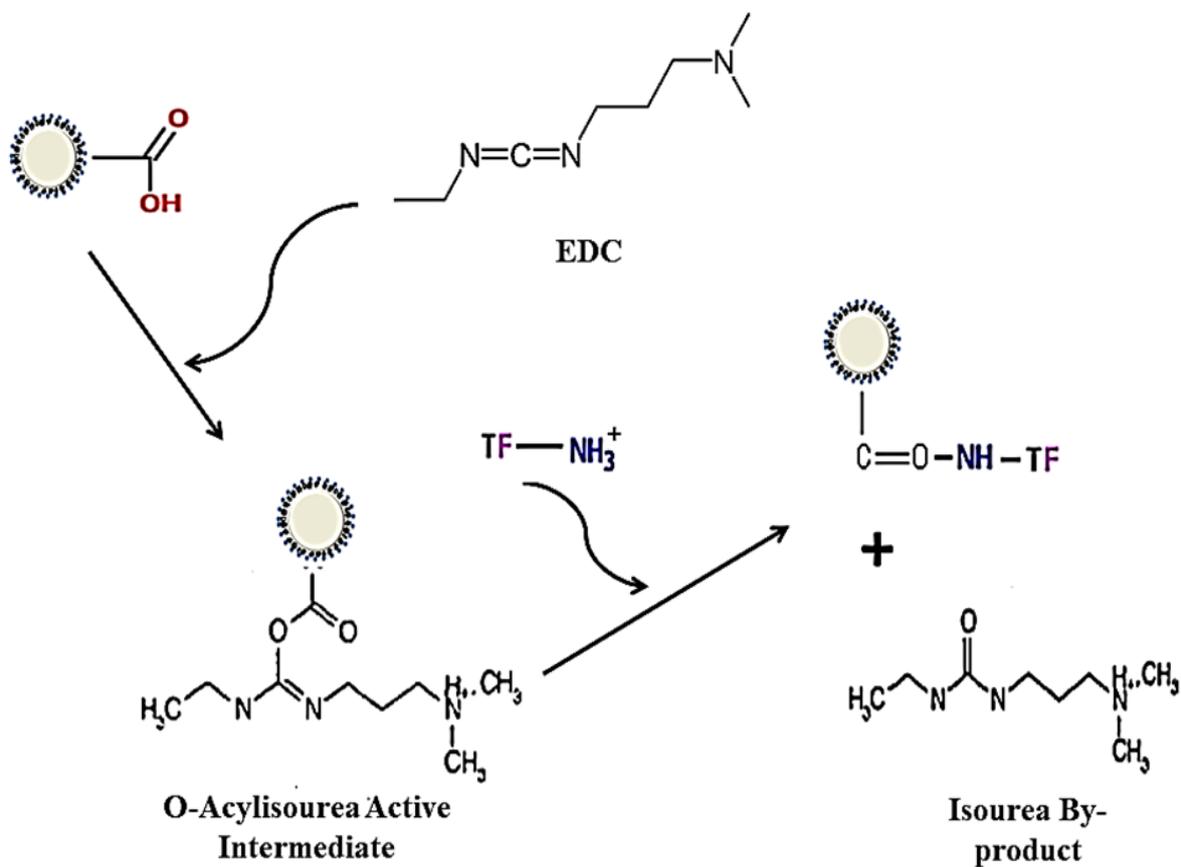
Figure 6. 1 Mechanism of conjugation (Bioconjugate Techniques by Greg T. Hermanson, Academic Press Inc. 1996)
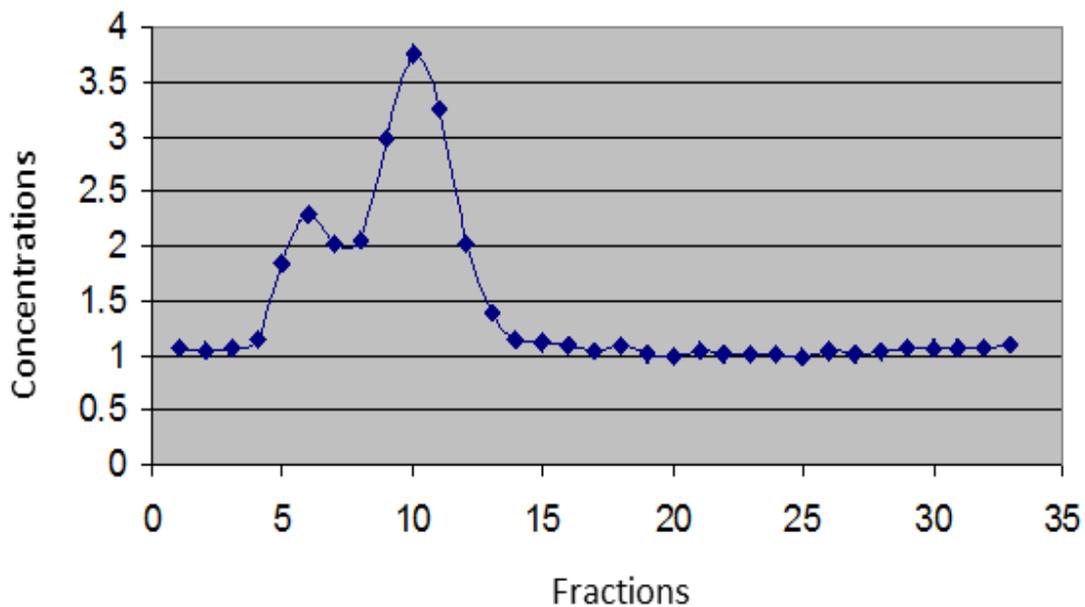
Figure 6. 2 In this graph the first curve represent SLN bounded to transferrin and second curve represents free transferrin.

These curves are the representation of bounded and un-bounded Tf on SLN surface, as the first curve represents SLN bounded to Tf and second curve represents free transferrin. The conjugation efficiency was found to be 7.3mg/ml (Tf) to 25mg/ml of lipid (Figure 6.2). It was found that the method used for conjugation was highly efficient for the conjugation of Tf (Mulik et al., 2010).
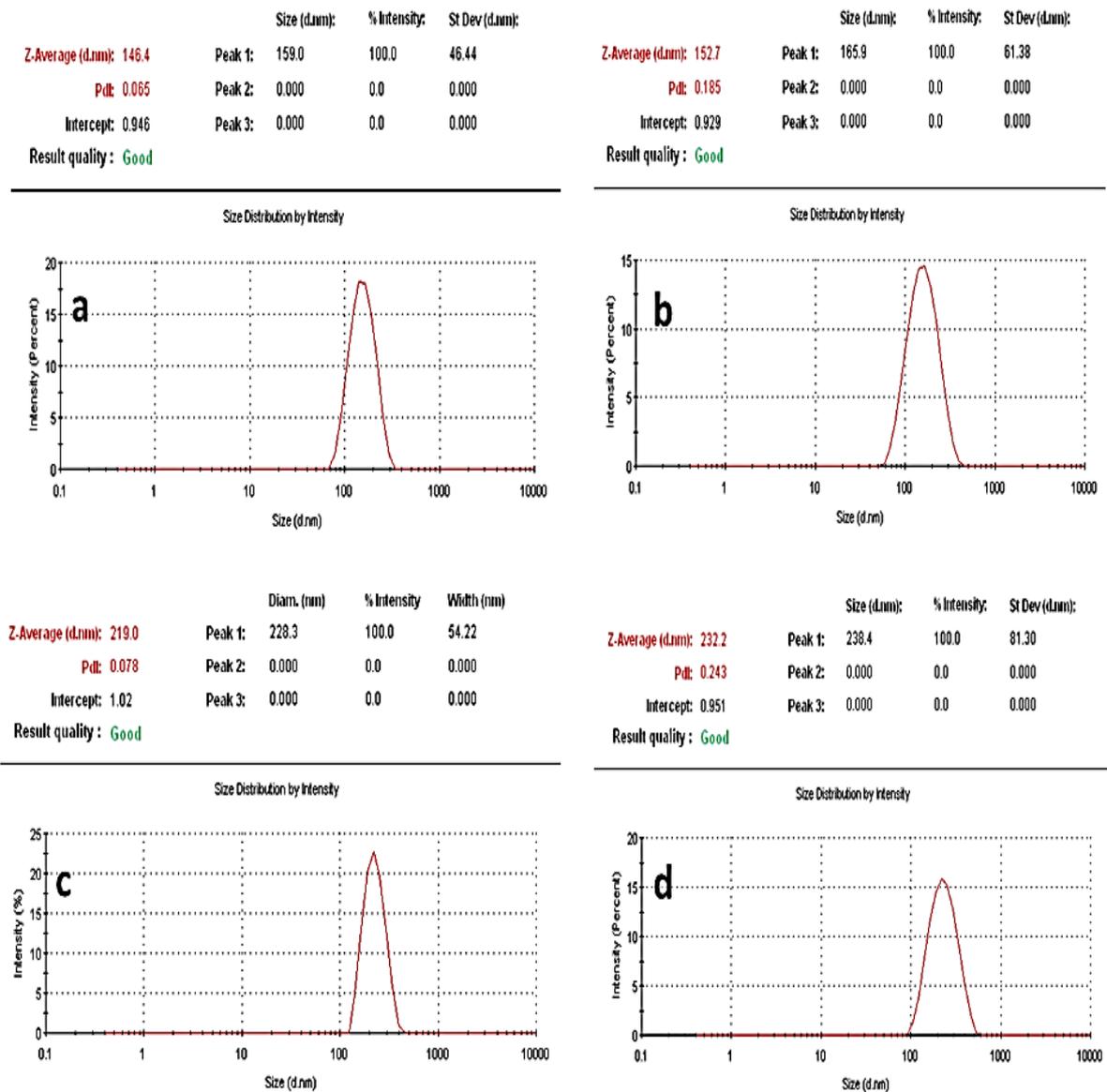
Figure 6. 3 Particle size distribution of (a) BL-SLN, (b) BL-Tf-SLN, (c) CRC-SLN, (d) Tf-CRC-SLN

6.4.2 Determination of encapsulation efficiency and drug loading

The encapsulation efficiency of both CRC-SLN and Tf-CRC-SLN showed high encapsulation efficiency. CRC-SLN showed an encapsulation efficiency of 91.7% while Tf-CRC-SLN demonstrated an encapsulation efficiency of 90.1%. Interestingly, the inclusion of Tf did not hamper the encapsulation efficiency of CRC in SLN. The solubility of drug in the lipid matrix is considered to be a vital factor for drug loading. Solubility of CRC in the lipid matrix has certainly facilitated the encapsulation of CRC inside the lipid matrix (Tiyaboonchai, et al., 2007). Table 6.2 represents a table comparing the encapsulation efficiency of CRC-SLN and Tf-CRC-SLN as both formulations demonstrated similar encapsulation efficiency.

Table 6. 2 Entrapment efficiency and drug loading of CRC-SLN and Tf-CRC-SLN

	Drug loading (%)	Encapsulation efficiency (%)
CRC-SLN	6.36	91.7
Tf-CRC-SLN	6.29	91.1

6.4.3 Antiproliferative effect of CRC

The antiproliferative effect of CRC-SLN and Tf-CRC-SLN was compared to an alcoholic solution of pure CRC and blank SLN formulations in LNCaP prostate cancer cells. The cytotoxicity studies of pure curcumin showed excellent anti-proliferative activity after 24 hours incubation (Figure 3.1). The LNCaP cell lines viability was reduced to almost 0% at a very low drug concentration of 40 µg/ml. Researchers has confirmed that CRC does have one of the most desirable characteristics of a cancer chemotherapeutic agent. These are known as the therapeutic selectivity or preferential killing of cancer cells by CRC. CRC is known to exert its effect on cancer cells without any significant effects on normal cells. According to Yang et al., (2006), CRC decreased the cellular proliferation and induced apoptosis in LNCaP cells in a concentration dependent manner. These effects can always be regarded advantageous in chemotherapy.

6.4.4 Antiproliferative effect of SLN formulations

The non-toxic characteristics of blank SLN (both conjugated and unconjugated) are considered to be an important feature. Cytotoxicity of empty formulations was evaluated to assess any significant changes in cell viability. In a dose dependent study, both blank and Tf-SLNs showed negligible effects on cell viability. As seen from the Figure 6.4 blank and Tf-SLN dispersions presented cell viability of 91.7% and 90% respectively. Moreover, there was no significant difference of cell viability between blank SLN and Tf-SLN, which indicated transferrin conjugation on blank SLN did not induce any toxic effects for the SLNs.
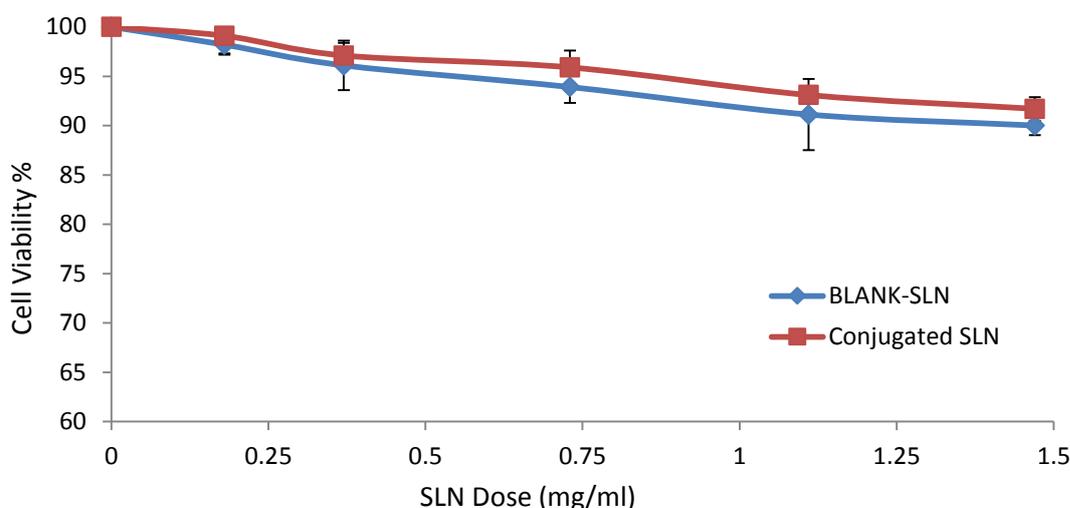
Figure 6. 4 Cytotoxicity of empty SLN formulations (blank and conjugated SLNs). (n = 3).

Cytotoxicity studies revealed that both CRC-SLN and Tf-CRC-SLN showed enhanced antiproliferative activity in a dose dependant manner (Figure 6.5). At the lowest dose of 12.5µg/ml both formulations showed substantial antiproliferative activity 90.56% and 75.96% respectively for CRC-SLN and Tf-CRC-SLN. Statistical t-test analysis showed significant difference between the anticancer potency of Tf-CRC-SLN (at 12.5 µg/ml CRC concentration) and blank Tf-SLN formulations (P=0.0001). At 25µg/ml CRC concentrations, an enhanced effect on cell viability was observed, as both CRC-SLN and Tf-CRC-SLN presented cell viability of 72.49% and 58.37% respectively. At increasing CRC concentrations (50µg/ml) cell viability was further reduced at 41.62%.
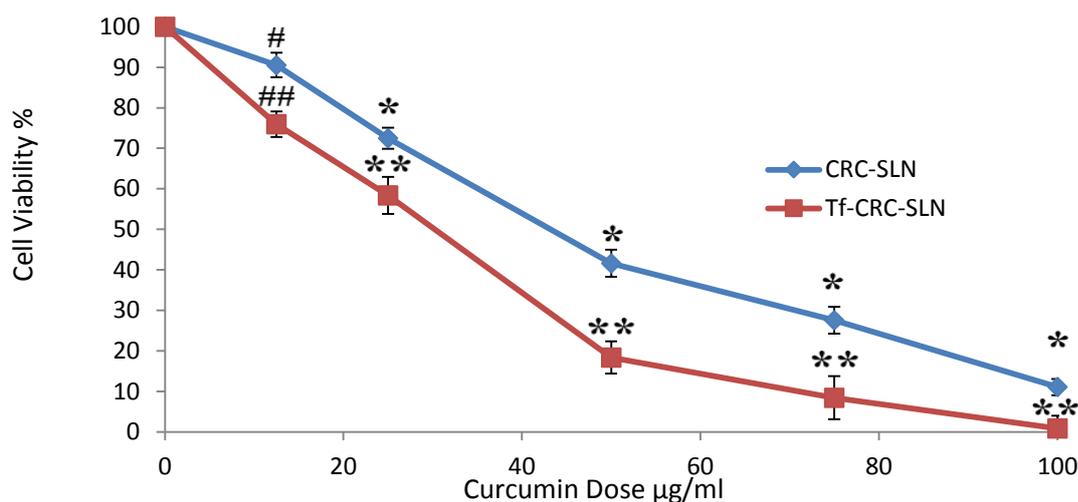
Figure 6. 5 Cytotoxicity of CRC-SLN and Tf-CRC-SLN after 24 hours. Data is represented as mean±S.D. (n = 3). #p=0.0366, *p< 0.0001, CRC-SLN (24 hours) vs. Blank SLN and ##p=0.0001, **p< 0.0001, Tf-CRC-SLN (48 hours) vs. transferrin conjugated blank SLN.

At the same CRC concentration the cell viability of Tf-CRC-SLNs was reduced at 18.36% demonstrating a significant effect compared to CRC-SLN formulations, and blank formulations (P<0.0001). At 75µg/ml dose, the effect was even more pronounced and cell viability was reduced to 27.58% for CRC-SLN and 8.43% for the Tf-CRC-SLN. At a CRC concentration of 100µg/ml, Tf -SLN samples taken the cell viability down to 0%, while for CRC-SLN the cell viability was 11.05%.These findings indicated that Tf-CRC-SLNs exhibits significantly higher potency then the other formulations (P<0.0001). As it can be seen from Figure 6.5, Tf-CRC-SLNs increased SLN active targeting which potentially could enhance the therapeutic potential of CRC. This study realized the efficiency of Tf-CRC-SLN as a targeted drug delivery system for human prostate cancer cells. According to Lemiux et al., (1994) both transferrin and CRC are capable of inhibiting p-glycoprotein efflux, bypass of membrane associated efflux could lead to increased cellular uptake and retention, which in turn results in an enhanced antiproliferative effect. In this dose dependent study blank SLN and Tf-SLN formulations showed negligible effect on cell viability after 24 hr incubation. The obtained results suggest that the antiproliferative effect observed with both CRC-SLN and Tf-CRC-SLN is attributed to the encapsulated CRC.

6.4.5 Cellular uptake by fluorescence microscopy

Internalization of the SLN formulations was confirmed by fluorescent microscopy where CRC-SLN and Tf-CRC-SLN were incubated in LNCaP prostate cancer cell line for 24 hours. Figure 6.6 reveals the cellular internalization of both CRC-SLN and Tf-CRC-SLN formulations in LNCaP prostate cancers cells. It can also be seen that the SLN particles are localised in the cytoplasm around the nucleus. Interestingly both CRC loaded SLNs (conjugated and unconjugated) showed similar uptake properties. The fluorescent intensity of encapsulated CRC was reduced due to the Tf conjugation on the surface of CRC-SLN. . Sevaral studies have proposed that SLNs are uptaken by the cells via the endocytosis mechanism pathway (Alam et al., 2012).
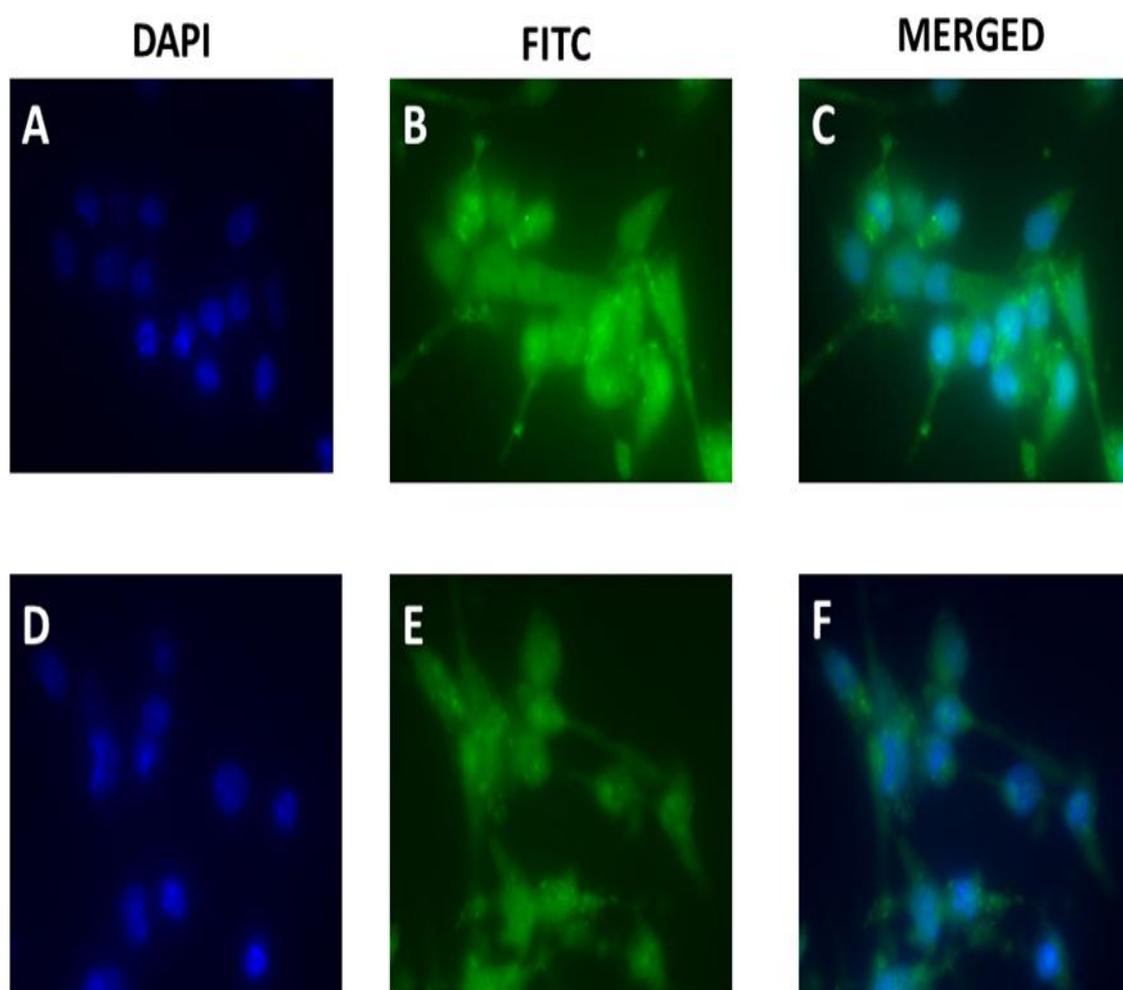
Figure 6. 6 Cellular uptake curcumin loaded SLNs. Green colour from FITC represents CRC. Blue colour from DAPI represents nuclei visualization. A-C shows the cellular uptake of Tf-CRC-SLN and D-F the cellular uptake of CRC-SLN

6.4.6 Flow cytometry analysis for cellular uptake of SLNs

Cellular uptake of CRC-SLN and Tf-CRC-SLN was examined quantitatively by using the intrinsic fluorescent property of CRC with fluorescent activated cell sorting (FACS) analysis. Figure 6.7 shows the relative extent of cellular uptake of CRC-SLN and Tf-CRC SLN in terms of fluorescent intensity. As seen in Figure 6.7, both CRC loaded SLN revealed an intensity percentage of more than 90%, which is directly related to the expression of high percentage of cellular uptake. Additionally, blank SLNs were also incubated in cells but no auto-fluorescence was observed for all batches.
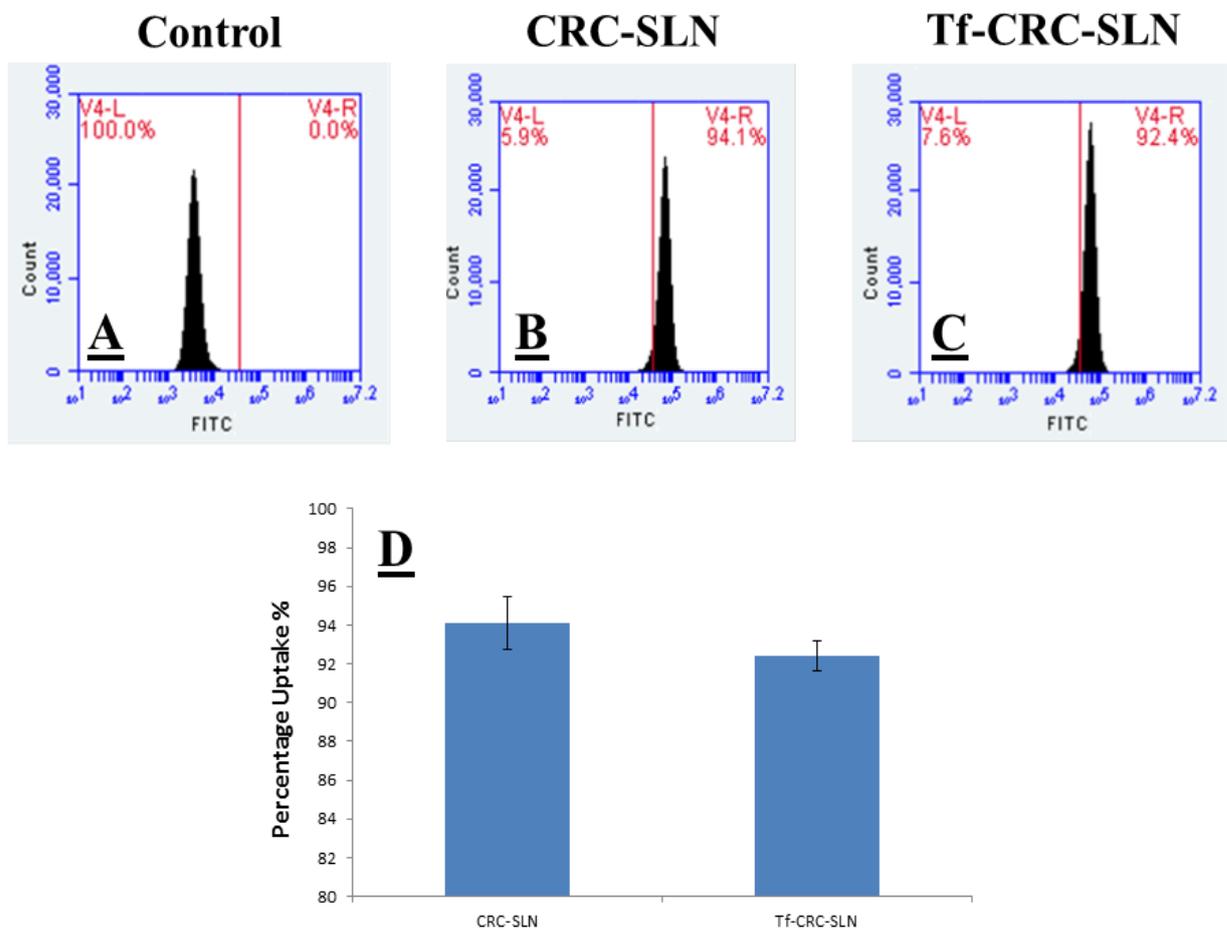
Figure 6. 7 Cellular uptake of SLNs by flow cytometric analysis. (A) Cellular uptake of control (Blank SLN). (B) Cellular uptake of CRC- SLN. (C) Cellular uptake of Tf-CRC-SLN. (D) bar graphs representing the uptake of CRC-SLN and Tf-CRC-SLN (n = 3).

6.4.7 *In vitro* apoptosis study

Externalization of phosphatidylserine (PS) at the outer plasma membrane is considered to be an early event in apoptosis, which is a consequence of loss of plasma membrane asymmetry. PS externalization was detected as an indicator of apoptosis by targeting for the loss of plasma membrane asymmetry (Speth et al., 1988). The induction of apoptosis by CRC after the treatment with both CRC-SLN and Tf-CRC-SLN was detected and also evaluated by using flow cytometric analysis (Figure 6.8). The ability to induce apoptosis was evaluated with PE Annexin V/ 7AAD staining, which binds to cells that express phosphatidylserine on the outer layer of cell membrane, for all SLN formulations (Speth et al. 1988). Annexin V allows discrimination of live cells from apoptotic cells and necrotic or late apoptotic pathway (stained with both PE Annexin V and 7AAD). Pure CRC treated cells (15µg/ml) demonstrated that 12% cells were early apoptotic and 24% cells were late apoptotic (Figure 6.8). Apoptotic cells were observed in cells treated with all CRC loaded formulations but the percentage of apoptotic cells varied with each formulation. Tf-CRC-SLN treated cells showed 19.9% early apoptotic and 50.0% late apoptotic/early necrotic cells populations respectively, when compared to CRC-SLN (20.2% and 34.0%) treated cells at 50µg/ml dose for 24 hours. At higher concentration of 100µg/ml, an increase in both populations was observed with both formulations. The percentage of early apoptotic and late apoptotic/early necrotic populations in cells treated with CRC-SLN and Tf-CRC-SLN at 100µg/ml dose were 12.1% and 80.3% and 6.4% and 88.9% respectively. Experiments with controls (Blank SLN and Transferrin conjugated Blank SLN) showed that they have negligible apoptotic effect indicating the apoptosis induced in all formulations were indeed because of CRC. These results indicated that CRC-SLN surface modification with anti-body or protein improves the apoptotic activity of designed drug delivery systems. Similar results were reported previously where the conjugation of transferrin on the surface of SLNs improves the inhibition efficiency of the formulations. (Li et al., 2009; Zhuo et al., 2013). Most anticancer drugs are necrotic which leadings to inflammation in other cells compartments and as a result cause various adverse side effects in patients when administered. These findings demonstrated the ability of CRC to induce apoptosis in LNCaP prostate cancer cells. Therefore, CRC could be considered as an effective drug candidate for prostate cancer treatment.
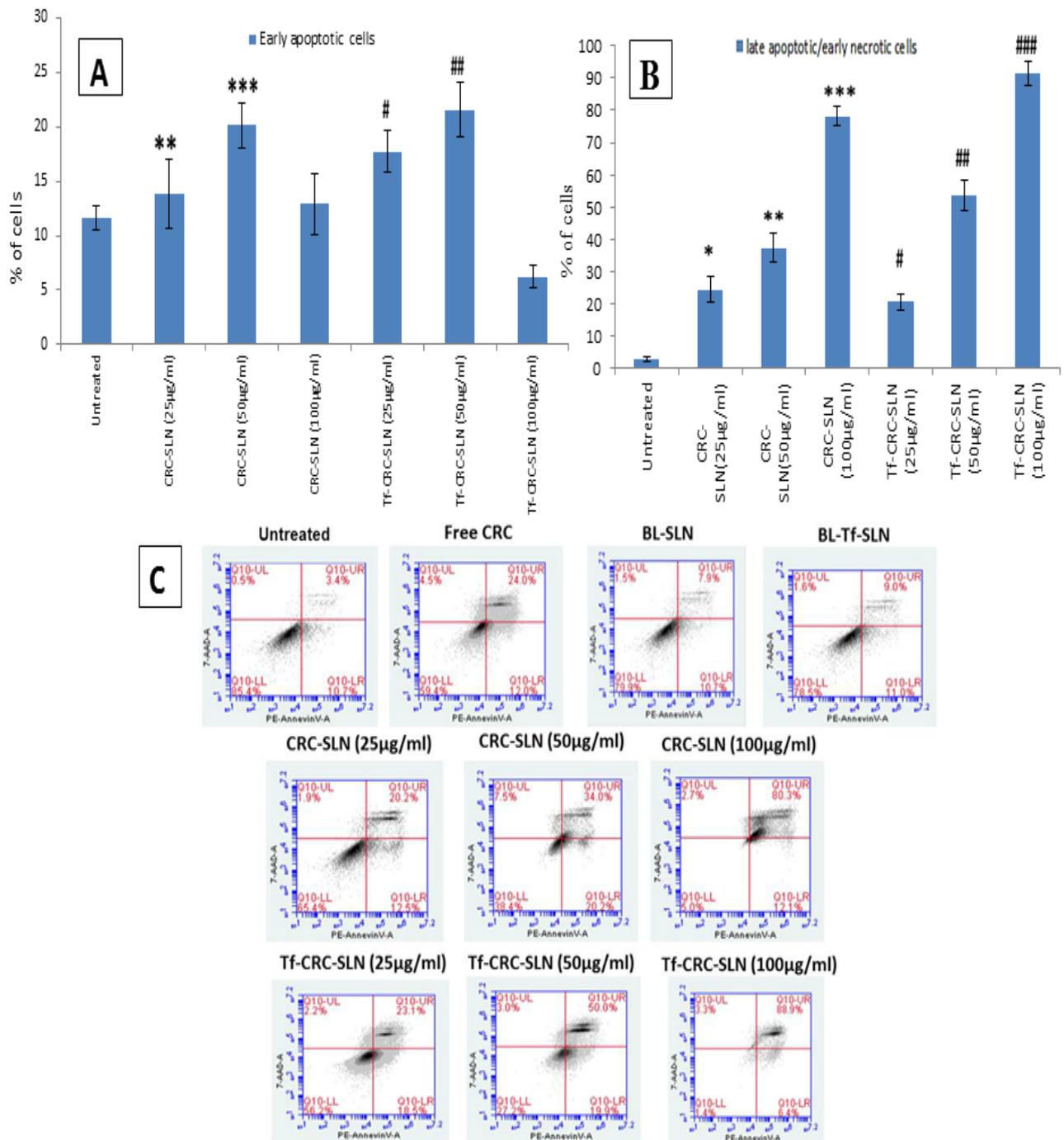
Figure 6. 8 Quantitative apoptotic measurement in LNCaP cells after treatment with Blank SLN, Conjugated SLN, free CRC, CRC-SLN and Tf-CRC-SLN(A) Dose dependent effect on early apoptosis by treatment with a concentration of 25, 50 and 100μg/ml of CRC-SLN and Tf-CRC--SLN dose for 24h determined by flow cytometry analysis. (B) Dose dependent effect on late apoptosis by treatment with a concentration of 25, 50 and 100μg/ml of CRC-SLN and Tf-CRC--SLN dose for 24h determined by flow cytometry analysis. The results are expressed as bar chart. Data as mean±S.D. (n = 3). (*) p<0.05, Control versus CRC-SLN(25μg/ml) and (#) p <0.05 Control versus vs Tf-CRC-SLN (25μg/ml), (**) p < 0.05, Control versus CRC-SLN and (##) p <0.05 Control versus vs Tf-CRC-SLN (50μg/ml), (***) p < 0.05, Control versus CRC-SLN and (###) p <0.05 Control versus vs Tf-CRC-SLN (100μg/ml)(B) Dose dependent effects are expressed as dot plot of PE AnnexinV versus 7-AAD. Dot plot from flow cytometry analysis reveals the four different populations of cells. Top left: necrotic cells; top right: late apoptotic cells/early necrotic cells; bottom left: live cells; and bottom right: early apoptotic cells.

.

130

6.4.8 *In vivo* anti-tumour activity of bio-conjugated SLN formulations on mice bearing LNCaP prostate cancer tumour.

CRC entrapped in TF conjugated SLNs slowed down the overall growth of LNCaP prostate cancer tumours compared to other treatments. Tumour inhibition growth in terms of mean tumour tissue weight (g) is presented in Figure 6.9. The examined therapeutic effects obtained by measuring the suppression of tumour growth in weight confirmed the formulations to have betters therapeutic efficacy compared to the drug solution.
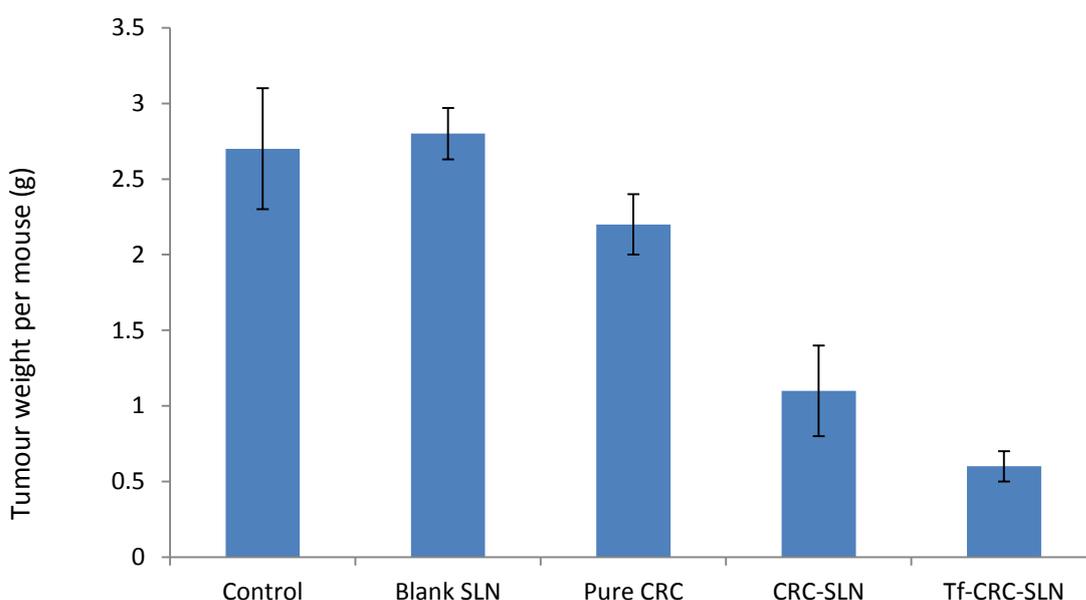
Figure 6. 9 Comparative therapeutic effects of control, blank SLN, pure CRC, CRC-SLN and Tf-CRC-SLN on tumour suppression of LNCaP prostate cancer.

CRC suppressed total tumour tissue mass by 19%, when compared to the control at the end of the treatment. Statistical analysis of an unpaired t-test revealed that, the effect of CRC on total tumour tissue weight upon treatment was significantly higher than the control, where the ($p<0.021$). The comparative anti-tumour activity of CRC-SLN formulations is given in Figure 6.10. Blank SLN dispersions did not show any significant anti-tumour activity when compared with the control samples (p .6742). However, significant difference can be seen in the therapeutic efficiency between blank SLN and CRC-SLN formulations ($P<0.0001$) where the inhibition of the tumour growth mass is 61% compared to blank SLN formulations. The comparison of CRC and CRC-SLN demonstrated a significantly higher anti-tumour activity

for the latter and the tumour mass was reduced up to 42%, compared to the pure CRC solution.

Figure 6.9 also depicts the therapeutic efficacy of Tf-CRC-SLN in terms of tumour weight per mouse. CRC encapsulated in Tf conjugated SLN formulations dramatically suppressed the tumour growth by 79%. This result corresponded to a major improvement of therapeutic efficacy of anti-cancer drug for the treatment of tumours as previously described by Fu et al., 2011. As shown in Figure 6.9 that the Tf-CRC-SLN dispersions significantly enhanced the anti-tumour effect compared to CRC-SLN (P <0.0003).The therapeutic improvement observed in Tf-CRC-SLN might result from various factors. First the entrapment of CRC within the lipid matrix of the SLN offers the opportunity to administer the drug intravenously while at the same time protecting it from degradation and metabolism. This in turn ensured sufficient circulating CRC available for reaching the tumours (Fue at al., 2011). Moreover a higher dose of CRC can be administered as a result of increased payload when encapsulated in delivery systems, subsequently improving the dosing regimen and therapeutic index. The increase of treatment duration (week 1- week 4) might also play a very important role in observed improvement. Furthermore, Tf-conjugated CRC-SLN systems could have different intracellular sorting pathway after uptake by Tf-receptor mediated endocytosis compared to unconjugated delivery systems via nonspecific pathway and this could increase the intracellular retention and hence, therapeutic efficacy of the encapsulated CRC (Mulik et al., 2010).The of tumour weight regression of the various groups was reduced in the following ascending order: CRC (19%) < CRC-SLN (61%) < Tf-CRC-SLN (79%).

The therapeutic effect examined by measuring the suppression of tumour growth specified in terms of tumour volume confirms that both CRC and CRC encapsulated SLN formulations can inhibit tumour growth (Figure 6.10). In terms of therapeutic effect efficacy pure CRC treatment produces higher tumour inhibition when compared with control (Figure 6.10). After treatment for 30 days with pure CRC the tumour volume was 1153.13 mm^3, while at the same time control exhibited a tumour volume of 1410.21 mm^3. Statistical analysis using t-test shows that CRC effect on tumour growth regression is significantly different from that of the control treatment (P <0.0001). These findings can confirm that, CRC can induce an effective therapeutic effect on the LNCaP prostate cancer tumours.

Figure 6.10 also shows that blank SLN formulation did not show significant decrease in tumour growth suppression, similar to the control treatment (P = 0.09). However, CRC-SLN

and Tf-CRC-SLN exhibited highly significant decrease in tumour growth when comparing to pure CRC treatment, blank SLN and control. Tf-CRC-SLN demonstrates the highest tumour growth inhibition by up to 72% when compared to the control. Tumour volume of mice treated with Tf-CRC-SLN was 392.64 mm^3 compared to CRC-SLN (754.59 mm^3), CRC (1153.13 mm^3), blank SLN (1354.08) and control 1410.21 mm^3). These results can be attributed to various factors Firstly, the elevated tumour accumulation of CRC due to the enhanced permeability and retention effect of CRC-SLN and secondly the utilization of active targeting based on the use of transferrin provided a tumour-selective targeting strategy, leading to an increased delivery of CRC to the tumours.
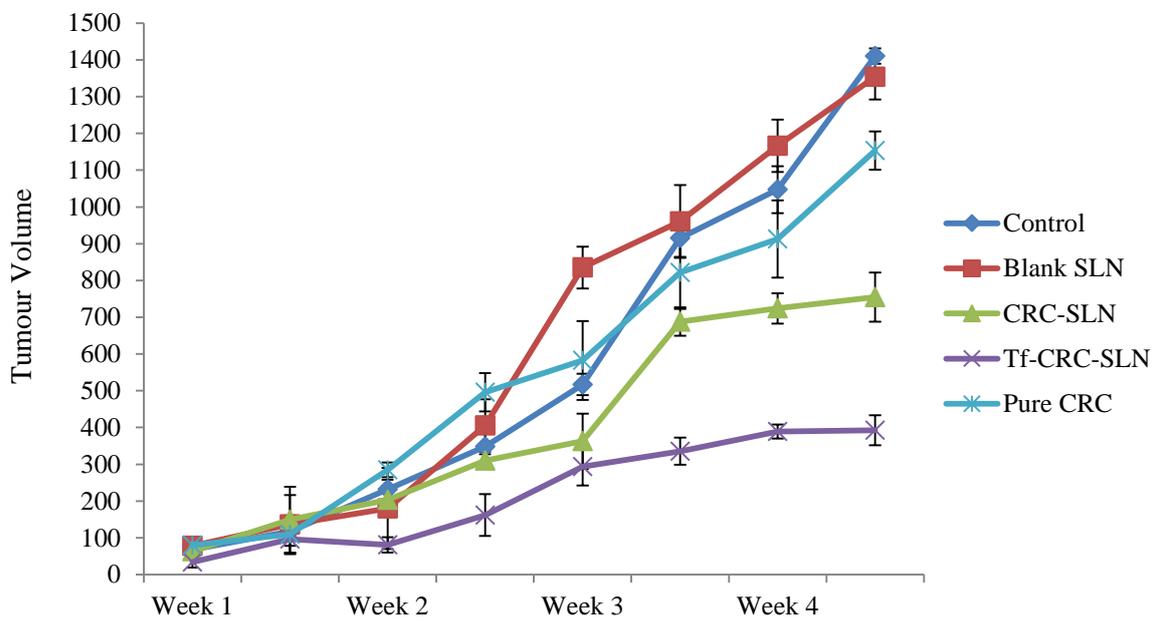

Figure 6. 10 Therapeutic effect of control, blank SLN, pure CRC, CRC-SLN and Tf-CRC-SLN on mice bearing tumour.
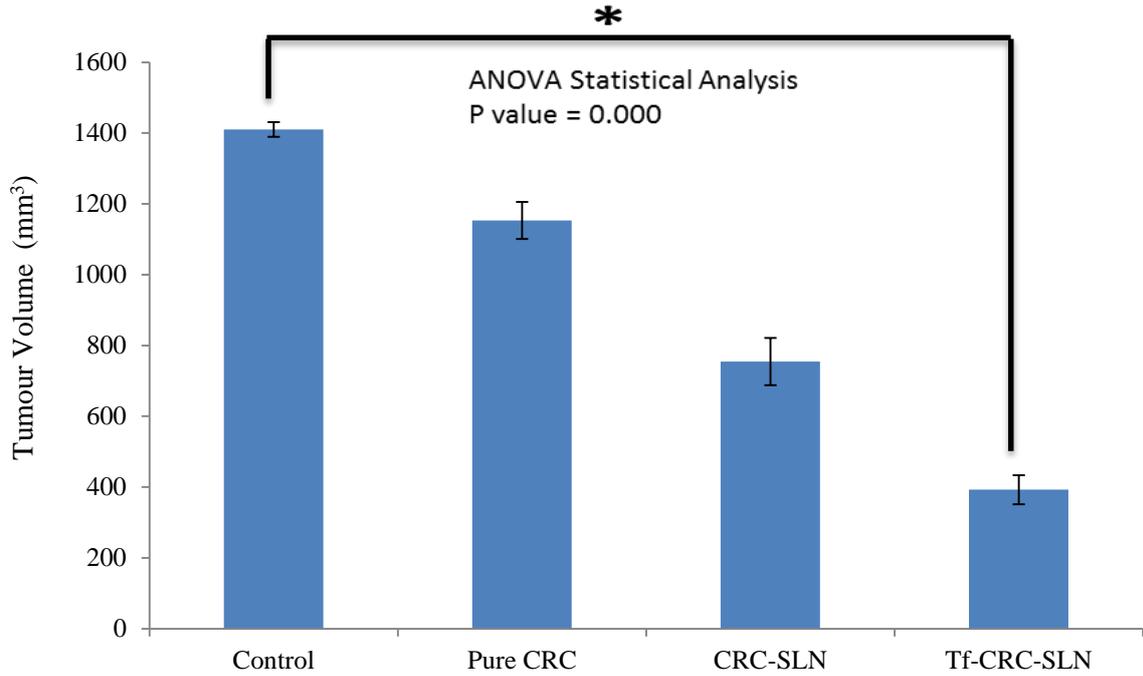
Figure 6. 11 Difference in therapeutic efficiency of control, pure CRC, CRC-SLN and Tf-CRC-SLN formulations in mice bearing tumour.
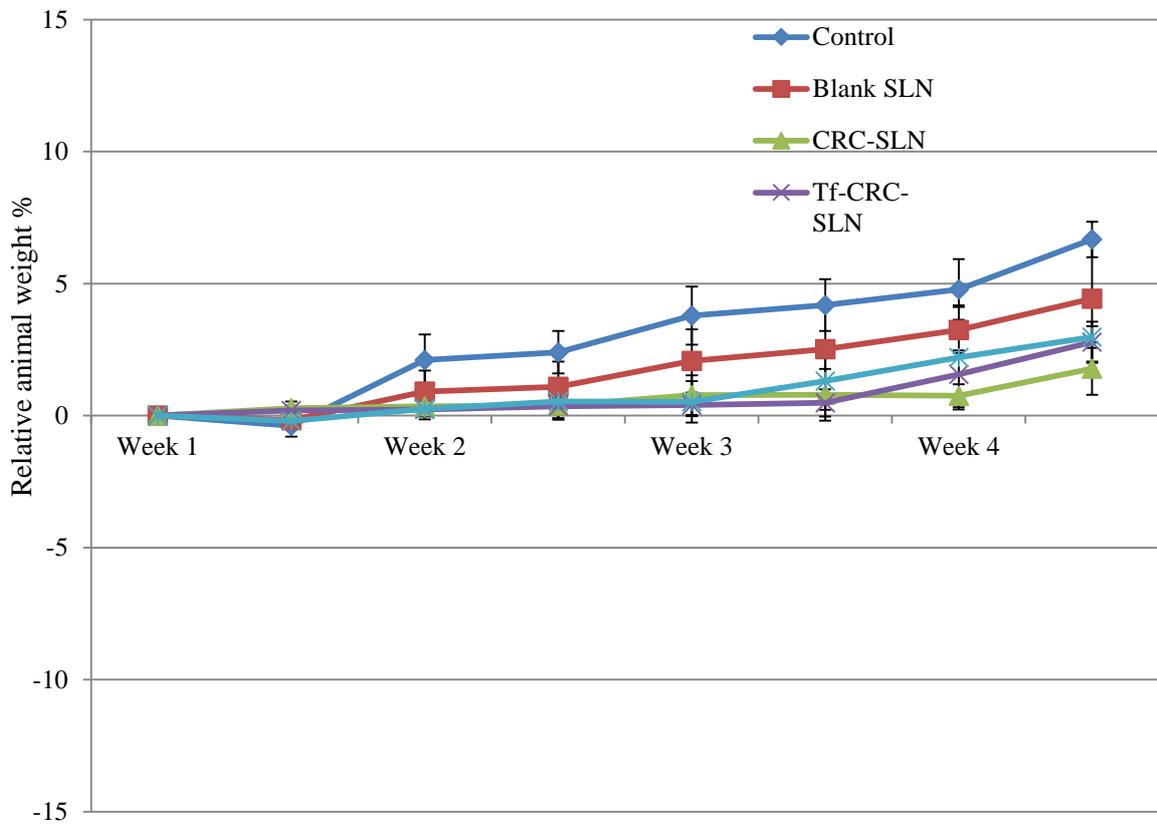

Figure 6. 12 Treatment tolerance by mice bearing tumour over the treatment study period of four weeks.

A summary graph of tumour regression efficiency of CRC and CRC loaded formulations is shown in Figure 6.11. Statistical analysis using ANOVA shows that difference of therapeutic efficacy between the treatments administered in tumour bearing mice is highly significant. The results of this study demonstrate that the CRC loaded formulations are highly effective against LNCaP prostate cancer tumours, where Tf-CRC-SLN was the most significantly efficient amongst all the formulations. Moreover, results shown in Figure 6.12 demonstrate formulations to be well tolerated by the mice with no seemly signs of toxicity of significant weight loss during the treatment.

CRC a major constituent of turmeric has been shown to be highly effective in affording protection against cancer in experimental animals induced by a variety of chemical carcinogens (Huang et al., 1988). Treatment of CRC initiated apoptosis and cell cycle arrest as well as cell growth inhibition, activation of signal transduction, and transforming activities in both androgen-dependent and androgen-independent prostate cancer cells. CRC also exerted strong antioxidant and anti-inflammatory activities by suppressing both constitutive and inducible nuclear factor- ƙB (NF-ƙB) and activator protein-1 activation (Hour et al., 2002). Despite all these properties of CRC, low bioavailability limits its therapeutic efficiency. However, CRC-SLN can successfully eliminate this particular limitation of CRC. As demonstrated from the *in vivo* trials, CRC-SLN significantly reduces tumour volume when compared to pure CRC. Targeted delivery of drugs to tumour has become a key trend in chemotherapy development. Nanotechnology consisting of SLN drug delivery system showed effective delivery of anti-cancer drug by targeting specific ligand in tumours. In this study, transferrin was conjugated on the surface of SLN and Tf-CRC-SLN significantly suppressed tumour growth, compared to unconjugated CRC-SLN. CRC and CRC encapsulated treatments (both conjugated and conjugated) regressed the tumour growth and also played a role in prolonging mice survival but did not totally eliminate tumour growth; similar findings were reported by Chen et al., (2012).

6.5 Conclusion

From the present investigation, it can be said that the proposed targeted delivery system is suitable for the therapeutically effective delivery of CRC being biocompatible and system capable of releasing drug in a sustained manner and tumour targeting. The enhanced therapeutic potential of Tf-CRC-SLN in the treatment of prostate cancer *in vivo* and *in vitro* was confirmed from the increased efficacy of CRC against LNCaP prostate cancer cells with

TF-CRC-SLN. Based on the results that have been obtained from the present investigation, conclusion of such manner can be proposed where transferrin mediated drug delivery system is worth exploring for other types of cancers like breast, neuroblastoma, etc.

6.6 References

1. Aggarwal, B. B., Kumar, A., & Bharti, A. C. (2003). Anticancer potential of curcumin: preclinical and clinical studies. *Anticancer research*, *23*(1), 363-398.

2. Alam, S., Panda, J. J., & Chauhan, V. S. (2012). Novel dipeptide nanoparticles for effective curcumin delivery. *International journal of nanomedicine*, *7*, 4207.

3. Caplan, A., & Kratz, A. (2002). Prostate-specific antigen and the early diagnosis of prostate cancer. *American journal of clinical pathology. 117*(1), 104-108.

4. Chen, Y., Wu, Q., Zhang, Z., Yuan, L., Liu, X., & Zhou, L. (2012). Preparation of curcumin-loaded liposomes and evaluation of their skin permeation and pharmacodynamics. *Molecules*, *17*(5), 5972-5987.

5. Das, M., & Sahoo, S. K. (2012). Folate decorated dual drug loaded nanoparticle: role of curcumin in enhancing therapeutic potential of nutlin-3a by reversing multidrug resistance. *PLoS one*, *7*(3), e32920.

6. Freitas, C., & Müller, R. H. (1998). Effect of light and temperature on zeta potential and physical stability in solid lipid nanoparticle (SLN™) dispersions. *International journal of pharmaceutics*, *168*(2), 221-229.

7. Fu, J. Y., Zhang, W., Blatchford, D. R., Tetley, L., McConnell, G., & Dufès, C. (2011). Novel tocotrienol-entrapping vesicles can eradicate solid tumors after intravenous administration. *Journal of controlled release*, *154*(1), 20-26.

8. Gupta, Y., Jain, A., & Jain, S. K. (2007). Transferrin-conjugated solid lipid nanoparticles for enhanced delivery of quinine dihydrochloride to the brain. *Journal of pharmacy and pharmacology*, *59*(7), 935-940.

9. Hermanson, G. T. (1996). *Bioconjugate techniques*. Academic press.

10. Hour, T. C., Chen, J., Huang, C. Y., Guan, J. Y., Lu, S. H., & Pu, Y. S. (2002). Curcumin enhances cytotoxicity of chemotherapeutic agents in prostate cancer cells

by inducing p21WAF1/CIP1 and C/EBPβ expressions and suppressing NF-κB activation. *The prostate*, *51*(3), 211-218.

11. Huang, M. T., Smart, R. C., Wong, C. Q., & Conney, A. H. (1988). Inhibitory effect of curcumin, chlorogenic acid, caffeic acid, and ferulic acid on tumor promotion in mouse skin by 12-O-tetradecanoylphorbol-13-acetate. *Cancer research*, *48*(21), 5941-5946.

12. Igartua, M., Saulnier, P., Heurtault, B., Pech, B., Proust, J. E., Pedraz, J. L., & Benoit, J. P. (2002). Development and characterization of solid lipid nanoparticles loaded with magnetite. *International journal of pharmaceutics*,*233*(1), 149-157.

13. Kutluay, S. B., Doroghazi, J., Roemer, M. E., & Triezenberg, S. J. (2008). Curcumin inhibits herpes simplex virus immediate-early gene expression by a mechanism independent of p300/CBP histone acetyltransferase activity. *Virology*, *373*(2), 239-247.

14. Lemieux, P., & Page, M. (1993). Sensitivity of multidrug-resistant MCF-7 cells to a transferrin-doxorubicin conjugate. *Anticancer research*, *14*(2A), 397-403.

15. Li, W., Khor, T. O., Xu, C., Shen, G., Jeong, W.-S., Yu, S., & Kong, A.-N. (2008). Activation of Nrf2-antioxidant signaling attenuates NF-κB-inflammatory response and elicits apoptosis. Biochemical Pharmacology, 76(11), 1485–1489. doi:10.1016/j.bcp.2008.07.017.

16. Li, X., Ding, L., Xu, Y., Wang, Y., & Ping, Q. (2009). Targeted delivery of doxorubicin using stealth liposomes modified with transferrin. *International journal of pharmaceutics*, *373*(1), 116-123.

17. Lim, S. J., & Kim, C. K. (2002). Formulation parameters determining the physicochemical characteristics of solid lipid nanoparticles loaded with all-trans retinoic acid. *International journal of pharmaceutics*, *243*(1), 135-146.

18. Liu, J., Chen, S., Lv, L., Song, L., Guo, S., & Huang, S. (2013). Recent progress in studying curcumin and its nano-preparations for cancer therapy. *Current pharmaceutical design*, 19(11), 1974-1993

19. López-Lázaro, M. (2008). Anticancer and carcinogenic properties of curcumin: considerations for its clinical development as a cancer chemopreventive and chemotherapeutic agent. *Molecular nutrition & food research*, *52*(S1), S103-S127.

20. Melmed, G. Y., Kwan, L., Reid, K., & Litwin, M. S. (2002). Quality of life at the end of life: trends in patients with metastatic prostate cancer. *Urology*, *59*(1), 103-109.

21. Mohanty, C., & Sahoo, S. K. (2010). The *in vitro* stability and *in vivo* pharmacokinetics of curcumin prepared as an aqueous nanoparticulate formulation. *Biomaterials*, *31*(25), 6597-6611.

22. Mulik, R. S., Mönkkönen, J., Juvonen, R. O., Mahadik, K. R., & Paradkar, A. R. (2010). Transferrin mediated solid lipid nanoparticles containing curcumin: enhanced *in vitro* anticancer activity by induction of apoptosis. *International journal of pharmaceutics*, *398*(1), 190-203.

23. Mulik, R. S., Mönkkönen, J., Juvonen, R. O., Mahadik, K. R., & Paradkar, A. R. (2012). Apoptosis-induced anticancer effect of transferrin-conjugated solid lipid nanoparticles of curcumin. *Cancer Nanotechnology*, *3*(1-6), 65-81.

24. Orlandi, M., Mantovani, B., Ammar, K., Avitabile, E., Dal Monte, P., & Bartolini, G. (2002). Retinoids and cancer: antitumoural effects of ATRA, 9-cis RA and the new retinoid IIF on the HL-60 leukemic cell line. *Medical principles and practice: international journal of the Kuwait University, Health Science Centre*, *12*(3), 164-169.

25. Potta, S. G., Minemi, S., Nukala, R. K., Peinado, C., Lamprou, D. A., Urquhart, A., & Douroumis, D. (2010). Development of solid lipid nanoparticles for enhanced solubility of poorly soluble drugs. *Journal of biomedical nanotechnology*, *6*(6), 634-640.

26. Powell, I. J. (2011). The precise role of ethnicity and family history on aggressive prostate cancer: a review analysis. *Archivos espanoles de urologia*, *64*(8), 711.

27. Sahoo, S. K., Ma, W., & Labhasetwar, V. (2004). Efficacy of transferrin-conjugated paclitaxel-loaded nanoparticles in a murine model of prostate cancer. *International journal of cancer*, *112*(2), 335-340.

28. Schulze-Tanzil G, Mobasheri A, Sendzik J, John T, Shakibaei M. (2004). Effects of Curcumin (Diferuloylmethane) on Nuclear Factor κB Signaling in Interleukin-1β-Stimulated Chondrocytes.*Annals of the New York Academy of Sciences*, *1030*(1), 578-586.

29. Souto, E. B., & Muller, R. H. (2007). Lipid nanoparticles (solid lipid nanoparticles and nanostructured lipid carriers) for cosmetic, dermal, and transdermal applications. *Drugs and pharmaceutical sciences*,*166*, 213.

30. Speth, P. A. J., Van Hoesel, Q. G. C. M., & Haanen, C. (1988). 2009, *15*(1), 15-31.

31. Sun, J., Bi, C., Chan, H. M., Sun, S., Zhang, Q., & Zheng, Y. (2013). Curcumin-loaded solid lipid nanoparticles have prolonged *in vitro* antitumour activity, cellular uptake and improved *in vivo* bioavailability. *Colloids and surfaces b: biointerfaces*, *111*, 367-375.

32. Tiyaboonchai, W., Tungpradit, W., & Plianbangchang, P. (2007). Formulation and characterization of curcuminoids loaded solid lipid nanoparticles.*International journal of pharmaceutics*, *337*(1), 299-306.

33. Yang, L., Chen, L., Meng, B., Suo, J., Wang, H., Xie, H., ... & Zhang, L. (2006). The effect of curcumin on proliferation and apoptosis in LNCaP prostate cancer cells. *Chinese journal of clinical oncology*, *3*(1), 55-60.

34. Zara, G. P., Cavalli, R., Bargoni, A., Fundarò, A., Vighetto, D., & Gasco, M. R. (2002). Intravenous administration to rabbits of non-stealth and stealth doxorubicin-loaded solid lipid nanoparticles at increasing concentrations of stealth agent: pharmacokinetics and distribution of doxorubicin in brain and other tissues. *Journal of drug targeting*, *10*(4), 327-335.

35. Zhuo, H., Peng, Y., Yao, Q., Zhou, N., Zhou, S., He, J., ... & Zhao, Y. (2013). Tumour imaging and interferon-γ–inducible protein-10 gene transfer using a highly efficient transferrin-conjugated liposome system in mice. *Clinical cancer research*, *19*(15), 4206-4217.

CHAPTER 7: OVERALL CONCLUSIONS

Promising therapeutic efficacy of curcumin and retinoic acid against cancer cells always gets hampered due to certain shortcomings such as low bioavailability. Moreover, systemic administration of curcumin and retinoic acid for cancer therapy is also not advisable owing to its uptake by mononuclear phagocytic system being lipophilic in nature and actual drug reaching the target sites will be very less. As a result, the need to develop a site specific targeted delivery system of these anticancer drugs capable of surpassing these aforementioned shortcomings is required. Several investigations have been done in the past to elucidate therapeutic potential of these anti-cancer drugs against cancer using *in vitro* cell culture techniques.

The use of anticancer drug loaded SLN as a drug delivery system for the treatment for LNCaP prostate cancer can be used effectively by bypassing the aforementioned drawbacks possessed by both curcumin and retinoic acid. Physicochemical properties of these loaded SLN played a significant role in its overall performance *in vitro* and *in vivo*. Dynamic light scattering properties of these SLN can actively affect the bio-distribution, release pattern and cellular uptake of nanoparticles. The encapsulation of anticancer drugs inside the SLN in an amorphous or molecularly dispersed form was confirmed by XRD and DSC analysis.

It was observed that, transferrin conjugated curcumin loaded SLN has shown more antiproliferative activity at lower dose when compared to CRC-SLN. Tf-conjugated delivery systems might have dissimilar intracellular sorting pathway after uptake by Tf receptor-mediated endocytosis compared to unconjugated delivery systems, this could intensify the intracellular retention and hence, therapeutic efficacy of the encapsulated anticancer drugs. However, both CRC-SLN and Tf-CRC-SLN showed significant increase in fluorescence intensity in terms of cellular uptake. Flow cytometric detection of apoptosis showed enhanced therapeutic potential of Tf-CRC-SLN compared with CRC-SLN. Cellular uptake of Tf-CRC-SLN by Tf receptor-mediated endocytosis might be the main influential factor in enhanced anticancer effect of Tf-CRC-SLN. The inhibitory effect of both CRC-SLN and Tf-CRC-SLN was also active in *in vivo* models. Mice bearing LNCaP prostate cancer xenografts were treated with CRC loaded formulations. Significant tumour growth inhibition was observed. Tumours from animals treated with curcumin loaded SLN demonstrated significant anti-tumour efficacy. However, just like *in vitro* conditions, *in vivo* models also tend to demonstrate a much greater anti-tumour effect for Tf-CRC-SLN

formulation. Blank SLN formulation did not alter or deviate tumour growth by any means, so blank SLN was considered to be totally non-toxic. Both CRC-SLN and Tf-CRC-SLN showed enhanced anti-tumour effect than that of curcumin alone at same dose level. This confirmed the efficacy and potency of these curcumin loaded SLN formulations. Hence, from our study, we conclude that developed Tf-conjugated drug delivery system offers innovative and effective therapeutic modality of curcumin in the treatment of LNCaP prostate cancer cells.

As discussed previously, Solid lipid nanoparticles (SLN) are a colloidal carrier for controlled drug delivery system. However, there are also some potential limitations associated with SLN, i.e. limited drug loading capacity, drug expulsion during storage, etc.

The Nanostructured lipid carriers (NLC) based on mixture of solid lipids with liquid lipids can overcome some of the problems that are associated with SLN. In contrast to the more or less highly ordered SLN being yielded from solid lipids, the incorporation of liquid lipid to solid lipid leads to massive crystal order disturbance. The resulting matrix of lipid particles shows great imperfections in the crystal lattice and leaves enough space to accommodate drug molecules, thus, leading to improved drug loading capacity. After the preparation of NLC by using the hot homogenization technique, NLC were characterised by size and zeta potential. NLC showed smaller size distribution than that of SLN; moreover the zeta potential of curcumin loaded NLC were way above the zeta potential values of CRC-SLN formulations. A smaller sized nanoparticle is always more favourable for intravenous drug delivery, since bigger particle can lead to embolism and many other difficulties in an *in vivo* condition. Particle size is also considered to be a major factor in influencing the permeance of lipid dispersions. Prepared NLC showed very narrow size distribution with zeta potential of higher than -40 mV, which is an indication of particles long term stability. *In vitro* release studies indicated sustained release with a very high encapsulation efficiency of CRC inside the lipid matrix. Another important factor is the higher drug loading due to usage of the solid and liquid lipid matrix which enables greater imperfection in crystal lattice. The release profiles of curcumin loaded NLC formulations displayed biphasic drug release pattern with burst release in initial stage and prolonged release afterwards. In addition efficacy of CRC-NLC as an anticancer agent was evaluated by *in vitro* fluorescent microscopy, FACS flow cytometry. *In vitro* cell viability assay displayed significant cell growth inhibition after treating the cells with CRC-NLC. Blank NLC did not alter the cell viability, which is an indication that only encapsulated CRC influenced the cell viability

findings. *In vivo*, animal studies demonstrated a significantly higher anti-cancer efficiency on mice bearing LNCaP prostate cancer xenografts. CRC-NLC exhibited greater anti-tumour effect on mice bearing LNCaP prostate cancer xenografts when compared with pure curcumin. Moreover, the blank NLC group did not exhibit any effect on tumour growth. Upon treatment for 4 weeks with the loaded and blank NLC formulations there were no considerable changes in animal weight too. These results indicated that CRC-NLC is a potent drug delivery system for the treatment of prostate cancer. Although, CRC-NLC did not necessarily show significantly better anti-cancer activities, various other aspects needs to be taken into consideration. Firstly, the inclusion of liquid lipid can slow down polymorphic changes within the lipid matrix, which can lead to complex stability issues (i.e lower zeta potential, bigger particle size, drug crystal formation etc). A higher zeta potential compared to SLN was an indication of NLCs improved stable characteristics. Moreover, NLC increased encapsulation efficiency and drug loading with a blend of solid and liquid lipid that can effectively protect encapsulated drug from damaging factors in aqueous phase.

CHAPTER 8: FUTURE WORK

Curcumin and retinoic acid loaded SLNs and curcumin loaded NLCs were successfully prepared by hot homogenization method maintaining temperatures above the lipids melting point. Potency of these SLN and NLC formulations as an anticancer agent was evaluated both *in vitro* and *in vivo*. However, several other modifications can be done in these lipid nanoparticles, as it has proven to be a promising drug delivery system in the treatment of LNCaP prostate cancer cells.

Future works for this project includes the following:

- Co-load retinoic acid and curcumin in SLN and NLC. Since both of these lipid nanoparticles have been shown to be a promising drug delivery system for anti-cancer drugs.

- Conjugation of transferrin to SLN has drastically improved its anti-tumour efficacy against mice bearing LNCaP prostate cancer xenografts. Similar studies can be performed on NLC as well, and see if similar or enhanced outcomes can be achieved.

- Load several other anti-cancer drugs such as Probucol, Camptothecin etc., in SLN and NLC and evaluate their efficiency on different cancer cell lines.

- Conduct further cellular studies using both conjugated and unconjugated SLNs. These studies can include measurements of reactive oxygen species, detection of mitochondrial membrane loss and cell cycle analysis.